UNIVERSITÉ DE SHERBROOKE
Faculté de génie
Département de génie mécanique

Développement d'outils de caractérisation de la mécanique pulmonaire en ventilation liquidienne totale

Mémoire de maîtrise
Spécialité : génie mécanique

Alexandre Beaulieu

Jury : Philippe MICHEAU (directeur)
Yvan CHAMPOUX (rapporteur)
Éric FOUCAULT (externe)
Hervé WALTI (externe)

Sherbrooke (Québec) Canada Juillet 2011

Library and Archives Canada

Published Heritage Branch

395 Wellington Street
Ottawa ON K1A 0N4
Canada

Bibliothèque et Archives Canada

Direction du Patrimoine de l'édition

395, rue Wellington
Ottawa ON K1A 0N4
Canada

Your file Votre référence
ISBN: 978-0-494-83716-0

Our file Notre référence
ISBN: 978-0-494-83716-0

RÉSUMÉ

Le projet de recherche présenté consiste à la mise en place de matériel et de méthodes pour la mesure de l'impédance du système respiratoire en ventilation liquidienne totale (VLT). Ce projet a été réalisé en majeure partie en collaboration avec un étudiant à la maîtrise en physiologie, M. Dominick Bossé.

Le matériel développé est un débitmètre instationnaire qui servira à mesurer le débit instantané à la trachée du patient. Le concept proposé consiste en un venturi symétrique comprenant trois prises de pression. La mesure du débit est obtenue en résolvant numériquement l'équation de Bernoulli légèrement modifiée. Un prototype a été validé expérimentalement en appliquant des débits sinusoïdaux de moyenne nulle. Les résultats ont montré que les écoulement quasi stationnaires sont mesurés précisément entre 5 ml/s et 60 ml/s et les oscillations de faible amplitude ($\leq$10 ml/s) sont correctement mesurés pour des fréquences sous 3 Hz.

De plus, une méthode pour appliquer la technique des oscillations forcées (TOF) en VLT est proposée. Elle consiste principalement à appliquer une excitation volumétrique sinusoïdale au système respiratoire, et à évaluer la fonction de transfert entre le débit délivré et la pression aux voies aériennes. Un modèle pulmonaire développé pour la ventilation gazeuse, le « *five-parameter constant-phase model* », est utilisé pour décrire les spectres d'impédance respiratoire observés. La méthode employée pour identifier les paramètres de ce modèle a été validée *in silico* sur des données générées informatiquement, et la méthode dans son ensemble a été validée *in vitro* sur un modèle mécanique reproduisant la dynamique pulmonaire. Les données *in vivo* sur 10 agneaux nouveau-nés suggèrent qu'un terme de compliance fractionnel est approprié pour décrire le comportement basse-fréquence des poumons, mais il n'a pas été possible de conclure sur la pertinence d'un terme d'inertance à ordre fractionnel.

Finalement, l'étude des aspects plus physiologique est présentée. En plus d'une description plus détaillée de la procédure expérimentale *in vivo*, on y observe l'influence de certains symptomes respiratoires (diminution de la compliance, augmentation de la résistance) sur l'impédance mesurée avec la TOF. Les conclusions sont que la résistance et l'inertance des voies aériennes sont grandement augmentées en VLT en comparaison de la ventilation gazeuse. La résistance et la réactance à 0.2 Hz sont sensibles à la bronchoconstriction et dilatation, autant que lors de la réduction de compliance. Ainsi, il est montré que la TOF à basse fréquence est un outil efficace pour suivre la mécanique respiratoire en VLT.

Mots-clés : Appareillage médical, Ventilation liquidienne totale, impédance pulmonaire, débitmètre à venturi, identification de système, système à ordre fractionnel, écoulements non stationnaires

REMERCIEMENTS

Mes premiers mots de remerciement vont évidemment à mon directeur de recherche M. Philippe Micheau qui, par ses connaissances approfondies — elles m'ont même souvent semblées infinies ! — dans les nombreux domaines touchées par ce projet, son ouverture aux nouvelles idées et sa patience a su me guider, me conseiller et m'épauler tout au long de ma maîtrise, en plus de me transmettre sa passion pour la recherche scientifique.

Je tiens par ailleurs à remercier M. Raymond Robert pour sa contribution inestimable au rojet Inolivent dans son ensemble, sans laquelle la poursuite de mes recherches n'aurait été possible, et M. Dominick Bossé qui a su préparer, mener et analyser les expérimentations *in-vivo* avec motivation et une puissance de travail contagieuses, mais sinon indescriptibles.

Il est tout aussi naturel de souligner la contribution du personnel de l'institut P' de l'Université de Poitiers, notemment Éric Foucault qui m'a encadré dans le développement du débitmètre instationnaire avec toute la rigueur et la souplesse nécessaires à la bonne conduite de tout projet scientifique. Et je ne peux passer sous silence l'assistance fournie par MM. Patrick Brault et Philippe Szeger lors du volet expérimental de ce projet.

L'apport des autres membres de l'équipe Inolivent, à commencer par les professeurs Dr. Hervé Walti et Dr. Jean-Paul Praud, mais sans oublier les étudiants et stagiaires ayant séjourné au laboratoire, notemment Benoît Beaudry, Mathieu Nadeau, Jaël Marchand et Lionel Thibault, a également été déterminant. C'est en évoluant dans ce milieu multisciplinanire dynamique, entouré d'experts mais aussi d'amis, que j'ai pu réaliser ces travaux de recherche qui, et j'en suis convaincu, apporteront une contribution manifeste au développement de ma carrière.

Finalement je tiens à remercier chaleureusement mes parents et amis qui m'ont toujours encouragés, par l'exemple et leurs bons mots, à poursuivre mes rêves et ambitions.

Merci !

TABLE DES MATIÈRES

LISTE DES FIGURES

LISTE DES TABLEAUX

CHAPITRE 1

Introduction

1.1 Contexte et problématique

1.1.1 Contexte global

La ventilation liquidienne totale (VLT) est une technologie médicale consistant à assurer la respiration d'un patient en utilisant un liquide oxygéné, typiquement un perfluorocarbone (PFC). À Sherbrooke, les recherches en VLT se font au sein du groupe de recherche Inolivent. Il s'agit d'une équipe multidisciplinaire qui regroupe des médecins chercheurs et cliniciens, des ingénieurs, et des étudiants dans les deux domaines.

L'équipe oeuvre au développement de la VLT dans le but de l'amener le plus tôt possible dans les unités de soins intensifs dans le cadre d'une étude pilote, car pour l'instant, l'essentiel des travaux en VLT dans le monde est validé par des expérimentations animales. Des protocoles antérieurs ont étudié entre autres les conséquences hémodynamiques de la ventilation liquidienne totale, son mode d'application et son efficacité à traiter les détresses respiratoires résultantes de l'aspiration gastrique ou de l'aspiration méconiale, en plus de valider les différentes fonctions et modes ventilatoires implantés sur le prototype. La VLT est donc en compétition directe avec d'autre modalités novatrices de respiration mécanique comme la ventilation haute fréquence ou encore des mesure plus invasives, telle l'oxygénation extra-corporelle (ECMO), utilisées en dernier recours en cas de grave insuffisance respiratoire. Se référer à (Yoxall *et al.*, 1997) pour une description un peu plus détaillée des techniques alternatives à la VLT.

Du côté de l'ingénierie, les principaux domaines impliqués sont la conception de systèmes mécatroniques (Robert *et al.*, 2006), les asservissements de systèmes mécaniques et biomécaniques (Robert *et al.*, 2009a), la modélisation des interfaces gaz-liquide (Beaudry, 2009) ainsi que le traitement de signal. Le dernier prototype développé par l'équipe Inolivent est montré à la figure 2.5 de la section 2.2.3.

Pour l'avenir, l'équipe se tourne vers le développement d'un appareil pour utilisation clinique, la modélisation de l'échange thermique entre le PFC et le sang dans les poumons ainsi qu'à la mise au point de la procédure de sevrage de la VLT, c'est-à-dire le passage de la VLT à la VMC, puis à la ventilation spontanée. Pour ce faire, les cliniciens doivent disposer d'au moins autant d'information sur l'état du patient que lors d'un traitement en ventilation mécanique conventionnelle (VMC).

1.1.2 Problématique

Comme pour toutes les techniques ventilatoires, il est essentiel en VLT pour le clinicien de connaître l'état des poumons et leur évolution au fil du traitement. Toutefois, alors que les modèles expliquant la dynamique pulmonaire en ventilation gazeuse sont bien documentés, il existe peu d'information pour la VLT.

Le projet de recherche proposé portera sur la caractérisation de l'impédance mécanique des poumons en ventilation liquidienne. Comme l'équipe de recherche se dirige vers l'optimisation des techniques de sevrage de la VLT, la caractérisation mécanique de l'appareil respiratoire apportera une information utile : elle sera un des indicateurs de l'évolution de la santé du patient au fil du traitement. Par ailleurs, une description plus fine de la dynamique pulmonaire, de pair avec sa plage de variation attendue, aidera la conception de contrôleurs en pression plus robustes. Notons au passage que le contrôle en pression est très important en VLT, car il s'agit du mode ventilatoire connu le plus efficace pour optimiser la ventilation minute (Robert *et al.*, 2009b).

Le problème posé est donc de s'inspirer des méthodes actuellement utilisées en VMC pour proposer une façon de mesurer l'impédance pulmonaire en VLT. Le projet couvrira donc l'exploration et l'implantation de la technique des oscillations forcées qui sera aussi utilisée pour valider les outils de mesure des paramètres dynamiques existants sur Inolivent-4.

De cet énoncé découle la question de recherche principale :

« *Comment mesurer la dynamique pulmonaire et son évolution lors d'un traitement en ventilation liquidienne totale ?* »

1.2 Objectifs du projet de recherche

L'objectif global du projet est de développer du matériel et des méthodes de caractérisation de la dynamique pulmonaire en ventilation liquidienne totale. L'accomplissement de cet objectif passera par l'atteinte des objectifs secondaires suivants :

1. concevoir et implanter un dispositif pour mesurer le débit instantané à la trachée ;
2. adapter la technique des oscillations forcées au contexte de la ventilation liquidienne totale ;
3. implanter les fonctionnalités sur le prototype Inolivent-4, et valider expérimentalement l'implantation finale ;
4. proposer un modèle décrivant l'impédance mécanique du système respiratoire des agneaux en VLT.

1.3 Contributions originales

Les contributions scientifiques amenées par le projet de recherche concernent à la fois le développement des respirateurs liquidiens ainsi que la mesure des propriétés physiologiques des poumons en VLT. Pour cette raison, les contributions majeures des travaux prennent la forme de publications à la fois dans des journaux de physiologie et d'ingénierie.

Premièrement, l'atteinte du sous-objectif N° 1 a mené à la rédaction d'un article publié dans *Flow Measurement and Instrumentation* (Beaulieu *et al.*, 2011). Cette publication, incluse dans le présent mémoire, propose une méthode pour déterminer la valeur d'un débit instationnaire à l'aide d'un tube de Venturi. Cette mesure rendra les futurs essais de caractérisation de la mécanique pulmonaire plus rapides, mais surtout répond à un besoin énoncé lors du 6^{e} Symposium International sur les Applications des Perfluorocarbones et la Ventilation Liquidienne par un groupe comprenant les principales équipes oeuvrant en VLT dans le monde : les ventilateurs liquidiens doivent inclure une mesure fiable du débit de liquide délivré au patient (Costantino *et al.*, 2009).

Deuxièmement, plus au coeur du sujet de maîtrise se trouve un manuscrit détaillant la méthodologie développée pour utiliser la technique des oscillations forcées en VLT. Comme il s'agit de la première fois, à notre connaissance, que de telles mesures sont tentées en VLT, la communauté scientifique pourra bénéficier du protocole proposé ainsi que des résultats obtenus pour mettre en oeuvre ses propres expériences et ainsi comparer les résultats et leur interprétation. Un modèle de dynamique pulmonaire tiré de la ventilation

gazeuse est appliqué sur les données et démontre que bien que les valeurs prises par les paramètres sont sensiblement différentes, la dynamique pulmonaire peut être décrite de la même façon qu'en VMC.

Ensuite, un article détaillant l'interprétation physiologique des données d'impédance mesurées par la TOF a été publié dans le *Journal of Applied Physiology* (Bossé *et al.*, 2010). Ce document est le fruit d'une collaboration entre Dominick Bossé, alors étudiant au doctorat en médecine et à la maîtrise en physiologie-biophysique (MD - M.Sc.) à l'Université de Sherbrooke. L'apport de ce dernier a été de définir et mettre en place le protocole d'expérimentation *in vivo*, et d'étudier les résultats en regard de la physiologie pulmonaire des agneaux et de la littérature médicale à ce sujet. De plus, la TOF a été expérimentée sur des modèles animaux ayant des pathologies respiratoires bien définies afin de déterminer l'utilité de la technique pour identifier ces dernières. Il n'est pas exagéré de dire que sans cet étudiant, la conduite de tout le volet *in vivo* du projet de recherche aurait été impossible. De la même façon, c'est le développement des outils exposés dans le présent mémoire qui a permis la récolte des données et leur traitement subséquent, nécessaires à la poursuite du projet de M. Bossé.

Pour finir, les travaux ont fait l'objet de communications dans des colloques locaux, nationaux et internationaux. En voici une liste sommaire :

- A. Beaulieu, P. Micheau, D. Bossé, R. Robert, O. Avoine, J.P. Praud et H. Walti. Mechanical impedance of the respiratory system during total liquid ventilation, *1st International Conference on Applied Bionics and Biomechanics*, Venise, Italie, 14 - 16 Octobre 2010

- D. Bossé, A. Beaulieu, O. Avoine, P. Micheau, J.P. Praud, H. Walti. Neonatal Total Liquid Ventilation: Is Low Frequency Forced Oscillation Technique Suitable for Respiratory Mechanics Assessment ?, *Pediatric Academic Societies' Annual Meeting (PAS)*, Vancouver, Canada, 1 - 4 Mai 2010

- A. Beaulieu, D. Bossé, O. Avoine, P. Micheau, J.P. Praud et H. Walti, La mécanique respiratoire en ventilation liquidienne totale : mise en oeuvre de la technique des oscillations forcées, *4e Journée Scientifique de l'Axe Mère Enfant*, Sherbrooke, Canada, 22 avril 2010,

- D. Bossé, A. Beaulieu, O. Avoine, P. Micheau, J.P. Praud et H. Walti, Total Liquid Ventilation : Is Low-Frequency Forced Oscillation Technique Suitable for Respiratory Mechanics Assessment ? *University of Giessen Molecular Biology and Medicine of the Lung 8th Annual retreat*, Giessen, Allemagne, Août 2010

1.4 Organisation du mémoire

Ce mémoire par articles se découpe en quatre parties principales. Le chapitre 2 regroupe une revue de la littérature utilisée dans le cadre de la recherche présentée de façon à mieux situer les travaux antérieurs. Cette revue traite des aspects principaux du projet : l'information disponible sur la technique des oscillations forcées et la modélisation de l'impédance respiratoire en ventilation gazeuse, la description plus globale de la ventilation liquidienne totale. Finalement les éléments propres aux dynamiques observées en ventilation liquidienne totale c'est-à-dire les paramètres physiologiques actuellement mesurés, les écoulements dans les conduites flexibles du prototype ainsi que les écoulements oscillants et leur mesure. Une revue plus technique des éléments appropriés est incluse dans chaque article.

Suite à cette section se trouve le premier article, traitant de la conception et de la validation d'un débitmètre instationnaire et publié dans le journal *Flow Measurement and Instrumentation.* La section suivante détaille la procédure de mesure de l'impédance pulmonaire au moyen de la technique des oscillations forcées. Dans cet article soumis à l'*IEEE Transactions on Biomedical Engineering*, on retrouve aussi une explication des dynamiques mesurées sous l'angle des écoulements dans l'arbre respiratoire. Finalement, un dernier article publié dans le *Journal of Applied Physiology* montre l'aspect plus physiologique du projet. Écrit par un étudiant en physiologie en collaboration avec l'auteur du présent mémoire, ce document étudie la sensibilité de la mesure à différents challenges respiratoires et son applicabilité pour obtenir l'impédance respiratoire en VLT.

CHAPITRE 2

État de la question et cadre théorique

2.1 Technique des oscillations forcées et traitement fréquentiel

2.1.1 Description générale de la technique

La technique des oscillations forcées (TOF) consiste à forcer une oscillation de débit à la trachée du patient, typiquement à l'aide d'un haut-parleur. Elle a été développée en VMC par DuBois *et al.* (1956) pour identifier la mécanique pulmonaire. Elle est toujours employée, en recherche (Bayat *et al.*, 2009) et en clinique (Goldman *et al.*, 2005), et parfois même en ventilation liquidienne partielle (VLP) (Schmalisch *et al.*, 2005), afin de caractériser les dynamiques associées à certains traitements et pathologies ou encore pour développer des modèles physiologiques du système respiratoire. Au meilleur de notre connaissance, toutefois, cette technique n'a jamais été implantée en VLT.

Étant donné que la TOF ne nécessite que peu ou pas de collaboration du patient, elle est très bien indiquée pour les mesures sur les enfants, les nouveaux nés ou les animaux, qu'ils soient anesthésiés, curarisés ou ventilés. En ce sens, elle est donc plus appropriée au projet que, par exemple, la spirométrie qui demande un effort du patient (Polak *et al.*, 2006).

La figure 2.1 montre comment est normalement implantée la technique. Lors des oscillations, le débit et la pression à la bouche sont mesurés simultanément et le rapport entre ces deux quantités fournit l'impédance pulmonaire, décrite plus en détail à la section 2.1.2.

Comme cette impédance est habituellement définie en fonction de la fréquence, l'analyse spectrale des signaux est nécessaire (Michaelson *et al.*, 1975). De ce fait, la linéarité du système mesuré et du système de mesure est supposée.

Cette linéarité implique naturellement que les mesures sont indépendantes de l'amplitude des signaux-tests employés si ceux-ci demeurent d'amplitude *raisonnable.* À titre d'indication, une réponse en pression d'environ 1-2 cmH_2O est mentionnée comme acceptable selon une revue critique sur le sujet (Navajas et Farre, 2001). Il existe une grande variété de signaux-tests pouvant être utilisés pour la TOF. La linéarité du système mesuré ouvre la porte à l'utilisation d'excitations contenant plusieurs fréquences, tels des bruits blancs (Michaelson *et al.*, 1975), des impulsions (Schmalisch *et al.*, 2005), ou encore des profils de respiration optimisés pour l'identification(Suki *et al.*, 1997). Mais cette approche doit être utilisée avec précaution pour les basses fréquences où le rapport signal/bruit s'en trouve diminué (Farre *et al.*, 1997). Pour y remédier ou en cas de doute, l'utilisation de signaux-tests harmoniques d'amplitude constante améliore ce rapport à la fréquence d'excitation (Navajas et Farre, 2001) et demeure valide dans le cas où la linéarité du système n'est pas assurée (Slotine et Li, 1990).

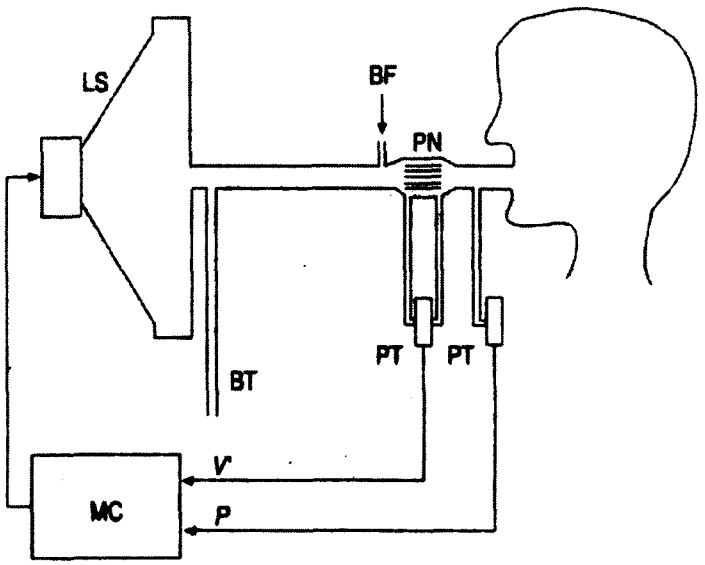

Figure 2.1 Schéma d'application typique de la technique des oscillations forcées (Navajas et Farré, 1999) MC: microcontrôleur, LS: haut-parleur ou générateur d'oscillations, BT: circuit de respiration, BF: débit respiratoire, PN: pneumotachographe, PT: capteur de pression, V': débit, P: pression.

2.1.2 Concept d'impédance du système respiratoire

L'impédance du système respiratoire est une façon usuelle de caractériser la mécanique pulmonaire, c'est-à-dire décrire, expliquer et prédire les variations dynamiques de pression en lien aux changements de volume (Farre *et al.*, 1994). Elle est définie par

$$Z_{RS} = \frac{\delta P_{aw}}{\delta \dot{V}} \tag{2.1}$$

où δP_{aw} est la réponse en pression trachéale à une petite perturbation de débit $\delta \dot{V}$ (la dérivée du volume pulmonaire). Comme pour l'impédance électrique, Z_{RS} est exprimée en fonction de la fréquence — ou de la pulsation $\omega = 2\pi f$ — et peut être séparée en une partie réelle et imaginaire :

$$Z_{RS}(j\omega) = R_{RS}(j\omega) + jX_{RS}(j\omega) \tag{2.2}$$

où $R_{RS}(j\omega)$ est la composante de l'impédance en phase avec le débit, la résistance du système respiratoire, alors que $X_{RS}(j\omega)$ est la réactance, soit la composante déphasée avec le débit. Cette dernière exprimera donc, en fonction de la fréquence, le lien entre la pression et le volume V et entre la pression et l'accélération volumique $\ddot{V}$ (Johnson et Bronzino, 1995; Navajas et Farre, 2001). Les relations entre les phases des différentes contributions à l'impédance sont illustrées à la figure 2.2. À titre d'exemple, le système représenté ici est plutôt caractérisé par sa résistance à cette fréquence car le débit y est presque en phase avec l'excitation.

2.1.3 Modélisation de l'impédance respiratoire en ventilation gazeuse

Modèle résistance-inertance-compliance (*RIC*)

L'analogie avec les circuits électriques peut se poursuivre avec les éléments fondamentaux de l'impédance pulmonaire. En effet, un modèle couramment utilisé pour décrire les dynamiques observées en VMC est le *RIC* qui se comporte comme un circuit *RLC* en série. Il s'agit d'un assemblage d'un terme dissipatif provenant de la résistance des voies aériennes à l'écoulement, un terme inertiel résultant du caractère instationnaire des écoulements et un terme de compliance émanant de l'élasticité du système respiratoire (Navajas et Farré, 1999; Pillow, 2005; Venegas et Fredberg, 1994). Il est aussi utilisé en VLT, où les effets inertiels deviennent plus importants (Bagnoli *et al.*, 2005; Costantino et Fiore, 2001). La

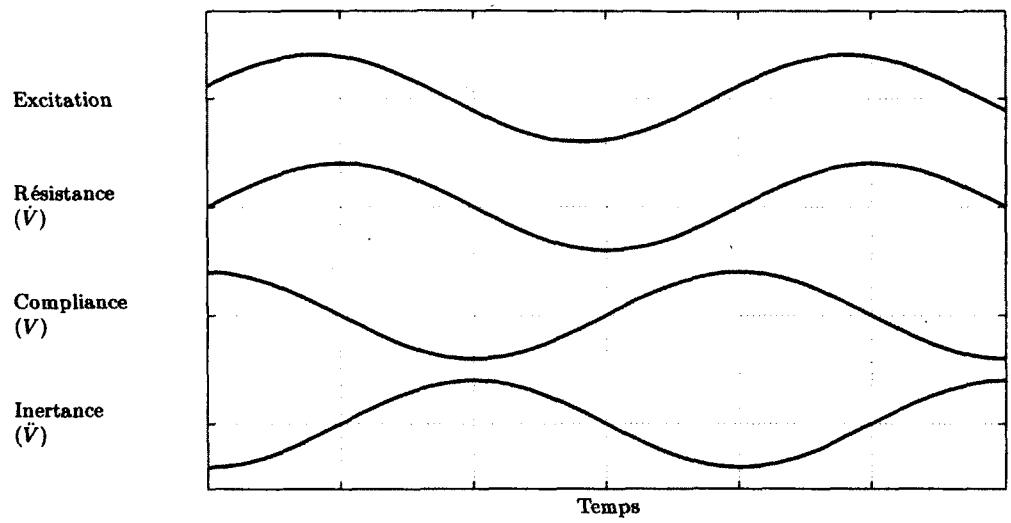

Figure 2.2 Relation de phase entre les éléments de d'un modèle simple d'impédance. La résistance est la contribution en phase avec le débit $\dot{V}$ alors que la compliance et l'inertance sont respectivement les contributions en phase avec le volume V et l'accélération $\ddot{V}$. Adaptée de (Lee *et al.*, 1999).

section 2.3.1 contient plus d'information sur l'état de l'art des mesures pulmonaires en VLT.

On peut représenter ce modèle sous forme d'un circuit électrique équivalent, montré à la figure 2.3.

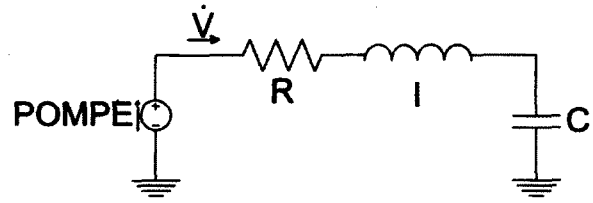

Figure 2.3 Schéma électrique équivalent du modèle RIC

Ainsi, l'impédance du système respiratoire avec ce modèle s'écrit

$$Z_{RS}(s) = \frac{I}{s}\left(s^2 + \frac{R}{I}s + \frac{1}{IC}\right), \tag{2.3}$$

où I est l'inertance pulmonaire, R est la résistance, C la compliance et s est la variable de Laplace ($s = j\omega + \sigma$). Ces trois éléments représentent donc respectivement une composante en phase avec l'accélération volumique, le débit volumique et le volume pulmonaire.

Des modèles d'impédances plus complexes ont été élaborés par différents auteurs et comparés par Ionescu et De Keyser (2008). Il s'agit pour la plupart de modèles d'ordres supérieurs

obtenus par différents assemblages des éléments simples R, I et C, un peu comme ce qui est décrit à la figure 2.3.

Modèle à déphasage constant

Cependant, la thèse de l'équipe de Ionescu montre que des modèles paramétriques d'ordre fractionnels représentent mieux la mécanique pulmonaire tout en réduisant le nombre de paramètres nécessaires(Ionescu et De Keyser, 2009; Ionescu *et al.*, 2010a). Ceci serait lié soit à la géométrie fractale de l'arbre pulmonaire (Ionescu *et al.*, 2010b, 2009b), ou encore à la viscoélasticité des tissus pulmonaire (Fredberg et Stamenovic, 1989; Suki *et al.*, 1994). Alors que la dernière interprétation prévaut actuellement dans les cercles des cliniciens et des physiologistes, l'explication de Ionescu rejoint la vision plus mathématique qui lie géométrie récursive et apparition d'opérateurs d'ordres non entiers (voir Mathieu et Oustaloup (1999), Annexe 2).

Hantos et ses collègues (Hantos *et al.*, 1992) sont parmi les premiers à proposer un tel modèle qui permet de décrire la dépendance fréquentielle de la partie réelle de l'impédance, ce qu'empêche un simple RIC. Son modèle revient à exprimer le RIC avec un terme de compliance à ordre fractionnel :

$$Z_{RS}(j\omega) = R_{aw} + j\omega I_{aw} + \frac{1}{(j\omega)^{\alpha} C} \tag{2.4}$$

où R_{aw} est un terme de résistance newtonienne liée aux voies respiratoires, I_{aw} est l'inertance associée à ces dernières, et C est la compliance d'ordre fractionnel. Afin de donner un sens physiologique, Hantos sépare les parties réelles et imaginaires du terme de compliance, et définit la viscance tissulaire

$$G = \frac{1}{C} \cos\left(\alpha \frac{\pi}{2}\right) \tag{2.5}$$

et l'élastance tissulaire

$$H = \frac{1}{C} \sin\left(\alpha \frac{\pi}{2}\right). \tag{2.6}$$

On obtient donc le modèle à déphasage constant [« *constant-phase model* » (CPM) en anglais], le modèle à ordre fractionnel le plus courant en VMC (Hantos *et al.*, 1992). Il vise à séparer les dynamiques appartenant aux voies aériennes centrales (avec R_{aw} et I_{aw}) de celles des régions périphériques (avec G et H). Il s'agit d'un modèle à quatre paramètres, soit

$$Z_{RS}(j\omega) = R_{aw} + j\omega I_{aw} + \frac{G - jH}{w^{\alpha}} \tag{2.7}$$

De (3.28) et (3.29), on obtient que la phase de G et H est liée par ω^{α}, où $\alpha = (2/\pi) \arctan(H/G)$.

Dans les faits, Yuan *et al.* (1998) et Thamrin *et al.* (2004) exposent que les paramètres R_{aw} et G sont fortement liés. Le modèle, même s'il arrive à décrire le comportement observé, ne permet donc pas toujours de bien séparer les dynamiques des voies aériennes centrales et périphériques, principalement dans les cas de pathologies pulmonaires bronchoconstrictives.

Modèle à deux ordres fractionnels

Par ailleurs, Ionescu et De Keyser (2009) proposent une amélioration du CPM en ajoutant un ordre fractionnaire au terme d'inertance, pour ainsi obtenir un modèle d'impédance pulmonaire à cinq paramètres :

$$Z_{RS}(j\omega) = R_{aw} + (j\omega)^{\beta}\mathcal{I}_{aw} + \frac{1}{(j\omega)^{\alpha}\mathcal{C}} \tag{2.8}$$

L'ajout de l'exposant β permet ainsi d'exprimer une dépendance en fréquence de la partie réelle de l'impédance à plus haute fréquence. Un tel modèle n'a jamais été employé auparavant pour décrire le mécanique respiratoire, ce qui soulève des questions quant au sens physique à apporter à ces exposants non entiers. Ionescu *et al.* (2010a) suggèrent qu'ils peuvent être liés à la pathophysiologie du système respiratoire.

2.1.4 Traitement des données

Analyse fréquentielle

Polak *et al.* (2006) décrivent clairement la procédure typiquement utilisée pour le traitement fréquentiel des signaux enregistrés lors d'un protocole de TOF. Les signaux de pression P et de débit $\dot{V}$ sont séparés en N_{seg} segments de durée T et fenêtrés afin d'en calculer les transformées de Fourier $\mathcal{F}(P)$ et $\mathcal{F}(\dot{V})$. Ceci permet de calculer des estimations des densités spectrales de puissance et d'interactions :

$$\hat{G}_{PP}(f) = \frac{2}{T}E\left[\mathcal{F}^{*}(P)\cdot\mathcal{F}(P)\right] \tag{2.9a}$$

$$\hat{G}_{\dot{V}\dot{V}}(f) = \frac{2}{T}E\left[\mathcal{F}^{*}(\dot{V})\cdot\mathcal{F}(\dot{V})\right] \tag{2.9b}$$

$$\hat{G}_{\dot{V}P}(f) = \frac{2}{T}E\left[\mathcal{F}^{*}(\dot{V})\cdot\mathcal{F}(P)\right] \tag{2.9c}$$

où E représente l'opérateur « espérance », et l'exposant $*$ indique le complexe conjugué. Ces autospectres et interspectres permettent d'avoir un estimé de la fonction de réponse

en fréquence du système $H_1(f)$ (équivalent ici à l'impédance), qui sera asymptotiquement non biaisé si du bruit non corrélé est seulement présent à la sortie (Bendat et Piersol, 1980).

$$Z_{RS}(f) = H_1(f) = \frac{\hat{G}_{\dot{V}P}(f)}{\hat{G}_{\dot{V}\dot{V}}(f)} \tag{2.10}$$

Finalement, la fonction de cohérence $\gamma^2(f)$ est l'indication la plus commune de l'acceptabilité des mesures et de l'hypothèse linéaire. Elle est en effet un indice du niveau de bruit et des non-linéarités du système (Bendat et Piersol, 1980).

$$\gamma^2(f) = \frac{\left|\hat{G}_{\dot{V}P}(f)\right|}{\hat{G}_{PP}(f)\hat{G}_{\dot{V}\dot{V}}(f)} \tag{2.11}$$

La limite d'acceptation de ce ratio est habituellement 0.95 (Bendat et Piersol, 1980; Lorino *et al.*, 1993). Certains auteurs rejettent toutefois ce critère d'acceptation des données, argumentant qu'il rend difficile, voire impossible, l'obtention de données fiables aux fréquences d'intérêt physiologique (Farre *et al.*, 1997; Maki, 1986).

2.2 La ventilation liquidienne totale

2.2.1 Description générale

Comme il a été vu en introduction, la ventilation liquidienne totale est une méthode de respiration assistée qui utilise les perfluorocarbones comme média pour assurer les échanges gazeux. Cette technique offre de nombreux avantages sur la ventilation mécanique conventionnelle (VMC), notamment la facilité à recruter les zones atélectasiées (ou collabées) des poumons, l'effet anti-inflammatoire des PFC (von der Hardt *et al.*, 2003) et la possibilité d'oxygéner un patient tout en pratiquant un lavage bronchoalvéolaire (Avoine *et al.*, 2011; Foust *et al.*, 1996; Marraro *et al.*, 1998).

Il existe deux principaux types de ventilation liquidienne, la VLP et la VLT. Dans le cas de la VLP, les poumons sont remplis à un certain niveau de PFC et l'oxygénation est assurée par un ventilateur gazeux (Hirschl *et al.*, 2002). En VLT, les poumons sont complètement remplis de PFC ce qui élimine l'interface air-liquide, permettant ainsi de bénéficier de tous les avantages de la ventilation liquidienne (Wolfson *et al.*, 1992). Le liquide est échangé, réoxygéné et réchauffé à l'aide d'un appareil dédié, un respirateur liquidien. Comme de tels appareils n'existent pas commercialement — la VLT étant encore au stade de recherche préclinique — chaque équipe doit disposer d'un prototype spécifique (Robert *et al.*, 2006).

Les deux aspects les plus distincts de la VLT en comparaison avec la ventilation mécanique conventionnelle sont donc l'emploi de ces liquides aux propriétés particulières, ainsi que le dispositif nécessaire pour assurer leur circulation. Ces deux éléments seront ainsi abordés ici dans l'optique d'une meilleure compréhension des travaux présentés et des résultats qui en sont issus.

2.2.2 Les perfluorocarbones

La ventilation liquidienne a vraiment débuté avec l'expérience de l'équipe de Gollan et Clark (1966), qui ont été les premiers à utiliser un perfluorocarbone comme médium respiratoire. De nombreux membres de cette famille de composés chimiques sont liquides à température ambiante, chimiquement et biochimiquement inertes, et possèdent une grande solubilité en oxygène et gaz carbonique (Wolfson et Shaffer, 2005). Ces propriétés les rendent idéaux pour la ventilation liquidienne. Deux liquides sont principalement utilisés par l'équipe Inolivent pour la ventilation liquidienne : le perfluorodécalin (PFDEC) et le perflubron (PFOB), schématisés à la figure 2.4. Comme le montre le tableau 2.1, ces PFC ont une densité près du double de celle de l'eau, mais une solubilité en O_2 et en CO_2 bien supérieures. On voit aussi que la densité et la viscosité des PFC sont très différentes de celles de l'air, ce qui suppose des dynamiques toutes autres pour les écoulements dans les voies respiratoires (Shashikant *et al.*, 2002).

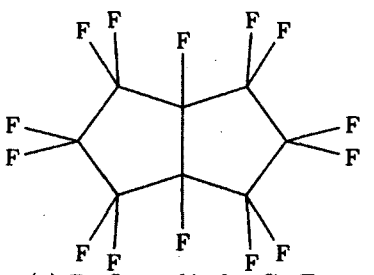

(a) Perfluorodécalin $C_{10}F_{18}$

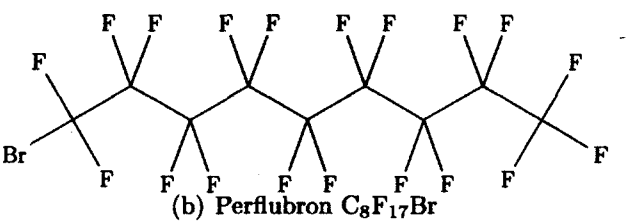

(b) Perflubron $C_8F_{17}Br$

Figure 2.4 Schémas de molécules de deux perfluorocarbones courants

Tableau 2.1 Propriétés de deux perfluorocarbones (Shaffer et Wolfson, 1992) (l'air et l'eau sont ajoutés à titre de comparaison (Lowe, 1991; White, 2008))

	Air	**Eau**	**PFDEC**[a]	**PFOB**[b]
Formule chimique	$N_2 + O_2 + \ldots$	H_2O	$C_{10}F_{18}$	C_8BrF_{17}
Poids moléculaire (uma)	29	18	462	499
Point d'ébullition (°C)	≈ -193	100	142	143
Densité à 25 °C (g/ml)	1.8×10^{-3}	0.997	1.95	1.93
Viscosité cinématique à 25 °C (cSt)	15.0	0.893	2.90	1.1
Pression de vapeur à 37 °C (kPa)	N/A	3.29	1.87	1.47
Tension de surface à 25 °C (N/m)	N/A	0.072	0.015	0.018
Solubilité en O_2 à 25 °C (%vol)	N/A	2.5	49	53
Solubilité en CO_2 à 37 °C (%vol)	N/A	65	140	210

[a] : Perfluorodécalin

[b] : Perflubron

2.2.3 Prototype Inolivent-4

Composantes de l'appareil

Le 4[e] prototype Inolivent est présenté à la figure 2.5. Il s'agit de l'évolution du dernier modèle (Robert *et al.*, 2006) dans le but de s'approcher d'une version acceptable pour mener des essais cliniques. Il est composé de deux pompes à piston pour assurer la circulation du PFC dans et hors des poumons et d'un système de filtration-oxygénation-chauffage afin de conditionner le PFC à être inspiré. Un condenseur recueille les vapeurs de PFC afin d'en limiter les pertes. Le liquide est dirigé par quatre valves à écrasement (« *pinch valves* »), et le tout est contrôlé par une station temps-réel tournant à 1 kHz (xPC Target, Mathworks, USA). Un second PC sert à l'affichage et au contrôle de l'appareil au moyen d'un écran tactile et d'une interface conçue sur mesure pour s'apparenter à celle d'un respirateur mécanique conventionnel. En plus de l'utilisation de composantes mieux adaptées à une utilisation clinique, le contrôle en pression de l'expiration, afin d'éliminer les collapsus respiratoires et d'augmenter les volumes/minute (Robert *et al.*, 2009a), est l'innovation la plus importante sur cette version.

Description d'un cycle de ventilation typique

Un cycle de ventilation liquidienne typique se découpe en quatre étapes principales : l'inspiration, la pause de fin d'inspiration, l'expiration et la pause de fin d'expiration. Le tableau 2.2 montre le comportement du prototype à chacune de ces étapes. Une description plus exhaustive de celles-ci et du fonctionnement des contrôleurs a été présentée par Robert *et al.* (2010).

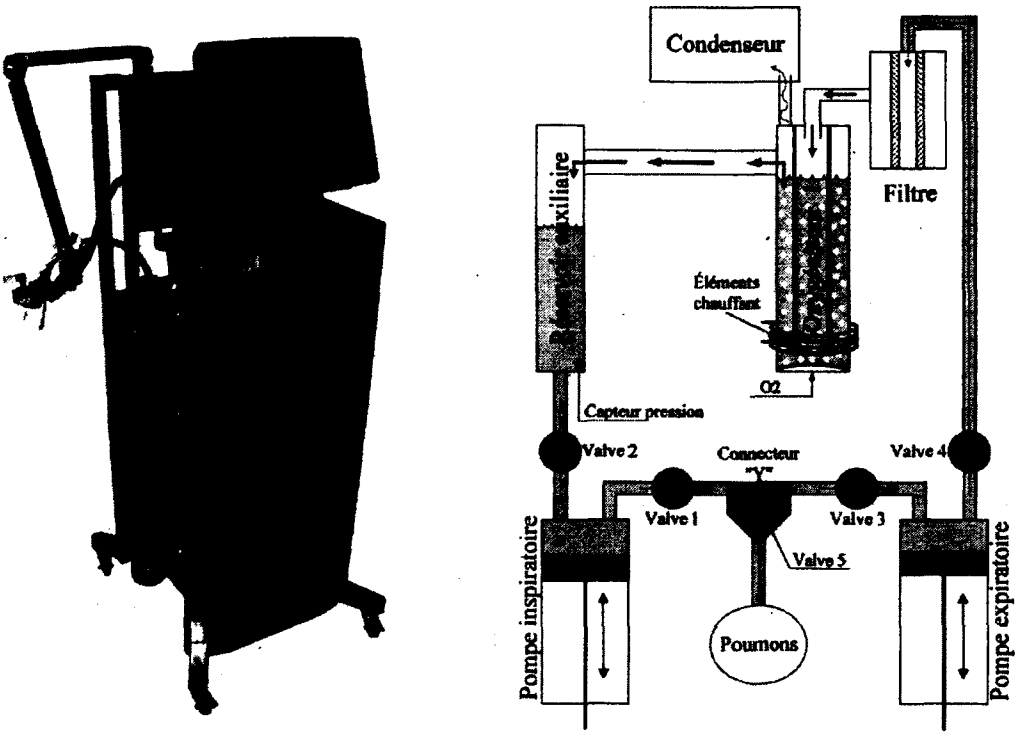

(a) Photographie (b) Schéma du circuit fluide

Figure 2.5 Représentations du dernier prototype de l'équipe : Inolivent-4

Tableau 2.2 Description d'un cycle de ventilation typique

	Pompe d'inspiration	Pompe d'expiration	Pression à la trachée (P_{aw})
Inspiration	Se vide dans le patient en suivant un profil volumique défini	Se vidange dans le système de filtration et d'oxygénation	Varie en fonction du débit imposé par la pompe d'inspiration
Pause de fin d'inspiration	-	-	Mesure de la PEIP[a] (≈ 15 cmH_2O)
Expiration	Se remplit de PFC propre et oxygéné à partir du réservoir tampon	Retire le PFC du patient en maintenant la pression P_{aw} constante	Contrôlée pour être fixe à la pression de référence définie par le clinicien
Pause de fin d'expiration	-	-	Mesure de la PEEP[b] (≈ 5 cmH_2O)

[a] : Positive end-inspiratory pressure

[b] : Positive end-expiratory pressure

Capteurs, acquisition et traitement des signaux

La mesure de la pression se fait à l'extrémité proximale du tube endotrachéal au moyen d'un cathéter métallique rempli de PFC et relié au capteur (Model 1620, Measurment Specialties, USA) par de la tubulure flexible. Le cathéter est bouché à son extrémité et muni de quatre prises de pression radiales pour mesurer la pression statique. La mesure du volume des pompes et l'estimation du débit se font quant à elles à partir de la position des pistons à l'aide d'un capteur de position linéaire (C-Series, MTS Temposonics, USA).

Les systèmes auxiliaires sont aussi munis de nombreux capteurs assurant leur bon fonctionnement. Le mélangeur des gaz dispose d'un débitmètre gazeux pour chacun des gaz, d'un capteur de concentration d'O_2 dans le gaz à être bullé. Les températures de PFC dans l'oxygénateur et le réservoir tampon sont aussi mesurées, ainsi que le niveau de liquide dans ce dernier. Finalement, la température du condenseur est aussi mesurée, car elle est régulée pour éviter la formation de givre en fonction du type de PFC.

Les signaux sont acquis sur une carte d'acquisition 16 bits (PCI-6225, National Instruments, USA) à une fréquence de 1 kHz, puis sous-échantillonnés à 50 Hz pour l'enregistrement. Comme les signaux de pression et de volume seront utilisés pour des analyses fréquentielles, on s'assure d'éviter le repliement spectral en les filtrant (Butterworth 6^e ordre, fréquence de coupure à 10 Hz) avant ce sous-échantillonnage. Les commandes envoyées aux pompes, valves et autres actionneurs du prototypes sont délivrées par une carte de sortie analogique 16 bits (PCI-DAC6702, Measurement Computing, USA).

2.3 Dynamiques propres à la VLT

2.3.1 Dynamiques du système respiratoire

Jusqu'à maintenant, la dynamique respiratoire en ventilation liquidienne totale n'est pas encore aussi bien connue qu'en ventilation gazeuse traditionnelle. Présentement, la majorité des équipes ont mis en place des méthodes pouvant mesurer la compliance pulmonaire et la résistance pulmonaire. Voici un survol de la mesure de ces deux grandeurs en VLT. Même si d'aucuns considèrent que les effets inertiels deviendront importants en VLT, il n'existe pas à ce jour de procédure standardisée pour mesurer l'inertance. C'est pourquoi une description de cette dernière est introduite à la section 2.3.2 avec d'autres éléments ayant trait aux écoulements instationnaires. Ensemble, ces trois grandeurs forment les éléments d'un modèle pulmonaire *RIC*, comme présenté à la section 2.1.3. Ce modèle est celui qui prévaut actuellement en VLT.

Estimation de la compliance

La compliance dynamique est évaluée à chaque cycle respiratoire selon (2.12) en utilisant directement la pression trachéale P_{aw} aux pauses (Gómez *et al.*, 2005; Robert, 2007).

$$C_{dyn} = \frac{V_T}{PEIP - PEEP} \tag{2.12}$$

où V_T est le volume courant (le volume de liquide échangé au cours d'un cycle normal), $PEIP$ (pour «*Positive End-Inspiratory Pressure*») est la pression mesurée au plateau de fin d'inspiration, et $PEEP$ (pour «*Positive End-Expiratory Pressure*») est celle mesurée à la pause de fin d'expiration. Par opposition, la compliance statique se calcule de façon identique, mais nécessite de plus longues pauses (typiquement 3 s) afin de s'assurer que l'écoulement de PFC dans les voies aériennes est bien nul. Elle ne peut donc pas être réalisée à chaque cycle, mais plutôt sur demande du clinicien.

Il convient de noter que la procédure de mesure de la compliance en VLT est identique à la méthode couramment utilisée en ventilation mécanique conventionnelle (Blom, 2004; Pilbeam et Cairo, 2006). Toutefois, en raison notamment de la faible tension de surface des PFC, la compliance observée en VLT est sensiblement plus élevée qu'en ventilation gazeuse (Alvarez *et al.*, 2009; Costantino et Fiore, 2001; Hirschl, 2004).

Estimation des résistances

La résistance est l'autre paramètre dynamique communément mesuré en VLT. Il s'agit du rapport pression/débit quand ces deux quantités sont en phase. On retrouve plusieurs approches pour la mesurer. Gómez *et al.* (2005) utilisent la technique proposée par Mead et Whittenberger (1953) :

$$R_{aw} = \frac{P_{ins} - P_{exp}}{\dot{V}_{ins} + \left|\dot{V}_{exp}\right|} \tag{2.13}$$

Cette résistance est calculée pour un volume pulmonaire donné, en mesurant la pression et le débit à ce volume durant la phase d'inspiration (P_{ins} et $\dot{V}_{ins}$ respectivement) et la phase d'expiration (P_{exp} et $\dot{V}_{exp}$). La résistance à l'inspiration, où le débit est très élevé, et celle à l'expiration, où le débit est plus lent, sont donc confondues dans une seule et même quantité alors qu'on s'attend à une bonne différence entre les deux en VLT (Alvarez *et al.*, 2009).

D'autres auteurs utilisent le travail de respiration (*work of breathing*) pour quantifier la résistance moyenne au cours d'un cycle (Larrabe *et al.*, 2001). Cette dernière approche se sert de l'aire de la boucle obtenue en traçant la pression en fonction du volume, la courbe

$P-V$, ainsi que de l'intégrale de $\dot{V}^2(t)$ dans le temps d'un cycle. Le principal avantage de cette méthode de calcul est qu'elle permettrait une mesure de résistance plus indépendante de la compliance que la première technique présentée (Alvarez *et al.*, 2009). Le caractère moyenné de cette approche la rend encore une fois moins pertinente en VLT en raison des importantes variations de débit au cours d'un cycle. Et encore ici, l'utilisation du carré du débit implique une connaissance précise de cette quantité.

Une dernière approche a été développée au sein de l'équipe (Robert *et al.*, 2009a) et considère la non-linéarité de la résistance sous la forme

$$R_{aw,NL} = R_1 + R_2\dot{V} \tag{2.14}$$

où R_1 et R_2 sont identifiés lors de l'expiration, par exemple à l'aide d'un algorithme des moindres carrés récursif. La technique est encore une fois inspirée de ce qui se fait en gazeux (Lauzon et Bates, 1991) mais avec un modèle ici adapté à la ventilation liquidienne. Cette approche a l'avantage de pouvoir fournir les paramètres en continu en plus de donner une bonne idée du degré de linéarité de la résistance pulmonaire. Cette linéarité est souvent supposée dans les modèles pulmonaires mais rarement quantifiée. Par contre, le temps de convergence de l'algorithme doit être savamment étudié avant de pouvoir analyser les données qui en sont issues, et les paramètres identifiés sont souvent bruités.

Comme pour la compliance, les propriétés des PFC donnent des valeurs de résistance beaucoup plus grandes en VLT qu'en VMC (Alvarez *et al.*, 2009; Costantino et Fiore, 2001). En effet, la viscosité dynamique de perfluorodécalin est environ 200 fois plus élevée que celle de l'air comme le montrent les données du tableau 2.1, ce qui nécessitera nécessairement des gradients de pression plus grands pour un même débit.

2.3.2 Dynamique des écoulements oscillants

Étant donné la nature même de la TOF, les écoulements oscillants seront omniprésents tout au long du projet. Un traitement analytique de ces derniers sera par conséquent utile que ce soit lors de l'étude du débitmètre instationnaire où lors de la conception de montages *in vitro* pour valider la TOF. De plus, c'est la non-stationnarité des écoulements qui amène le terme d'inertance dans les modèles pulmonaires *RIC*.

Concept d'inertance

L'inertance est définie comme la pression nécessaire pour faire accélérer un fluide sans tenir compte des effets visqueux $\left(I = P/\ddot{V}\right)$. Toutefois, cette grandeur n'est que peu ou pas

utilisée en clinique car sa valeur diagnostique demeure controversée et difficile à déterminer (Schmalisch *et al.*, 2005). On la retrouve tout de même dans certains modèles pulmonaires utilisées pour des fins de recherche à la fois en VLT et en ventilation gazeuse (Alvarez *et al.*, 2009; Bagnoli *et al.*, 2005). L'expression suivante est typiquement utilisée pour calculer l'inertance I d'une conduite circulaire.

$$I = \frac{\rho L}{A} \tag{2.15}$$

où L est la longueur de la conduite et A sa section. On voit tout de suite que la densité 1000 fois plus grande du médium de ventilation donnera un terme d'inertance aussi 1000 fois plus grand, et donc que les effets inertiels sont appelés à jouer un rôle plus important en VLT. On peut estimer la grandeur de l'inertance en prenant l'équation précédente et en l'appliquant à un modèle physiologique des poumons, comme celui décrit par Weibel (Weibel, 1963). Cependant, il est important de garder en tête qu'il s'agit d'une expression *simplifiée*, dérivée des hypothèses d'écoulement non visqueux et non stationnaire. L'utilisation de cette expression en conjonction avec un terme résistif dérivé pour un écoulement visqueux et stationnaire représenterait donc une approche inconsistante (Morris et Forster, 2004).

Modélisation des écoulements oscillants

Ainsi, un modèle qui considère les effets dissipatifs et inertiels dans une seule et même équation pourrait donner de meilleures prédictions, toujours selon Morris et Forster. La modélisation des écoulements instationnaires est un sujet de recherche bien vivant depuis les travaux de Lambossy (1952) et Womersley (1955), qui ont proposé une solution analytique exacte des équations de Navier-Stokes pour des écoulements développés, laminaires et incompressibles sous un gradient de pression périodique. Schlichting (1979) présente les résultats obtenus pour des écoulements en canal rectangulaire et en conduite circulaire. Seule cette dernière sera rapportée ici. Si le gradient de pression appliqué est de forme $\partial P/\partial x = \Re\{K \exp(j\omega t)\}$, la vitesse en tout point du tube sera

$$u(r,t) = \Re\left\{\frac{K}{\rho j\omega}\exp(j\omega t)\left[1 - \frac{J_0\left(r\sqrt{-j\omega/\nu}\right)}{J_0\left(R\sqrt{-j\omega/\nu}\right)}\right]\right\}. \tag{2.16}$$

La quantité $\mathrm{Wr} = R\sqrt{\omega/\nu}$, connue comme le nombre de Womersley (mais initialement proposé par Lambossy), est un nombre sans dimension qui décrit l'importance des effets instationnaires pour un écoulement donné. Quand Wr est petit (1.32 ou moins (Çarpinlio-

glu et Yasar Gündogdu, 2001)), la fréquence des pulsations est suffisamment faible pour qu'un profil de vitesse parabolique ait le temps de se former à chaque cycle, donc l'écoulement sera en phase avec le gradient de pression. Quand Wr est grand (10 ou plus), le profil de vitesse est relativement plat et le débit moyen est en retard d'environ 90° avec le gradient de pression. Un cas intermédiaire (Wr=5) est présenté à la figure 2.6. On y voit aussi l'apparition de l'effet « annulaire » où l'écoulement est plus rapide près des parois qu'au centre du tube.

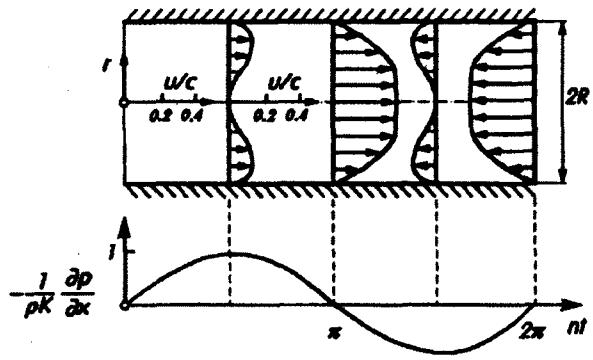

Figure 2.6 Représentation des profils de vitesse pour un écoulement oscillant de Wr=5 (Schlichting, 1979).

Certains auteurs ont utilisé (2.16) et les données d'un modèle morphologique pour calculer un terme d'inertance qui dépend de la fréquence pour chaque génération de l'arbre pulmonaire (Ionescu *et al.*, 2010c). Bien que l'approche semble également prometteuse en VLT, son application directe ne reproduit pas bien les données expérimentales. Dans le cadre du projet de maîtrise présenté, c'est donc pour la mesure des débits instationnaires dans des conduites rectilignes à section constante que l'utilité d'une telle modélisation s'est avérée.

Mesure des débits pulsés

Pour un écoulement laminaire, on peut injecter une valeur de gradient de pression mesuré dans (2.16) et intégrer la vitesse sur le rayon pour obtenir une mesure plus précise du débit lors des accélérations brusques ou des oscillations (Brereton *et al.*, 2006). De la même façon, si seulement la vitesse au centre de la conduite est connue, on peut retrouver la vitesse en chaque point radial pour calculer le débit de façon plus précise que de simplement supposer un profil *a priori* (Brereton *et al.*, 2008; Durst *et al.*, 1996; Uchiyama et Hakomori, 1983).

Une autre approche pour mesures des débits instationnaires est d'implanter un élément déprimogène dans l'écoulement fluide et de mesurer la différence de pression de part et d'autre. Il s'agit donc de débitmètres différentiels, mais dont l'équation caractéristique pour lier débit et différence de pression doit être modifiée pour faire intervenir les ef-

fets inertiels. Par exemple, si l'élément déprimogène est un venturi assez important pour pouvoir négliger les effets visqueux, l'équation de Bernoulli instationnaire permet d'en arriver à une première estimation des différences de pression attendues (White, 2008). Après quelques manipulations ceci donne la relation compacte (2.17), dont la solution fournira la débit instantané

$$A\frac{dq(t)}{dt} + B|q(t)|q(t) = \frac{\Delta p(t)}{\rho} \tag{2.17}$$

où Δp est la différence de pression entre l'entrée et le col, et A et B sont deux paramètres tirés de la géométrie du dispositif :

$$A = \int_{x_1}^{x_2} \frac{dx}{S(x)} \tag{2.18}$$

$$B = \frac{1}{2}\left(\frac{1}{S_2^2} - \frac{1}{S_1^2}\right). \tag{2.19}$$

Comme cette relation est utilisée pour mesurer des écoulements bidirectionnels, le terme $q^2(t)$ doit être sensible aux changements de direction, en le remplaçant par $|q(t)|q(t)$ (Catania et Ferrari, 2009; Foucault *et al.*, 2005).

Il existe un dispositif breveté (Foucault *et al.*, 2005) qui utilise ce principe et pourrait être adapté aux besoins de l'équipe Inolivent. Une schématisation de l'appareil est montrée à la figure 2.7.

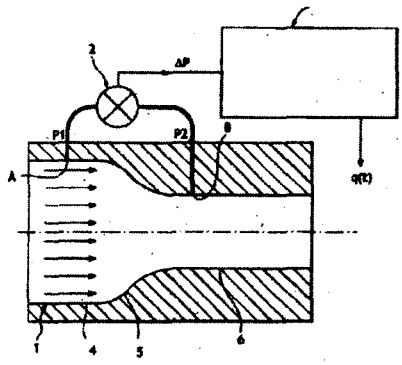

Figure 2.7 Schéma du principe du débitmètre instationnaire, ici montré avec un convergent comme organe déprimogène (Foucault *et al.*, 2005).

Pour conclure, notons qu'il est difficile d'inclure l'effet venturi à un modèle analytique d'écoulement instationnaires semblable à (2.16) : cette dernière solution analytique des équations de Navier-Stokes peut être obtenue pour un écoulement développé et incompressible dans des conduites de section uniforme, ce qui annule le terme d'advection $(\mathbf{v}\cdot\boldsymbol{\nabla})\,\mathbf{v}$. En ajoutant un changement de section, le problème devient passablement plus compliqué.

CHAPITRE 3

Matériel et méthodes

3.1 Article : «Un débitmètre pour les mesures d'écoulements instationnaires liquides»

3.1.1 Avant-propos

Auteurs et affiliation : A. Beaulieu : Étudiant à la maîtrise, Université de Sherbrooke, Faculté de génie, Département de génie mécanique.

E. Foucault : Maître de Conférence, Université de Poitiers - ENSMA - CNRS, Département Fluides, Thermique, Combustion, Labo Pprimme.

P. Brault : Ingénieur d'Études, Université de Poitiers - ENSMA - CNRS, Département Fluides, Thermique, Combustion, Labo Pprimme.

P. Szeger : Ingénieur de Recherche, Université de Poitiers - ENSMA - CNRS, Département Fluides, Thermique, Combustion, Labo Pprimme.

P. Micheau : Professeur titulaire, Université de Sherbrooke, Faculté de génie, Département de génie mécanique.

Date de soumission : 24 août 2010

Date d'acception : 31 janvier 2010

État de l'acceptation : Accepté pour publication

Revue : Flow Measurement and Instrumentation

Titre français : Un débitmètre pour les mesures d'écoulements instationnaires liquides

Contribution au document : Cet article contribue au mémoire en décrivant le dispositif conçu pour répondre au premier objectif spécifique du projet de maîtrise : la mesure du débit instantané à la trachée. Un prototype a été conçu et fabriqué dans le cadre du projet de maîtrise, à l'Université de Sherbrooke. L'article résulte principalement du travail de validation réalisé à l'automne 2009 au Laboratoire d'Études Aérodynamiques de l'Université de Poitiers.

Résumé français : Un débitmètre instationnaire a été développé pour le prototype de ventilateur liquidien Inolivent-4. Le concept proposé consiste en un venturi symétrique comprenant trois prises de pression. La mesure du débit est obtenue en résolvant numériquement l'équation de Bernoulli légèrement modifiée. Un prototype a été validé expérimentalement en appliquant des débits sinusoïdaux de moyenne nulle. La caractérisation à basse fréquence a fourni le coefficient de décharge en fonction du nombre de Reynolds, et des essais à plus haute fréquence ont fixé la bande passante utile du capteur. Les profils de vitesse ont été mesurés dans le venturi par vélocimétrie par imagerie de particules (PIV), et le dispositif a été calibré expérimentalement par comparaison avec un débitmètre ultrasonore et la mesure d'une pompe à piston. Les résultats ont montré que les écoulements quasi stationnaires sont mesurés précisément entre 5 ml/s et 60 ml/s, et les oscillations de faible amplitude ($\leq$10 ml/s) sont correctement mesurés pour des fréquences sous 3 Hz. Finalement, les expérimentations PIV ont montré que l'hypothèse des profils de vitesse plats, requise pour une solution simple de l'équation du débitmètre, est valide dans la plage d'opération.

Note : Le contenu rapporté est identique à la version publiée.

A Flowmeter for Unsteady Liquid Flow Measurements

A. Beaulieu[a], E. Foucault[b], P. Braud[b], P. Micheau[a], P. Szeger[b]

[a] *Département de génie mécanique - Université de Sherbrooke, Sherbrooke (Québec), J1K 2R1, Canada*

[b] *Institut Pprime CNRS - Université de Poitiers - ENSMA Département Fluides, Thermique, Combustion - SP2MI Boulevard Marie et Pierre Curie, BP 30179, F86962 Futuroscope Chasseneuil Cedex, France*

Abstract

An unsteady flowmeter was developed for implementation in the Inolivent-4 total liquid ventilator prototype. The proposed design consists of a symmetrical venturi tube comprising three pressure sensors and in which flow measurement is obtained by numerically solving a slightly modified version of the unsteady Bernoulli equation. A prototype was validated experimentally by applying zero-mean sinusoidal flows. Low-frequency characterization determined the venturi discharge coefficient as a function of the Reynolds number, and higher-frequency ($\leq$4 Hz) measurements determined the applicable bandwidth of the device. The velocity profiles were measured in the venturi by particle image velocimetry (PIV), and the device was calibrated experimentally by comparison with an ultrasonic flowmeter and measurements from a piston pump. Results showed that quasi-steady flows could be accurately measured in the 5 ml/s–60 ml/s range, while low-amplitude ($\leq$10 ml/s) oscillatory flows were well measured for frequencies below 3 Hz. Finally, PIV experiments showed that the flat velocity profile assumption required for a simple solution of the flowmeter equation was valid within the operating range.

Keywords: Unsteady flows, Venturi, Total Liquid Ventilation, Perfluorocarbons, Medical devices,

Nomenclature

A, B	Flowmeter geometric parameters
C^{st}	Arbitrary constant
C_v	Venturi discharge coefficient
f	Frequency
$G_{x,y}(f)$	Cross-power spectrum between x and y
$H(f)$	Frequency response function
j	Imaginary unit $= \sqrt{-1}$
J_0	Zero order Bessel function of the first kind
K	Arbitrary complex constant
n_d	Number of averaged segments
P	Pressure
q	Volume flow
r	Radial coordinate
R	Duct radius
Re	Reynolds Number $= \frac{2q}{\pi R\nu}$
S	Cross-section area
t	Time
u	Velocity
V	Volume
Wr	Womersley Number $= R\sqrt{\omega/\nu}$
x	Axial coordinate
β_0, β_1	Discharge coefficient parameters
ΔP	Pressure difference
γ^2	Coherence function
μ	Fluid dynamic viscosity
ν	Fluid kinematic viscosity
ω	Angular frequency $= 2\pi f$
ρ	Fluid density
φ	Velocity potential

Subscripts

1,2,3	Related to one of the three pressure sensors
p	Related to the piston pump
piv	Related to particle image velocimetry
st	Evaluated using steady assumptions
thr	Evaluated at venturi throat
uns	Evaluated by the unsteady model
us	Related to ultrasonic measurements
v	Related to the venturi

Superscripts

c	Corrected value
m	Indicates a measurement
p	Indicates a prediction

Other symbols

$\hat{(\ )}$	Estimate of quantity ( )
$\bar{(\ )}$	Mean of quantity ( )
$\Re(\ )$	Real part of complex quantity ( )
$\mathcal{U}(\ )$	Standard uncertainty on variable ( )

3.1.2 Introduction

Total liquid ventilation (TLV) is a respiratory support technique in which blood oxygenation and carbon dioxide elimination are ensured by a liquid media – typically a perfluorocarbon (PFC) – instead of a gas (Wolfson *et al.*, 1998). Liquid ventilator development is an active field of research, as most components cannot be directly imported from gas ventilators and must be completely redesigned. According to most active teams in TLV (Costantino *et al.*, 2009), liquid ventilators must provide a reliable measurement of the liquid flow in and out of the lungs.

During a typical TLV respiratory cycle, both the inspiratory and the expiratory flows exhibit acceleration and deceleration phases, hence the flowmeter must take into account these unsteady effects to produce accurate measurements. Moreover, concomitant works involving measurement of the respiratory system mechanical impedance using sinusoidal flow oscillations of frequencies up to 2 Hz and 7.5 ml/s amplitude (Bossé *et al.*, 2010) are currently ongoing. This method is the forced oscillation technique (FOT) and requires a reliable measurement of the associated low-amplitude pulsating flows. In addition to an adequate frequency response and the ability to measure laminar and turbulent bidirectional flows, the application context also poses a number of design constraints such as being sterilizable or disposable, low cost, exhibit a fail-safe operation or redundancy as well as small physical dimensions. Flow measurement by means of a venturi tube is well known and has the potential to comply with the above criteria.

The venturi principle first needed be adapted to unsteady flow conditions. Thus, a new flowmeter equation, developed using the methodology proposed in (Foucault *et al.*, 2005), had to be slightly modified because of the present use of three pressure sensors. Furthermore, there is no theoretical evidence that the hypotheses required for the development of the equations hold for all flow conditions encountered by the prototype. These hypotheses must therefore be validated experimentally or correctly compensated.

An analogous approach had already been developed for automotive engine intake measurements (Foucault *et al.*, 2005), in the simpler case when viscosity effects were neglected. Other authors developed a similar momentum balance technique based on pressure gradient measurement in a high-pressure hydraulic pipeline application, where compressibility effects and wave travel speeds had to be taken into account (Catania et Ferrari, 2009). On the other hand, for laminar and incompressible unsteady flows, some authors used an analytical flow model to enhance flow measurements obtained from pressure gradient (Brereton *et al.*, 2006) or centerline velocity (Brereton *et al.*, 2008; Durst *et al.*, 1996;

Uchiyama et Hakomori, 1983). These latter centerline velocity methods use laser Doppler velocimetry which implies high setup costs, while other velocimetry methods such as hot wire (Durst *et al.*, 2007) can be difficult in the presence of mucus or other impurity deposits. Consequently, the the design of the method herein focused on pressure measurement-based approaches. A critical review on pulsatile pipe flow studies can be found in (Çarpinlioglu et Yasar Gündogdu, 2001).

The present report focuses on the development of a flowmeter and an algorithm destined to be implemented in total liquid ventilators as well as the experimental approach used for its validation with unsteady flows.

The objectives of this study are

1. to select and validate an analytical model for retrieving flow from the measured pressure difference,
2. to assess the performances of the flowmeter for steady flows,
3. to determine the bandwidth of the device for low amplitude oscillating flows.

The originality of this document resides in that, by utilizing a typical venturi with the unsteady Bernoulli relation, this principle is adapted to measurement of partially developed flows with laminar to turbulent Reynolds numbers, either quasi-steady or oscillating.

3.1.3 Description of the prototype

Concept and components

The concept of a symmetrical unsteady venturi flowmeter, with three pressure sensors, was explored for this application. A schematic drawing of the prototype is shown in figure 3.1. The prototype was constructed of clear polycarbonate, and was vapor polished to enhance

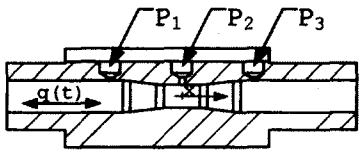

Figure 3.1 Scaled drawing of the unsteady venturi flow meter. Gray arrow indicates positive velocity direction. Major diameter is 5.5 mm, diameter ratio is 0.73, and overall length is 60 mm.

its optical properties for particle image velocimetry (PIV) measurements. The endotracheal tube is attached to the right of the device, and the left side fitting is to be bonded to the

liquid ventilator's wye-piece (see (Robert *et al.*, 2006) for a description of the ventilator's main components). The device comprises three medical grade pressure sensors (Model 1620, Measurement Specialties Inc., USA), allowing to measure the pressure difference between the entrance and the throat, regardless of flow direction, while simultaneously measuring gauge pressure near the upper airways for ventilator control purposes.

Modeling

The usual unsteady Bernoulli equation for an irrotational, constant density flow in the absence of gravity effects (White, 2008) is

$$\frac{\partial\varphi(x,r,t)}{\partial t} + \frac{1}{2}u^2(x,r,t) + \frac{P(x,r,t)}{\rho} = C^{st} \tag{3.1}$$

where φ is a velocity potential, $u(x,r,t)$ is the time varying velocity field, $P(x,r,t)$ is the pressure field and C^{st} a constant.

If a uniform (or flat) 1D velocity profile is assumed, $u(x,r,t) \approx \overline{u}(x,t)$ and the volume flow becomes

$$q_v(t) = S(x)\overline{u}(x,t) \tag{3.2}$$

where $\overline{u}(x,t)$ is the time-varying flow speed (section-averaged velocity) and $S(x)$ is the tube section versus axial position.

Equation 3.1 could then be evaluated at two axial positions, say x_1 at the entrance and x_2 at the throat of the venturi, so that

$$\varphi(x,t) = q_v(t)\int_{x_1}^{x_2}\frac{dx}{S(x)}, \tag{3.3}$$

and the unsteady Bernoulli relation can be expressed in terms of flowrate and differential pressure:

$$\frac{dq_v(t)}{dt}\int_{x_1}^{x_2}\frac{dx}{S(x)} + \frac{q_v^2(t)}{2}\left(\frac{1}{S_2^2} - \frac{1}{S_1^2}\right) + \frac{P_2(t) - P_1(t)}{\rho} = 0. \tag{3.4}$$

This shows that the relation between differential pressure is only governed by the fluid's density and two geometric parameters,

$$A = \int_{x_1}^{x_2}\frac{dx}{S(x)} \tag{3.5}$$

$$B = \frac{1}{2}\left(\frac{1}{S_2^2} - \frac{1}{S_1^2}\right) = \frac{1}{2}\left(\frac{1}{S_2^2} - \frac{1}{S_3^2}\right). \tag{3.6}$$

Since this relation is used for measuring bidirectional oscillating flows, the $q_v^2(t)$ term has to be direction-sensitive, and is replaced by $|q_v(t)|q_v(t)$ (Catania et Ferrari, 2009; Foucault *et al.*, 2005). This yields the compact differential relation (2.17), of which the solution gives the instantaneous flowrate.

$$A\frac{dq_v(t)}{dt} + B|q_v(t)|q_v(t) = \frac{\Delta P(t)}{\rho} \tag{2.17}$$

where ΔP is the pressure difference between the throat and the entrance (or between the other entrance and the throat depending on the direction of the flow). When unsteady effects are negligible, this difference has to be positive for forward flows (as defined in in figure 3.1) and negative for reverse flows.

3.1.4 Oscillating flows theory

Unsteady flow modeling and measurement is an active field of study since the work of Lambossy (Lambossy, 1952) and Womersley (Womersley, 1955) who proposed an exact analytical solution to the Navier-Stokes equation for laminar and incompressible pipe flow undergoing periodic pressure gradient $\partial P/\partial x = \Re\{K\exp(j\omega t)\}$:

$$u(r,t) = \Re\left\{\frac{K}{\rho j\omega}\exp(j\omega t)\left[1 - \frac{J_0\left(r\sqrt{-j\omega/\nu}\right)}{J_0\left(R\sqrt{-j\omega/\nu}\right)}\right]\right\}. \tag{2.16}$$

The quantity $\mathrm{Wr} = R\sqrt{\omega/\nu}$, known as *Womersley Number*, denotes the phase lag between pressure gradient and flow. When Wr is small (1.32 or less (Çarpinlioglu et Yasar Gündogdu, 2001)), the frequency of pulsations is sufficiently low that a parabolic velocity profile has time to develop during each cycle, thus the flow will be very nearly in phase with the pressure gradient. When Wr is large (10 or more), the velocity profile is relatively flat or plug-like and the mean flow lags the pressure gradient by about 90 degrees. However, when the flow is turbulent (Re over 2300), the time averaged velocity profile in pipes remains approximately flat even if the Womersley number is relatively small.

3.1.5 Numerical exploration of unsteadiness effects

Numerical application of equation 2.17 allows to determine the conditions for which the consideration of the unsteady effect is mandatory. The modeled differential pressure was calculated, with $A = 795.1\ \mathrm{m}^{-1}$ and $B = 2.281 \times 10^9\ \mathrm{m}^{-4}$ according to the experimental

device described in section 3.1.3. Flow calculation neglecting unsteady effects, q_{st}, was evaluated by

$$q_{st}(t) = \mathrm{sgn}\big(\Delta P(t)\big)\sqrt{\frac{|\Delta P(t)|}{\rho B}} \tag{3.7}$$

where

$$\mathrm{sgn}\big(\Delta P(t)\big) = \begin{cases} 0 & \text{if } \Delta P = 0 \\ \frac{\Delta P}{|\Delta P|} & \text{else} \end{cases} \tag{3.8}$$

and $q_{uns}(ft)$ was evaluated by solving (2.17).

In order to characterize the influence of the unsteady effects, the complex ratio $q_{uns}(f)/q_{st}(f)$ was calculated at the fundamental frequency of each numerical experiment. This ratio was obtained using the standard weighted-overlapped segment averaging (WOSA) procedure (50% overlapped hamming windows, 10 s segments of 2048 samples each) (Bendat et Piersol, 1980). Results are reported in table 3.1 in terms of modulus (the ratio of the amplitudes) and phase shift between the two signals. An acceptable error for the steady model was defined as a modulus higher that 0.95 and a phase shift of less than 10°.

Tableau 3.1 Predicted behavior of the ratio q_{uns}/q_{st} at the fundamental frequency (expressed as modulus∠phase shift). Bold figures indicate scenarios where steady model is applicable.

Amplitude (ml/s)	Frequency (Hz)				
–	0.1	0.5	1.0	2.0	4.0
2.0	0.994∠-11.0°	0.895∠-36.3°	0.759∠-53.0°	0.585∠-68.4°	0.425∠-78.9°
5.0	**0.999∠-5.2°**	0.976∠-19.0°	0.925∠-31.4°	0.811∠-47.6°	0.642∠-64.2°
10.0	**1.000∠-2.9°**	0.994∠-11.0°	0.977∠-19.0°	0.925∠-31.4°	0.812∠-47.8°
20.0	**1.000∠-1.6°**	**0.999∠-6.2°**	0.994∠-11.0°	0.977∠-19.0°	0.926∠-31.5°
40.0	**1.000∠-0.9°**	**1.000∠-3.5°**	**0.999∠-6.2°**	0.994∠-11.0°	0.978∠-19.1°
60.0	**1.000∠-0.6°**	**1.000∠-2.4°**	**1.000∠-4.4°**	**0.998∠-7.9°**	0.990∠-13.9°

These simulations show that high amplitude flows are less sensitive to unsteady effects than low amplitude ones. Particularly, the usual venturi model is adequate for measuring which are typical of FOT excitations (5-10 ml/s), accounting for flow components up to 2 Hz at 60 ml/s. For low amplitude flows unsteadiness is mandatory in order to obtain a valid measurement of the flow components above 0.1 Hz. This behavior is directly related to the form of (2.17), in which unsteady effects are proportional to f and $|q|$ while venturi effect is proportional to q^2. It is also important to mention that these results are independent of the fluid and are only a function of the geometry of the model.

3.1.6 Experimental validation methods

Experimental setup

Due to experimental constraints – mainly minimizing PFC usage – the flow is driven by a piston pump (Model SPS 3891, ViVitro Systems, Canada) as shown in figure 3.9. The three pressure signals from the venturi were independently conditioned (9300 Series, Sensorex, France) and calibrated (Druck DPI 610, GE Sensing, USA). All signals were digitized to 24 bits at 1 kHz (PCI-4472, National Instruments, USA). Tests were conducted with two fluids: distilled water and perfluorodecalin (F2 Chemicals Ltd, United Kingdom), a PFC having $\rho = 1917$ kg/m^3 and $\mu = 5.33$ mPa $\cdot$ s at 25 °C.

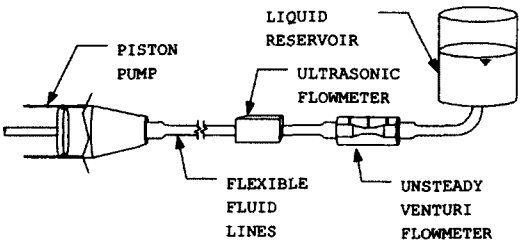

Figure 3.2 Scheme of the experimental setup

Other flow measurements

Ultrasonic flowmeter An ultrasonic flowmeter (T110R, Transonic Systems Inc., USA) was used to measure instantaneous flow near the proposed venturi meter. Its relative accuracy was ±4 % after on-site calibration, and the measurement bandwidth was 100 Hz. The flowmeter was calibrated by comparing its quasi-steady flow response with the piston pump volume output. However, without hardware modification, this flowmeter cannot be used with PFC because of its high density.

Piston pump volume The piston pump controller outputs the piston position measured by a linear variable displacement transducer (LVDT), measuring the pump volume with a maximal error of 0.64 ml. This value is used to obtain a measurement of the flow at the pump for subsequent ultrasonic flowmeter calibrations, and for low-frequency tests with PFC when the ultrasonic flowmeter is unusable. Herein, the flowrate was estimated by harmonic analysis: the Fourier coefficients of the volume signals were calculated from spectral density function estimates and then multiplied by $j2\pi f$.

Particle Image Velocimetry PIV measurements provided velocity fields in the venturi (Flowmaster 2DPIV, LaVision, Germany ; Nd:YAG laser). Liquids were seeded with 0.5 g/l of 10 μm silver-coated hollow glass spheres (S-HGS-10, Dantec Dynamics A/S, Denmark). The main difficulty was to precisely position the laser sheet in the meridional plane of the 4 mm diameter venturi throat. The velocity fields were computed using multi-pass cross-correlations with 50% overlap for an interrogation window of 16 pixels, providing a spatial resolution of approximately 0.16×0.16 mm (i.e., 0.04 mm per pixel). The maximal particle displacement was approximately 4 pixels with a sub-pixel error of ± 0.1 pixel. The time-periodic flow signals allowed phase averaging of the velocity fields: each period was divided into 20 frames, and 100 records were acquired for each frame. The PIV-measured flow was calculated by integration of the velocity profiles at the throat, and the scale was corrected as with the ultrasonic flowmeter. In addition, the experimental PIV velocity profiles were compared with the theoretical profiles given by (2.16) to determine the applicability of this model to enhance frequency response in the context of our studies.

Experiment design and data processing

Steady flow characterization: the discharge coefficient The venturi flowmeter performance was first assessed in quasi-steady flows to determine its discharge coefficient C_v as a function of the throat Reynolds number. The steadiness of the flow was determined by the results developed in section 3.1.5. Flows ranging from 5 ml/s to 40 ml/s were generated at a 0.1 Hz frequency while a 0.2 Hz signal was used for 60 ml/s experiments. The piston pump was taken as the flow reference because these experiments were conducted with both water and PFC.

The discharge coefficient corrects the measured flow q_v^m to account for all unrecoverable pressure losses that arise from friction along the walls, pressure ports effects or separation of the flow, in such a way that

$$q_v^c = C_v q_v^m. \tag{3.9}$$

The low flow rates associated with the present application make C_v highly dependent on Re. Experimental data showed that C_v can be estimated by a correlation having the form

$$\hat{C}_v = \beta_0 + \frac{\beta_1}{\sqrt{\mathrm{Re}_{thr}}} \tag{3.10}$$

where Re_{thr} is the Reynolds number based on the throat diameter, and β_0, β_1 are determined by regression analysis on experimental data. The prime reason for choosing this form was its concordance with experimental data. It is also analogous to other known empiri-

cal correlations such as that suggested for long radius flow nozzles (ISO, 1980). Because measurement errors were present in both axes (C_v and Re), the least products linear regression, also known as the geometrical mean functional relationship, was applied(Draper et Smith, 1998).

Experimental data for C_v and Re were obtained by spectral analysis of the pump volume and venturi flow signals, again using the WOSA procedure (90% overlapped hamming windows, 10 s segments of 10000 samples each). The measured discharge coefficient C_v^m was calculated as the ratio between the amplitude of the flow measured at the pump q_p and the flow estimated by the venturi q_v at the excitation frequency

$$C_v^m(f) = \frac{\hat{G}_{V_p,V_p}(f)}{\hat{G}_{V_p,q_v}(f)} j2\pi f \tag{3.11}$$

Measurement uncertainties on C_v arose from three major components:

- $\mathcal{U}(\hat{C}_v)$: prediction errors due to uncertainty on the regression,
- $\mathcal{U}_a(C_v^m)$: random errors involved with frequency analysis,
- $\mathcal{U}_b(C_v^m)$: uncertainty due to the sensors themselves.

The detailed procedure for evaluating these values follows ISO's *Guide to the Expression of Uncertainty in Measurement* (GUM) guidelines (ISO/IEC, 1995), and is reported in appendix 3.1.9. For a given measured flow, the squared standard uncertainty on the predicted C_v will be given as the sum of the squares of these three contributors:

$$\mathcal{U}^2(C_v^p) = \mathcal{U}^2(\hat{C}_v) + \mathcal{U}_a^2(C_v^m) + \mathcal{U}_b^2(C_v^m). \tag{3.12}$$

Unsteady flow characteristics The measurement of unsteady flows was again addressed by applying harmonic flow signals with the piston pump. The experiments were only conducted with water. Two different amplitudes were tested: 5 ml/s and 10 ml/s. Investigated frequencies were 0.1 Hz, and 0.5 Hz to 4 Hz at 0.5 Hz intervals. The recorded data were then processed using the same WOSA frequency analysis procedure described in section 3.1.5 (50% overlapped hamming windows, 2 s segments of 2000 samples each). Only spectral data at the excitation frequency where the measured coherence function respected $\gamma^2 > 0.999$ were kept. As with table 3.1 data, acceptable performance was defined as a modulus of 1.00 ± 0.05 and an angle of $0^\circ \pm 10^\circ$.

Validation experiments with simultaneous PIV measurements were also conducted with both fluids, at frequencies of 0.1 Hz, 1 Hz, 2 Hz and 4 Hz for amplitudes of 5 ml/s and 10 ml/s and at 0.2 Hz for the 60 ml/s amplitude.

3.1.7 Results and discussion

Quasi-steady flow characteristics

The venturi discharge coefficient is plotted versus throat Reynolds number in figure 3.3. The experimental correlation linking the quantities is

$$C_v = 1.06 - \frac{8.2}{\sqrt{\mathrm{Re}_{thr}}} \tag{3.13}$$

for Re_{thr} ranging from 740 to 23 000.

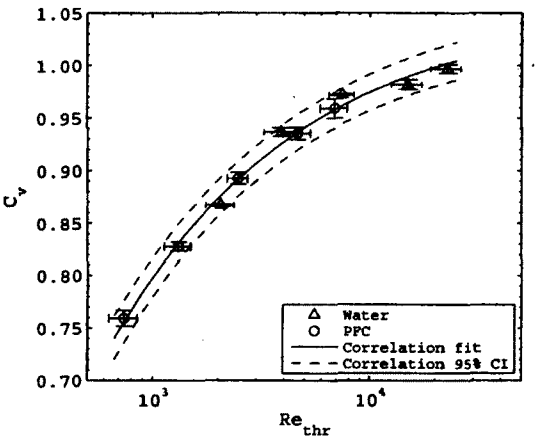

Figure 3.3 Venturi discharge coefficient (C_v) versus throat Reynolds number (Re_{thr}). Error bars indicate random errors obtained from spectral analysis. Dotted lines indicate the 95% nonsimultaneous prediction confidence interval of the regression.

Since it is expressed in terms of Reynolds number, and determined using two fluids of different mechanical properties, this quasi-steady calibration curve allows the device to be used with all fluids of interest in TLV.

For all data points, the first two uncertainty components can be bound at $\mathcal{U}(\hat{C}_v) \leq 0.009$ and $\mathcal{U}_a(C_v^m) \leq 0.005$. Uncertainty due to the sensors was dependent on the fluid and flow rate, since low throat flows or lower densities yielded a smaller pressure difference. This component was thus negligible at high flows whereas it became critical at the low end of the operating range. The expanded uncertainty on the measured flow ranged from

±0.6 ml/s to ±1.4 ml/s for PFC flows from 5 ml/s to 60 ml/s respectively. Uncertainty on water measurements was higher (±1 ml/s) at low amplitudes but comparable above 10 ml/s.

Unsteady flow characteristics

Figure 3.4 shows the frequency response function $H(f)$ between the ultrasonic and venturi flowmeters, both after applying the calibration coefficients calculated in section 3.1.7.

$$H(f) = \frac{q_v(f)}{q_{us}(f)} \tag{3.14}$$

The figure shows that, at 10 ml/s, the proposed venturi flowmeter adequately reproduced the measurements obtained with the commercially available ultrasonic meter for frequencies up to 3 Hz. Beyond that limit, the confidence interval of the data lies entirely outside the acceptable magnitude range. For 5 ml/s experiments, all data were within the acceptable values intervals, although their relative uncertainties were much larger as explained in section 3.1.7. The 5 ml/s, 0.1 Hz point was removed due to a low γ^2 value.

It is unclear whether the observed 10 ml/s behavior at $f > 3$ Hz was due to the ultrasonic flowmeter or departure of the discharge coefficient from the relation determined in section 3.1.7. First, the ultrasonic flowmeter needed to be installed on flexible tubing few inches before the venturi. This flexible section was reduced to a minimum, but still could have induced resonant dynamics between the two sensors. On the other hand, the discharge coefficient was determined for steady flows and its applicable frequency range can also be questioned. For this reason, the authors prefer to remain conservative and limit the specific frequency range to 3 Hz even though previous works (Foucault *et al.*, 2005) have shown good performance at much higher frequencies. However, the main purpose of a good frequency response in the current medical device application is the correct measurement of low-frequency lung mechanical impedance. Existing studies showed that most data of interest lie in the 0.05 Hz – 2 Hz range (Bossé *et al.*, 2010), hence justifying the adequateness of a 3 Hz upper limit.

Limit scenarios and velocity profiles

Figures 3.5 to 3.7 show the flow behavior throughout an oscillation cycle for three limit cases. The upper portion of the figure represents the time evolution of the measured velocity profiles compared with values obtained analytically using (2.16). This information shows that the flat profile assumption was reasonable in the application context, thus validating the flowmeter equation of section 3.1.3. The lower portion represents the flow

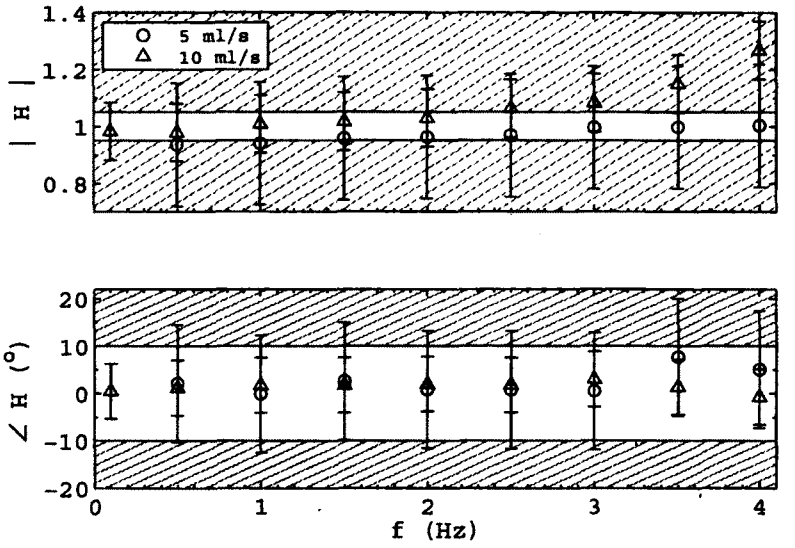

Figure 3.4 Frequency-response function between venturi and ultrasonic flowmeter, tested with water. Hatched regions: inadequate response.

rate evolution for a complete cycle, offering a comparison of all available methods. For all explored scenarios except 4 Hz cases, all available measurement methods were in agreement relative to their precision.

High velocity - low frequency (60 ml/s - 0.2 Hz with water) These conditions correspond to $\mathrm{Re}_{thr} = 21\,500$ and $\mathrm{Wr}_{thr} = 2.4$, and a typical oscillation cycle is reported in figure 3.5. After steady calibration, all four measurements coincided with each other with good accuracy for the overall 0.2 Hz cycle. Furthermore, the venturi measurement tracked the tube oscillations at higher frequencies whereas the pump measurement did not. This feature is desirable in the TLV context in order to adequately characterize tube resonances. The velocity profiles were relatively flat, due to the turbulent regime in the throat. This demonstrates that the flat profile assumption needed for development of (2.17) is valid. However, as expected, the pulsatile flow model (2.16) cannot be used for describing the unsteady flow behavior at this moderately high Re.

Low velocity - low frequency (10 ml/s - 0.1 Hz with PFC) These conditions correspond to $\mathrm{Re}_{thr} = 1150$ and $\mathrm{Wr}_{thr} = 0.95$, and a typical oscillation cycle is reported on figure 3.6. For this scenario, the venturi measurement again tracked the sinusoidal flow delivered by the pump with good accuracy throughout the cycle, despite the much lower amplitude.

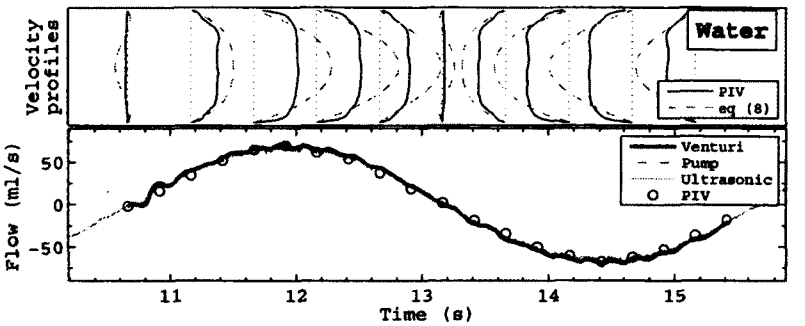

Figure 3.5 Multi-method measurements at 60 ml/s - 0.2 Hz with water (Re_{thr} = 21 500 and $Wr_{thr} = 2.4$)

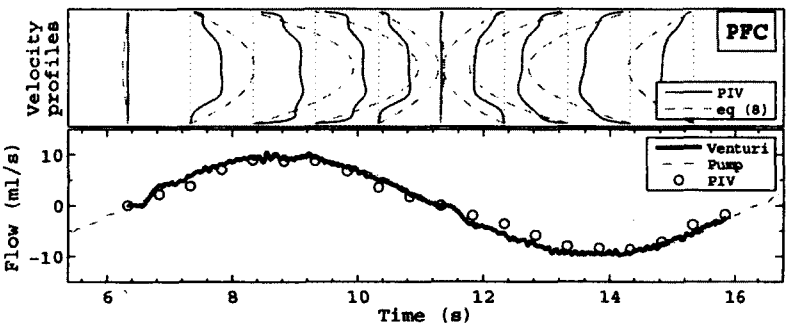

Figure 3.6 Multi-method measurements at 10 ml/s - 0.1 Hz with PFC (Re_{thr} = 1150 and $Wr_{thr} = 0.95$)

The profiles were again more flat than parabolic, even in this instance which should produce a laminar Poiseuille flow according to the developed model (2.16). Consequently, the latter cannot be used to enhance the frequency response of our device since it does not yield valid results for low Wr either. A likely explanation for this phenomenon is that the flow is affected by the section changes between the venturi body and the connecting fluid lines. The resulting profiles are then flattened because the flow is still in the "entrance region" of the venturi body. The existence and behavior of an entrance length for oscillating pipe flows have previously been reported, and yields flatter velocity profiles than for fully developed equivalent flows (Çarpinlioglu et Yasar Gündogdu, 2001; Yamanaka *et al.*, 2002).

Low velocity - high frequency (10 ml/s - 4.0 Hz with water) These conditions correspond to $\mathrm{Re}_{thr} = 3600$ and $\mathrm{Wr}_{thr} = 11$, and a typical result is reported in figure 3.7. As expected from the frequency response data in section 3.1.7, the venturi-measured flow rate was of higher amplitude than the ultrasonic-measured one. However, the general shape of the signal, which is not purely sinusoidal, was preserved and also reproduced by PIV-measured flow. At these frequencies, the pump measurement was clearly inadequate to measure flow rate near the venturi: most of the oscillatory flow is filtered by the flexible tubing.

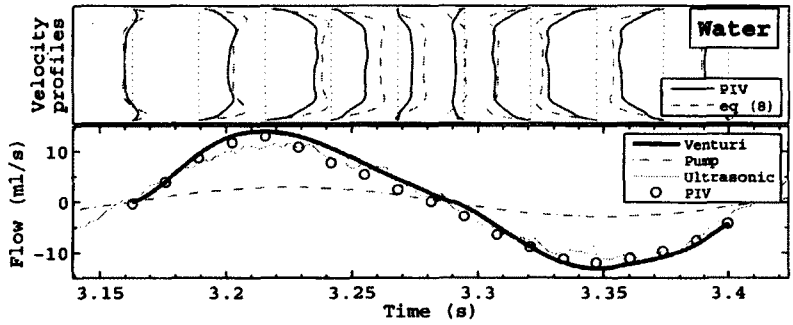

Figure 3.7 Multi-method measurements at 10 ml/s - 4.0 Hz with water ($\mathrm{Re}_{thr} = 3600$ and $\mathrm{Wr}_{thr} = 11$)

This last experiment illustrates that the oscillating flow theory and the corresponding exact Navier-Stokes solution (2.16) are in good agreement with results for $\mathrm{Wr} \geq 5$. Other authors reported a reduction of flow development effects at higher Wr (He et Ku, 1994), which concur with the present observation.

As for venturi exit profiles, unpresented data show explicitly that the flow distribution varies greatly with Re, sometimes resulting in flow reversals or jet formations. The exit

pressure sensor cannot be used to retrieve flow information, thus justifying the use of a third sensor.

3.1.8 Conclusions

A venturi flowmeter and a method for retrieving unsteady flowrate from the differential pressure was presented. The device was tested with both water and perfluorodecalin, for quasi-steady and oscillating flows. The venturi discharge coefficient was determined as a function of Reynolds number. Water unsteady characterization presented acceptable dynamic response for low flows up to 3 Hz, with less than 5% amplitude difference with the reference meter and a $< 10^{\circ}$phase shift. The different measurement methods all agreed within instrument precision in this frequency range, for flows from 5 ml/s to 60 ml/s.

A more detailed flow model will be needed to explain the higher sensitivity and phase lag for frequencies above 3 Hz, and more precise differential pressure sensors are recommended to lower the uncertainty at very low flows. Nonetheless, the presented device and methodology yield highly adequate performances for the liquid ventilator application context.

Acknowledgements

The authors gratefully acknowledge M. Raymond Robert for his technical assistance, Patrick Lévesque for the mechanical fabrication of the prototypes.

3.1.9 Appendix A: Expression of the uncertainty in C_v and q_v measurement

$U(\hat{C}_v)$: prediction errors due to uncertainty on the regression

The least products regression renders proper estimation of the prediction confidence bounds difficult. Linear regression theory was therefore used to give an order of magnitude, considering the regression coefficients were almost equal (less than 0.5% difference). The standard deviation on $\hat{C}_v$ for a new observation is

$$U(\hat{C}_v) = s\left[1 + \frac{1}{n} + \frac{\left(\mathrm{Re}_0^m - \overline{\mathrm{Re}^m}\right)^2}{\sum_i \left(\mathrm{Re}_i^m - \overline{\mathrm{Re}^m}\right)^2}\right]^{1/2} \tag{3.15}$$

where s is the standard deviation of the residuals, n is the number of data points, $\overline{\mathrm{Re}^m}$ is the mean of the individual observations (Re_i^m) used for the regression, and Re_0^m is a new observation of the Reynolds number (Draper et Smith, 1998).

$\mathcal{U}_a(C_v^m)$: random errors on measured C_v involved with the frequency analysis

The WOSA method used for determination of the measured C_v and Re also provides an expression of the uncertainty due to random errors on these components (type A uncertainties). After proper propagation (ISO/IEC, 1995),

$$\mathcal{U}_a(C_v^m) = 2\pi f \frac{[1-\gamma^2(f)]^{1/2}}{\gamma(f)\sqrt{2n_d}} C_v^m(f) \tag{3.16}$$

$$\mathcal{U}_a(\mathrm{Re}^m) = \frac{1}{2\sqrt{2n_d}} \mathrm{Re}^m(f). \tag{3.17}$$

where $\gamma^2(f)$ is the ordinary coherence function between the two signals and n_d is the number of averaged segments (see (Bendat et Piersol, 1980), Chap 11).

$\mathcal{U}_b(C_v^m)$: uncertainty due to the sensors themselves

Type B uncertainties evaluation accounted for the limited sensors precision. Applying the uncertainty propagation rule to (3.9) (using q_p as the "corrected" value) yields

$$\mathcal{U}_b^2(C_v) = \left(\frac{1}{q_v}\right)^2 \mathcal{U}^2(q_p) + \left(\frac{-q_p}{{q_v}^2}\right)^2 \mathcal{U}^2(q_v) \tag{3.18}$$

where

$$q_p = 2\pi f V_p \tag{3.19}$$

$$\mathcal{U}^2(q_p) = (2\pi f)^2 \mathcal{U}^2(V_p) \tag{3.20}$$

and

$$q_v = \sqrt{\frac{1}{B}\frac{\Delta P}{\rho}} \tag{3.21}$$

$$\mathcal{U}^2(q_v) = \frac{1}{2\sqrt{\Delta P\, B^{-1}\rho^{-1}}} \frac{1}{B\rho} \mathcal{U}^2(\Delta P). \tag{3.22}$$

These equations are obtained from the propagation rule on (2.17) for quasi-steady flows ($dq/dt \approx 0$). Fluid properties, flowmeter dimensions and measured frequencies were of negligible uncertainties compared to sensors. $\mathcal{U}(\Delta P)$ was determined by the standard de-

viation of nonlinearity and hysteresis errors of in-house recalibration within the application pressure range.

$$\mathcal{U}(\Delta P) = 13 \text{ Pa}$$

Finally, since $\mathcal{U}(\ )$ denotes a standard uncertainty, the final value of $\mathcal{U}(C_v)$ was enlarged by a factor 2 in order to express a $\approx 95\%$ confidence interval for this coefficient.

3.2 Article : «La mesure des paramètres d'un modèle d'impédance respiratoire d'ordre fractionnaire en ventilation liquidienne totale»

3.2.1 Avant-propos

Auteurs et affiliation : A. Beaulieu : Étudiant à la maîtrise, Université de Sherbrooke, Faculté de génie, Département de génie mécanique.

D. Bossé : MD-MSc, Université de Sherbrooke, Faculté de médecine et des sciences de la santé, Département de physiologie-biopysique.

P. Micheau : Professeur titulaire, Université de Sherbrooke, Faculté de génie, Département de génie mécanique.

O. Avoine : étudiant au doctorat, Université de Sherbrooke, Faculté de médecine et des sciences de la santé, Département de physiologie-biopysique.

J.P. Praud : Professeur titulaire, Université de Sherbrooke, Faculté de médecine et des sciences de la santé, Département de pédiatrie.

H. Walti : Professeur titulaire, Université de Sherbrooke, Faculté de médecine et des sciences de la santé, Département de pédiatrie.

Date de soumission : 17 mai 2011

État de l'acceptation : Révision mineure demandée

Revue : IEEE Transactions on Biomedical Engineering

Titre français : La mesure des paramètres d'un modèle d'impédance respiratoire d'ordre fractionnaire en ventilation liquidienne totale

Contribution au document : Cet article contient l'essentiel de la méthodologie développée et employée dans le cadre du projet de maîtrise. Il consiste donc en une partie centrale du mémoire de par sa description complète du matériel et des méthodes, ainsi que la dérivation et la justification du modèle d'impédance pulmonaire utilisé au long du projet. Les résultats sont énoncés selon le modèle « *five-parameter constant-phase model* » et justifient l'emploi d'un tel modèle à ordre fractionnaire, mais leur analyse est moins détaillée du point de vue physiologique que dans la section 4.1. Pour des raisons de synchronisme avec M. Dominick Bossé, l'étudiant

qui s'occupait du volet médical du projet, cette étude ainsi que celle présentée à la section 4.1 ont été menées sans le débitmètre instationnaire.

Résumé français : Une méthode pour appliquer la technique des oscillations forcées en ventilation liquidienne totale (VLT) est proposée. Elle consiste principalement à appliquer un excitation volumétrique sinusoïdale au système respiratoire, et à évaluer la fonction de transfert entre le débit délivré et la pression aux voies aériennes. La plage de fréquence étudiée est $f \in [0.05, 4]$ Hz, à une amplitude de débit constante de 7.5 mL/s. Les cinq paramètres d'un modèle pulmonaire à ordre fractionnel existant, le « *five-parameter constant-phase model* », ont été identifiés à partir des spectres d'impédance mesurés. La méthode d'identification a été validée *in silico* sur des données générées informatiquement et la méthode dans son ensemble a été validée *in vitro* sur un modèle mécanique de dynamique pulmonaire. Les données *in vivo* sur 10 agneaux nouveau-nés suggèrent qu'un terme de compliance fractionnel est approprié pour décrire le comportement basse-fréquence des poumons, mais il n'a pas été possible de conclure sur la pertinence d'un terme d'inertance à ordre fractionnel. Une réponse en fréquence typique du système respiratoire est présentée, ainsi que les données statistiques des paramètres d'un modèle d'impédance pulmonaire mesurés sur agneau. Cette information sera utile pour la conception d'un contrôleur en pression robuste pour la VLT en plus du suivi de l'état du patient durant le traitement.

Note : Cet article correspond à la soumission initiale du manuscrit. Comme des corrections mineures ont été demandées, la version publiée sera légèrement différente du texte présenté ici.

Measurement of Fractional Order Model Parameters of Respiratory Mechanical Impedance in Total Liquid Ventilation

A. Beaulieu[a], D. Bossé[b], P. Micheau[a], O. Avoine[b], J.P. Praud[b] and Hervé Walti[b]

[a] *Faculté de génie de l'Université de Sherbrooke, Département de génie mécanique, Sherbrooke (Québec), Canada*

[b] *Faculté de Médecine et des Sciences de la Santé de l'Université de Sherbrooke, Département de Pédiatrie, Sherbrooke (Québec) Canada.*

Abstract

A methodology for applying the forced-oscillation technique in total liquid ventilation is proposed. It mainly consists of applying sinusoidal volumetric excitation to the respiratory system, and determining the transfer function between the delivered flow rate and resulting airway pressure. The investigated frequency range was $f \in [0.05, 4]$ Hz, at a constant flow amplitude of 7.5 mL/s. The five parameters of a fractional order lung model, the existing "5-parameter constant-phase model", were identified based on measured impedance spectra. The identification method was validated *in-silico* on computer-generated data sets and the overall process was validated *in-vitro* on a simplified single-compartment mechanical lung model. *In-vivo* data on 10 newborn lambs suggested the appropriateness of a fractional-order compliance term to the mechanical impedance to describe the low-frequency behavior of the lung, but was unable to conclude on the relevance of a fractional-order inertance term. Typical respiratory system frequency response is presented, together with statistical data of the measured *in-vivo* impedance model parameters. This information will be useful for both the design of a robust pressure controller for total liquid ventilators and the monitoring of the patient's respiratory parameters during the TLV treatment.

Keywords: Total Liquid Ventilation, Lung Mechanics, Forced Oscillation Technique, Biomedical Systems, Frequency-Domain System Identification, Fractional Order Systems

3.2.2 Introduction

Context

Liquid ventilation, or the use of an oxygenated liquid as ventilatory medium, is an emerging and promising mechanical ventilation method. It offers many advantages over conventional mechanical ventilation, such as

the use of lower inflation pressure by increasing lung compliance, the reduction of barotrauma risk, the recruitment of atelectatic zones of the lung (Wolfson *et al.*, 1992), the homogenization of ventilation (Wolfson et Shaffer, 2005), the perfluorocarbons (PFC)-induced anti-inflammatory effects (von der Hardt *et al.*, 2003) and the wash out of alveolar and bronchial remnants (Wolfson *et al.*, 2008). The Inolivent team focuses on advancement of total liquid ventilation (TLV), where a tidal volume of liquid is withdrawn form the lungs, filtered, oxygenated, heated and reinserted into the lungs at every respiratory cycle (Wolfson et Shaffer, 2005). Compared to other forms of liquid ventilation, TLV has the main advantages of eliminating the liquid-gas interface in the lungs, as well as ensuring homogenous pressure and lung expansion (Wolfson et Shaffer, 2005). TLV can also be applied outside of the pure respiratory support field, for instance to induce protective hypothermia (Tissier *et al.*, 2007) or performing a broncho-alveolar lavage to wash out of alveolar and bronchial remnants while ensuring proper ventilation and gas exchange (Foust *et al.*, 1996; Marraro *et al.*, 1998).

A dedicated liquid ventilator is prerequisite for TLV development and since no commercial device is available, many authors reported designing their own (Corno *et al.*, 2003; Larrabe *et al.*, 2001; Robert *et al.*, 2006; Sekins *et al.*, 1999). Though there is an international consensus on the main functions that a device must realize to be called a liquid ventilator (Costantino *et al.*, 2009), the lung mechanics measurement capabilities varies from one prototype to another.

Knowledge of the lung mechanical properties is of prime interest while applying mechanical ventilation (Bhutani et Sivieri, 2001; Grinnan et Truwit, 2005b). In conventional gas ventilation (CGV), number of methods are available such as time domain pressure and flow signals analysis (Lauzon et Bates, 1991), occlusion techniques (Oswald-Mammosser *et al.*, 2010; Pierce *et al.*, 2005) and forced-oscillation technique (FOT) (DuBois *et al.*, 1956; Navajas et Farre, 2001). This article solely focus on FOT and readers are refered to ref. (Polak *et al.*, 2006) for details on these techniques. Briefly, this method consists of applying a volumetric excitation profile to the airway opening, and calculating lung impedance as the ratio between recorded airway pressure and flow. This can be done during

pauses at the end of expiration and inspiration, or continuously during the spontaneous or mechanical ventilation (Birch *et al.*, 2001). Prior results showed that low-frequency FOT enables reliable respiratory mechanics characterization during neonatal total liquid ventilation (Bossé *et al.*, 2010).

Parametric models can then be used to interpret the experimental impedance data. While a great number of these models are developed and used in CGV, previous works in liquid ventilation showed that a fractional order linear model such as the constant-phase model (CPM) (Hantos *et al.*, 1992), can be successfully fitted to experimental data (Bossé *et al.*, 2010). This four-parameter model incorporates a fractional order integral on the compliance term:

$$Z_{CPM}(j2\pi f) = R + \frac{G - jH}{(2\pi f)^{\alpha}} + I(j2\pi f) \tag{3.23}$$

where $\alpha = (2/\pi)\arctan(H/G)$ is the fractional order. While the usual interpretation of the CPM in gas ventilation link the fractional order to the viscoelasticity of the lung tissue, giving physical meaning to parameters G and H (Fredberg et Stamenovic, 1989; Hantos *et al.*, 1992; Suki *et al.*, 1994), recent works suggest flows in the recursive (*i.e.* fractal) morphology of a compliant airway tree can also explain this behavior (Ionescu *et al.*, 2010b, 2009a,b). Was also added another fractional order derivative for the inertance term to form what is called the 5-CPM (Ionescu et De Keyser, 2006, 2008; Ionescu *et al.*, 2010b, 2009a). Because of the high density of PFCs, yielding more important inertial effects, it was hypothesized that such behaviors would also be observed in TLV, and the 5-CPM was explored in the present study.

Problem and relevance

Prior to the works of Bossé and colleagues (Bossé *et al.*, 2010), impedance measurements in TLV remained unexplored. As no information was available, proposing an adequate respiratory impedance model for TLV was challenging and there was a real need to develop a methodology to obtain valid experimental data to work on. Some authors already experimented FOT measurement in partial liquid ventilation (PLV) where the lungs are only partially filled with a PFC liquid (Schmalisch *et al.*, 2003). However, the very large disparity between air and perfluorocarbon as a medium to convey volume excitations and pressure wave responses, and the presence of a liquid-gas interface are sufficient for expecting many differences between PLV and TLV results and their interpretation. On the modeling point of view, this disparity between air and PFC should yield very different parameter values, and even the adequacy of CGV-derived models is yet to be demonstrated, hence the necessity of respiratory impedance measurements in TLV.

Aim of work

The aim of the presented work is twofold. First, propose a protocol for applying FOT in TLV and analyzing data using material already implemented in the authors' liquid ventilator prototype, together with well-known signal analysis and frequency-domain system identification methods. The second goal is to propose a respiratory impedance model for TLV, and show it's applicability by presenting experimental results and suggest appropriate parameters values. This paper uses the same data set as a previous study (Bossé *et al.*, 2010), but presents a more technical description of the methodology and its validation. It also proposes a slightly different model to express the lung impedance by incorporating a fractional order on the inertance term as well. It thus consists of a broader and updated description of the work presented earlier (Beaulieu *et al.*, 2010).

3.2.3 Materials and Methods

Experimentation material: Inolivent-4 liquid ventilator prototype

Experiments were conducted using Inolivent-4 liquid ventilator (Robert *et al.*, 2009a) an optimized version of Inolivent-3 (Robert *et al.*, 2006). It was designed for experimental research on animals representing newborns and infants weighing 0.5-9 kg and to include the new pressure controlled ventilation mode (Robert *et al.*, 2009b).

A schematic representation of the prototype is shown in figure 3.8. The device comprises two independent piston pumps, respectively for inspiration and expiration. Each of these pumps is connected to the wye piece by means of flexible tubing and a pinch valve to direct the flow of PFC. The wye piece is in turn connected to the patient with a 5.5-G cuffed endotracheal tube (ET) (Mallinckrodt, St. Louis, MO)..

Each of the pumps is also connected to the oxygenator unit (comprising a filter, a bubble gas exchanger, heating elements, a condenser and a buffer reservoir) by flexible tubing and a pinch valve. During the cycles, used PFC in the expiration pump is pushed in the filter and the oxygenator. The filtered, heated and oxygenated PFC pours in the buffer reservoir, and will fill the inspiration pump for next cycle.

The control unit consists of two fully integrated computers (PC). The first computer runs real-time control of the ventilator (xPC-target, Mathworks, USA) and records data from the ventilator as well as the other medical devices. The second PC supports a touch-screen graphical user interface for entering orders from the clinician. All control parameters and

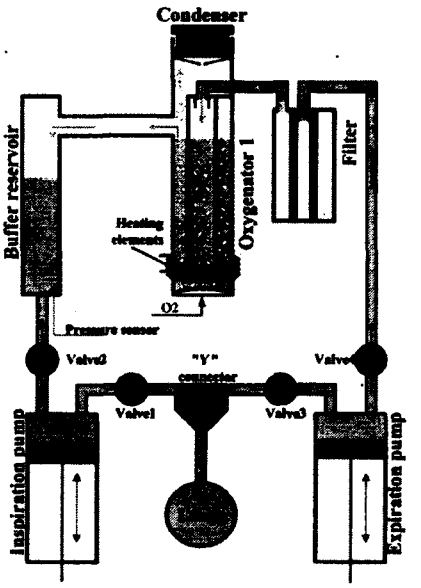

Figure 3.8 Representation of the Inolivent-4 prototype

monitored data are accessible via an interface similar to any typical gas ventilator, but adapted to TLV practice.

Figure 3.9 shows a schematic representation of the experimental setup of FOT tests: during end-inspiratory and end-expiratory pauses, valve 3 is open, valve 4 is closed and the oscillations are generated by the expiration piston pump. It is only a specific configuration of the ventilator described by figure 3.8: no external component is needed.

A linear displacement sensor [CS-250-AD, MTS Sensors, Cary (NC), USA] measures piston position which is sent to a controller allowing precise tracking of the volume reference, $V_{ref}(t)$. The controller is a proportional feedback with $K_p = 1.0$ V/mL, with a slight offset $V_{off} = 0.6$ V to overcome static friction. The estimated bandwidth of the electromechanical system greater than 10 Hz. The airway pressure $P_{AW}(t)$ is recorded by a disposable blood pressure sensor [Model 1620, Measurement Specialties inc, Hampton (VA), USA], connected to a metallic capillary inserted in the endotracheal tube. The catheter is capped, and four pressure openings are made on it's circumference in order to measure static pressure about 1 cm above ET's proximal end. Measurement inside the constant-section ET minimises any "venturi effect" on the pressure reading. The sensor and the capillary are connected with a 30 cm perfusion flexible tubing.

The signals were digitized [PCI-DAS1602/16, Measurement Computing, Norton (MA), USA (16 bits resolution, 2 kHz sampling rate)], then digitally low-pass filtered (6th order Butterworth, -3dB cutoff at 10 Hz) and downsampled at 50 Hz for recording.

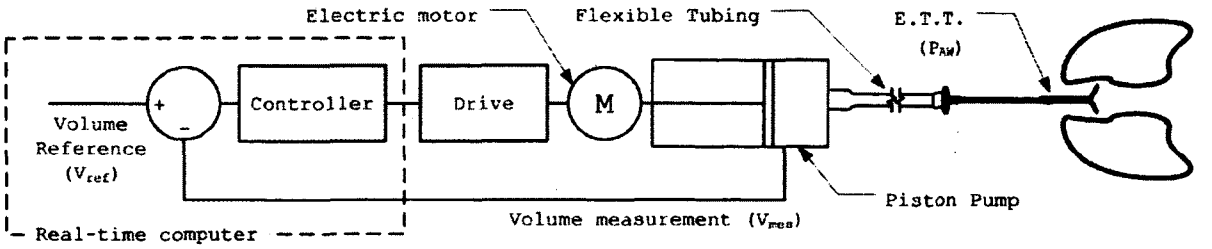

Figure 3.9 Schematic representation of the FOT setup. V_{ref}: Volume reference, V_{mes}: Volume measurement, P_{aw}: Airway pressure sensor, ET: Endotracheal tube.

Impedance spectra measurement protocol

Two types of pump volume reference, $V_{ref}(t)$, were used to generate flow disturbances:

1. A random excitation was first generated by the piston pump during 30 s. The random signal reference had a uniform probability distribution of 1 mL amplitude (generated by the *Simulink* Uniform Random Number generator). This test was used to measure the transfer function of the system between 2 Hz and 4 Hz.

2. Harmonic flow signals were generated by specifing a sinusoidal volume movement of the pump

$$V_{ref}(t) = \frac{A_{flow}}{2\pi f}\left[1 - \cos\left(2\pi f t\right)\right] + V_0 \tag{3.24}$$

where f is the excitation frequency (Hz), A_{flow} the specified flow amplitude and V_0 is initial volume in the pump (mL). The amplitude was $A_{flow} = 7.5$ mL/s excepted at $f = 0.05$ Hz where a lower amplitude $A_{flow} = 5$ mL/s was used to limit non-linearities associated with large lung volume variations. The frequencies were varied from $f = 1$ Hz to $f = 2$ Hz by 0.02 Hz increments, and from $f = 0.1$ Hz to $f = 0.9$ Hz by 0.1 Hz increments. These excitation signals also lasted 30 s, except for $f = 0.05$ Hz which lasted 45 s to mimimise influence of the transient on the spectra.

The airway pressure, $P_{aw}(t)$ and pump volume $V_{pump}(t)$ were recorded and post-processed off-line to calculate the measured input impedance

$$Z_m(f) = \frac{G_{VP}(f)}{j2\pi f G_{VV}(f)} \tag{3.25}$$

where $G_{VP}(f)$ is the averaged cross-spectral density function between P_{aw} and V_{pump}, $G_{VV}(f)$ is the averaged autospectral density function of V_{pump} and $j2\pi f$ is the time de-

rivative in the frequency domain. The cross-spectral density and the autospectral density function were calculated by using a Welch's overlapped-segment averaging (WOSA) procedure (Welch, 1967b). The overlapping segments were 20 s, 75% overlap ($\Delta f = 0.05\ Hz$) for harmonic signals and 10 s, 67% overlap ($\Delta f = 0.1\ Hz$) for noise signals. Hanning windows were used in both cases.

The coherence function γ^2 was also computed from spectral analysis.

$$\gamma^2(f) = \frac{|G_{VP}(f)|^2}{G_{VV}(f)G_{PP}(f)} \tag{3.26}$$

where $G_{PP}(f)$ is the averaged autospectral density function of P_{aw}. A value of $\gamma^2 \geq 0.95$ was used as the criterion for test acceptance (Sly *et al.*, 1996). This overall process is similar to typical gas ventilation forced-oscillation technique analysis (Polak *et al.*, 2006).

Parametric model

The measured input impedance model of the system can be broken down in two parts as shown in Figure 3.10. where $Z_{RS}(f) = P_{aw}(f)/\dot{V}_{aw}(f)$ is the mechanical input impedance

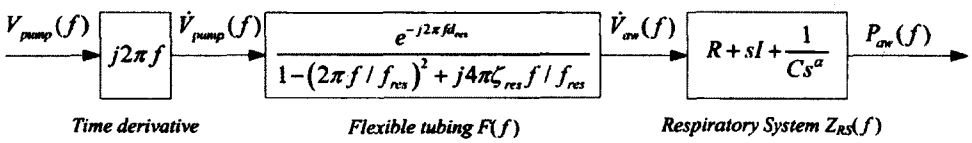

Figure 3.10 Block diagram representing the experimental setup model's components

of the respiratory system and $F(f) = \dot{V}_{aw}(f)/\dot{V}_{pump}(f)$ the tube transfer function.

The model of the respiratory impedance was a fractional order model known as the five-parameter constant-phase model (5-CPM):

$$Z_{RS}(f) = R + \frac{1}{C\,(j2\pi f)^{\alpha}} + I\,(j2\pi f)^{\beta} \tag{3.27}$$

where R is the linearized resistance ($\mathrm{cmH_2O \cdot s \cdot mL^{-1}}$), C is the linearized compliance ($\mathrm{mL \cdot cmH_2O^{-1}}$), I is the airway inertance ($\mathrm{cmH_2O \cdot s^2 \cdot mL^{-1}}$), and α and β are respectively the fractional orders of the compliance and the inertance terms (Ionescu et De Keyser, 2006). Of note is that the compliance terms of (3.27) and (3.23) are the exact same, but with different parametrization:

$$G = \frac{1}{C}\cos\left(\alpha\frac{\pi}{2}\right) \tag{3.28}$$

and

$$H = \frac{1}{C}\sin\left(\alpha\frac{\pi}{2}\right). \tag{3.29}$$

The tube transfert function was modeled as a 2nd order underdamped oscillation and a time delay.

$$F(f) = \frac{1}{1-(2\pi f/f_{res})^2 + j4\pi\zeta_{res}f/f_{res}} e^{-j2\pi f d_{res}} \tag{3.30}$$

where f_{res} is the natural frequency of the tube resonance, ζ_{res} its damping factor and d_{res} is the time delay associated with the pressure wave travel speed limitation in flexible tubing.

Parametric identification

The seven parameters were identified by a nonlinear weighted least squares minimization routine, Matlab's `lsqnonlin` function [The MathWorks, Natick (MA), USA] that uses the trust-region-reflective algorithm (Coleman et Li, 1996). This routine yields an optimal estimate of the parameters according to

$$\hat{\boldsymbol{\theta}} = \arg_{\boldsymbol{\theta}} \min \sum_i |Z_m(f_i) - Z(f_i,\boldsymbol{\theta})|^2 w(f_i)^2 \tag{3.31}$$

where $\boldsymbol{\theta} = [R \quad I \quad C \quad \alpha \quad \omega_{res} \quad \zeta_{res} \quad d_{res}]^T$ is the vector of the parameters and $Z_m(f_i)$ is the measured impedance at the frequency f_i. If no data point was rejected (*e.g.* based on a low coherence value), $i = 1, 2, \ldots, 16$ correspond to harmonic data from 2 Hz to 0.05 Hz respectively, while $i = 17, \ldots, 37$ are data from the random test signal. The weights, $w(f_i)$, were set inversely proportionally to the frequency step between data points.

The confidence intervals around the parameters are estimated by linearization of the objective function by the `nlparci` function (Donaldson et Schnabel, 1987; Seber et Wild, 2003). The variance-covariance matrix $\hat{\mathbf{V}}$ is first computed by

$$\hat{\mathbf{V}} = s^2\left(\hat{\mathbf{J}}^T\hat{\mathbf{J}}\right)^{-1} \tag{3.32}$$

where

$$s^2 = \frac{\sum_i |Z_m(f_i) - Z(f_i,\boldsymbol{\theta})|^2 w(f_i)^2}{n-p} \tag{3.33}$$

is an estimate of the residual variance, also called the mean-squared error (MSE) (Draper et Smith, 1998), and $\hat{\mathbf{J}}$ is the jacobian matrix evaluated at $\hat{\boldsymbol{\theta}}$. Both are outputs of the optimization algorithm. The $100(1-\alpha)\%$ confidence interval for the r^{th} element of $\boldsymbol{\theta}$ is

then

$$\theta_r \pm t_{n-p}^{\alpha/2}\sqrt{\hat{V}_{rr}}. \tag{3.34}$$

where $t_{n-p}^{\alpha/2}$ is the t-distribution with $n-p$ degrees of freedom.

Validation experiments

***In-silico* validation of the identification method** The identification procedure was validated *in-silico* to assess its performance devoid of any measurement-induced error. 1000 simulated impedance spectra were generated with a given value of $\boldsymbol{\theta}$ and an added uncorrelated complex white normal noise with 0.1 $cmH_2O \cdot s/mL$ standard deviation. The methodology described in section 3.2.3 was then applied and the identified parameters were compared with the exact ones.

***In-vitro* validation of the measurement procedure** An *in-vitro* model of the respiratory system in TLV was constructed for validations of the measurement protocol and signal processing methods, as well as the parametric identification on experimental data. It comprises a vertical column of diameter D_c to reproduce compliance, and a long narrow tube (diameter D_t and length L_t) entering in the column that bring inertance and resistance, thus reproducing a typical *RIC* system. This latter model is a special case of the 5-CPM when both α and β are equal to unity, and is more common in the literature. The resistance-compliance (*RC*) mechanical impedance model is usually used to represent and describe respiratory mechanics for most ventilation modes in CGV (Chatburn et Primiano, 2001). The physical dimensions were set so as to produce comparable dynamics as the ones expected from an average lamb.

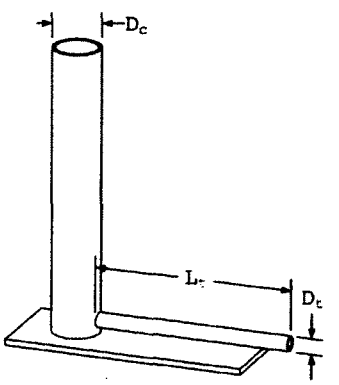

Figure 3.11 Schematic representation of the respiratory system in-vitro model. $D_c = 22.5$ mm, $D_t = 5.45$ mm and $L_t = 115$ mm.

This model lung is similar to an already published one (Bagnoli *et al.*, 2005), but the linear pressure-drop element is replaced here by a long narrow tube which also brings a calculable inertance. The compliance of the model, C_{mod}, is given by hydrostatic theory (White, 2008)

$$C_{mod} = \frac{\pi D_c^2}{4\rho g} \tag{3.35}$$

where ρ is the liquid's density and g the gravitational acceleration.

The inertance and resistance terms were treated together as they arose from the same long narrow tube. The modeled tube impedance (Z_{mod}) was derived by solving the Navier-Stokes equation for an oscillatory flow in a straight circular duct, under hypotheses that the flow is newtonian, laminar, incompressible and fully developed (Schlichting et Gersten, 2000).

$$Z_t(f) = \frac{4\rho L_t \omega}{\pi D_t^2} j \left[1 - \frac{2}{\sqrt{-j\mathrm{Wr}^2}} \frac{J_1\left(\sqrt{-j\mathrm{Wr}^2}\right)}{J_0\left(\sqrt{-j\mathrm{Wr}^2}\right)} \right]^{-1} \tag{3.36}$$

where J_0 and J_1 are respectively zeroth and first order Bessel functions of the first kind, Wr is the Womersley number $\left(\mathrm{Wr} = (D_t/2)\sqrt{2\pi f \rho/\mu}\right)$ (Morris et Forster, 2004). Furthermore, the junction of the horizontal tube and the column will bring extra resistance to the flow. It was approximated by a head loss coefficient $K_{exit} \approx 1$ (White, 2008), so that around a typical flowrate $\dot{V}_{typ}$, the total impedance of the mechanical model lung is

$$Z_{mod} = Z_t(f) + \frac{1}{C_{mod} j 2\pi f} + K_{exit} \frac{\rho \dot{V}_{typ}}{2S_t^2} \tag{3.37}$$

where $S_t = \pi D_t^2/4$. Resistance, inertance and compliance parameters were then fitted to this expression using the procedure given in section 3.2.3, and subsequently used as references for *in-vitro* validations.

In-vivo measurements

The developed methods were then applied to 13 healthy newborn lambs. The lambs, weighing 2.5 ± 0.4 kg (mean ± SD), were premedicated, intubated, anesthetized, and instrumented according to the protocol approved by our institutional Ethics Committee for Animal Care and Experimentation. Lambs were allowed 20 minutes for surgical recovery and then gradually shifted from conventional mechanical ventilation to a volume-controlled pressure-limited total liquid ventilation using Inolivent-4 prototype. Transitions were made as quickly as possible using 10 mL aliquots of warmed (39 °C), preoxygenated perfluorocarbon (Perfluorodecalin, F2 Chemical, Lancashire, UK) and by increasing

gas-ventilator PEEP from 4 to 7 cmH_2O . Total number of PFC aliquots was adjusted to achieve lamb calculated functional residual capacity (25 ml/kg). Gas ventilation was then interrupted and total liquid ventilation was performed at the following initial ventilator settings: pressure-regulated volume control mode, 5.6 breaths/min with an inspiration/expiration ratio of 1:3 ; end-inspiratory and end-expiratory pause = 0.5 second ; tidal volume = 28 ml/kg ; $PEEP_{ref}$ = $5cmH_2O$ and fraction of oxygen of 1.0. Inspiration was volume-regulated while expiration was pressure-regulated ; both were volume-controlled, pressure-limited and time-cycled. The FOT experiments procedure of section 3.2.3 was then initiated, with a sufficient period between measurements to maintain normal blood gases.

Two typical points of linearization were considered, both where the mean airway flow is zero:

1. during the end-expiratory pause, the lung volume is at the end expiratory lung volume (EELV) ;
2. during the end-inspiratory pause, the lung volume is at the end inspiratory lung volume (EILV).

The measurements were repeated three times. As in the previous study (Bossé *et al.*, 2010), only the last two series were considered to eliminate variation due to the adaptation to TLV period. Also, the two series were pooled together whenever possible to have enough data points for the optimisation routine to converge on every lamb.

3.2.4 Results

In-silico results

Computer-generated data allowed assessment of the identification performance with an added noise of 0.1 $cmH_2O{\cdot}s \cdot mL^{-1}$ standard deviation, which matches most experimental spectra. The identification was run on 1000 data sets, and the mean identified values and theirstandard deviation (SD) are presented in Table 3.2 together with the exact value used for the data generation. All parameters are identified with a $\leq 2\%$ bias error.

In-vitro results

The identified parameters of both the measured spectrum and the theoretical model are reported in Table 3.3. The theoretical model, described by equations (3.35) to (3.37), exhibits fractional orders both close to unity, showing this mechanical model should behave

Tableau 3.2 *In-silico* validation of the identification procedure

Parameter	Identified		Exact	Error
	Mean	S.D.		
R (cmH_2O s/ml)	0.484	0.072	0.500	-1.1 %
I (cmH_2O s^2/ml)	0.0510	0.0095	0.050	2.0 %
β (-)	1.20	0.07	1.20	0.2 %
C (ml/cmH_2O)	2.00	0.24	2.00	0.1 %
α (-)	0.699	0.067	0.700	-0.1 %
ω_{res} (rad/s)	15.0	0.4	15.0	-0.2 %
ζ_{res} (-)	0.300	0.014	0.300	0.1 %
d_{res} (s)	0.0203	0.0041	0.0200	1.3 %
MSE (cmH_2O s/ml)^2	6.03×10^{-3}	1.27×10^{-3}	–	–

as a typical RIC system. The relatively small MSE of the model fit also points towards this direction. The identified values of the "respiratory parameters" of the mechanical lung are within 10% of the modeled ones, except for the resistance which is 30% higher than what was predicted. On the other hand, the theoretical values lie in the 95% confidence interval of every respiratory parameter.

One interesting thing to observe is that the inertance of the long narrow tube can not be calculated by the typical expression $I = \rho L_t/S_t$ (Alvarez *et al.*, 2009; Bagnoli *et al.*, 2005), which would give $I = 0.0963$ cmH_2O s^2/ml. The measured I is almost 60% higher. This justifies a more coherent model of inertial effects, as described by equation (3.36), which considers the influence of the shape of the velocity profile to estimate I.

Tableau 3.3 In-vitro theoretical parameter values for PFC, identified values and confidence bounds (95% C.B.)

Parameter	Identified		Model	Error[a]
	Mean	95% C.B.		
R(cmH_2O s/ml)	0.509	[0.351 - 0.666]	0.391	30 %
I(cmH_2O s^2/ml)[b]	0.153	[0.108 - 0.198]	0.142	7 %
β (-)	0.900	[0.781 - 1.019]	0.930	-3 %
C(ml/cmH_2O)[b]	2.08	[1.59 - 2.56]	2.03	3 %
α (-)	0.983	[0.838 - 1.13]	0.986	-0.3 %
ω_{res} (rad/s)	23.4	[23.0 - 23.9]	23.0	2 %
ζ_{res} (-)	0.31	[0.29 - 0.34]	0.35	-11 %
d_{res} (s)	0.0111	[0.0055 - 0.0167]	0.0126	-12 %
MSE (cmH_2O s/ml)^2	2.24×10^{-2}		3.60×10^{-6}	–

[a] Error indicates relative error between theory and mean identified

[b] Unit is frequency dependant. Given here for ω=1 rad/s.

Fig. 3.12 shows the spectra of the theoretical model, of the measured data from the *in-vitro* experiment and of its corresponding fit. Qualitatively, the identification describes correctly the discrete data points, though the larger dispersion at frequencies above 3 Hz are responsible for the high MSE of the fit. Moreover, as reflected by the difference on R in Table 3.3, the real part of the experimental impedance is slightly above the theoretical one. The two reactances, however, are close to each other up to approximately 2 Hz which is the frequency range where the mechanical lung dynamics are driving the impedance.

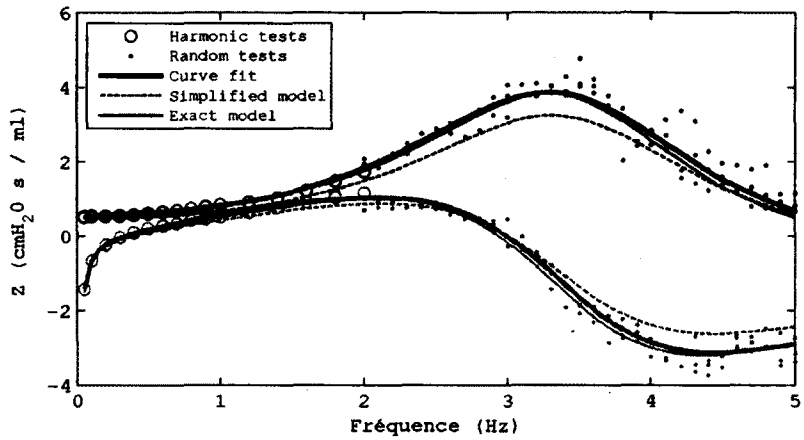

Figure 3.12 Impedance spectrum of the mechanical model lung with PFC. Black lines: real part, gray lines: imaginary part. MSE=0.0224 $(\mathrm{cmH_2O\ s/ml})^2$

In-vivo results

10 lambs out of the 13 were kept, because one had a perfluorothorax, another had idiopathic hemothorax (prior to total liquid ventilation initiation) and the data for the last one exhibited extraordinary large dispersion: the MSE of the fits (both at the end of inspiration and expiration) were more than twice higher than the average MSE of all *in-vivo* experiments. Similarly, only one of the two measurement series was considered for three of the remaining lambs. Their state evolved too much between the two series and pooling the data would have produced a too large MSE.

Fig. 3.13 shows an example of an *in-vivo* measurement. The most remarkable difference with *in-vitro* tests is the curvature of the real part of Z_{RS} at the lower frequencies. This qualitatively indicates the presence of a dissipative phenomenon at low frequency, suggesting the expression of a fractional order behavior. However, this fractional behavior can difficultly be observed in a Bode plot representation, as in Fig. 3.13(b), where this quantity is the ratio $\phi(f)/90^\circ$ for $f \to 0$ because the phase $\phi(f)$ is not constant.

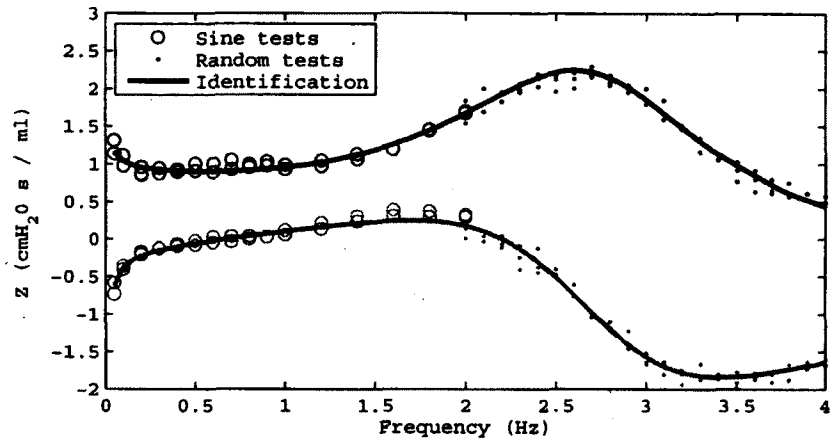

(a) Re-Im representation. Black lines: real part, gray lines: imaginary part.

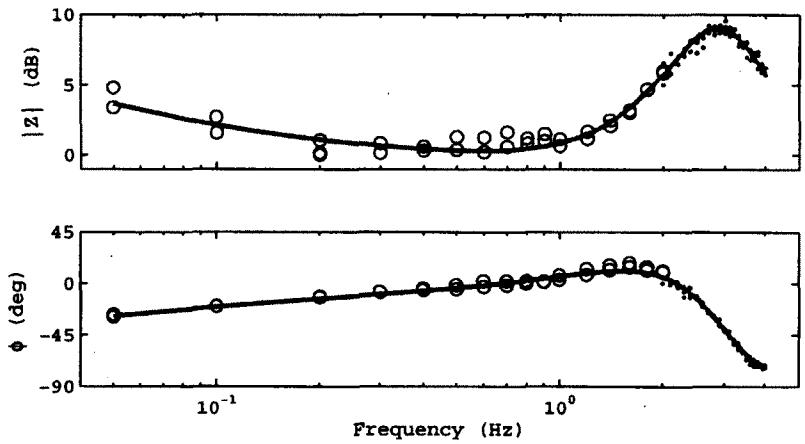

(b) Bode plot representation. Solid lines: Identified model

Figure 3.13 Example of an *in-vivo* impedance spectrum with PFC. $MSE = 0.0065$ $(\text{cmH}_2\text{O s/ml})^2$

Results for the identified parameters of the curves of Fig. 3.13 are presented in Table 3.4. These numbers reflect more evidently the fractional order of the compliance, with an identified α value of 0.71 [0.614 - 0.806], and the one of the inertance with $\beta = 1.17$ [1.10 - 1.23].

The respiratory system parameters for all considered lambs are shown as box plots on Fig. 3.14. The major observation, that also arose in (Bossé *et al.*, 2010), to make from this box plot is that there were no significant difference on the mechanics between end inspiratory (E.I.) and end expiratory (E.E.) experiments.

Tableau 3.4 Example of *In-vivo* measured parameter values and 95% confidence bounds [95% C.B.]

Parameter	Identified	
	Value	95% C.B.
R(cmH_2O s/ml)	0.868	[0.807 - 0.929]
I(cmH_2O s^2/ml)	0.0534	[0.0464 - 0.0604]
β (-)	1.17	[1.10 - 1.23]
C(ml/cmH_2O)	3.26	[2.71 - 3.81]
α (-)	0.710	[0.614 - 0.806]
ω_{res} (rad/s)	17.9	[17.6 - 18.3]
ζ_{res} (-)	0.314	[0.299 - 0.329]
d_{res} (s)	0.0140	[0.0100 - 0.0180]
MSE (cmH_2O s/ml)^2	6.5×10^{-3}	–

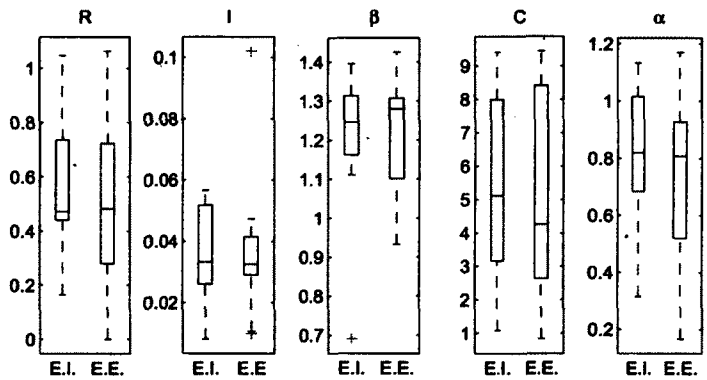

Figure 3.14 Box plots for the identified respiratory system parameters. n=10. E.I.: End of inspiration; E.E.: End of expiration

The median values for the combined (E.I. & E.E.) data for all considered lambs are presented in Table 3.5. Of note is the high variability of many parameters (R, I, α, C, d_{res}), where the interquartile range is of comparable magnitude than the median value. By opposition, β was always close to 1.2-1.3, suggesting that the fractional order of the inertance would be more characteristic to the system than the one of the compliance.

3.2.5 Discussion

Validity of the identification procedure

In-silico results show that the identification procedure runs successfully, despite the added noise. This noise addition yields a mean MSE of 6.03×10^{-3}, which is also typical of the *in-vivo* measurements (see Table 3.5), so it can be concluded that the routine was tested

Tableau 3.5 Summary of the combined results for the 10 lambs. Data presented as median [interquartile range]

Parameter	Value	
R (cmH_2O s/ml)	0.482	[0.369]
I (cmH_2O s^2/ml)[a]	0.0325	[0.0171]
β (-)	1.26	[0.17]
C (ml/cmH_2O)[a]	5.10	[5.40]
α (-)	0.807	[0.395]
ω_{res} (rad/s)	16.6	[3.1]
ζ_{res} (-)	0.289	[0.027]
d_{res} (s)	0.0362	[0.0273]
MSE (cmH_2O s/ml)^2	0.0050	[0.0046]

[a] Unit is frequency dependant. Given here for ω=1 rad/s..

in realistic experimental conditions. The identification is considered unbiased because the maximal relative bias of 2% is much less than the usual confidence intervals around the parameters found with experimental data.

Validity of the measurements

The identified systems were excited by periodic signals, as close to pure sine waves as practically realizable. Under the hypothesis that the measured system (i.e. the flexible tubing and the respiratory system) behaves as a low-pass filter, the transfer function at the test frequency is considered as the ratio of the output to the input at that given frequency only, independent of any higher-frequency component. In typical system analysis, the describing function is obtained by varying the test signal amplitude and plotting the system gain versus excitation amplitude (Slotine et Li, 1990). This approach was not realizable *in-vivo* with single-frequency excitations for the overall measurement time would be excessively long. A fixed-amplitude approach — aimed to remain in the linear regime — was instead used for this first FOT study in TLV. The fact that C does not vary with lung volume (see Fig. 3.14) validates the assumption of the linearity of the PV curve for the chosen TLV settings. Moreover, a low Reynolds number (Re < 1000) associated with the 7.5 ml/s flow amplitude in the ET makes it reasonable to assume linearity of the resistance as well.

As pointed out in the description of the *in-vitro* results, the very low MSE ($\approx 10^{-6}$ cmH_2O s/ml) of the fit over the theoretical model, as well as α and β values close to 1, indicate the mechanical model lung should behave as a RIC system. Whereas I, β, C and α are adequately close to the expected values, the large difference between expected and measured R values is most probably due to use of K_{exit} to model the resistance due

to the connection between the vertical column and the horizontal tube. It is known that such coefficients are only rough approximations to describe much more complex flows so this difference doesn't affect the validity assessment of the measurement method, specially since all the other parameters are correctly measured.

Concerning the ventilator tubing dynamics, only the resonant frequency varies significantly between *in-vitro* and *in-vivo*. This shift is most probably caused by the fact that *in-vitro* tests were conducted at room temperature while the tubing softens with increasing temperature.

Fractional order behavior of the respiratory system

The fractional behavior of the inertance term is not evident on either representation of the measured respiratory system impedance. The fact that it manifests itself in the same frequency range as the tube resonance can certainly account for this, so does it's relatively close to unity value. Consequently, the presented experiments can not conclude whether or not the median $\beta = 1.26$ represents a real dynamic of the respiratory system or an artefact from the respirator tubing oscillations. Future experiments incorporating a measurement of the unsteady flow directly at the trachea should be able to provide a more definitive answer.

However, the influence of the α parameter is clearly visible in the Re-Im representation of Z_{RS}, indicating different dynamics than what a RIC system would exhibit. In the explored frequency range, these dynamics are adequately modeled by a fractional order of the compliance term. The Bode plot representation of Fig. 3.13(b) alone doesn't allow the authors to conclude about the presence of such fractional order because the data don't extend enough in the low frequencies for the phase to be constant. Though this seems to call for an exploration of the very low frequency impedance, such experiments would be unpracticable on an *in-vivo* model since they would require very large volume variations for a given measurable flow, as well as test durations that would seriously impair the quality of the animals' blood gases. For this practical reason, together with the fact that these models are more and more common in gas ventilation, a fractional order compliance term was determined to be the best way to explain the frequency-dependance of the real part of Z_{RS} observed in TLV.

Limitations of this study: next steps towards clinical practice

The method proposed here should be developed a little further prior to its application in the clinical context. First, the use of multifrequency signals would considerably shorten the duration of the mechanics measurement protocol, thus reducing time-evolution biases

and making the overall procedure easier both for the clinician and the patient. However the linearity of the measured system has to be more broadly assessed prior to the use of such test signals. Concretely, this means that the presented procedure should be conducted in a range of excitation amplitudes and show no notable difference between those.

Second, a measurement of the unsteady flow at the trachea should be implemented to remove any ambiguity of the behavior of Z_{RS} at frequencies close to the flexible tubing resonance. This element will be crucial to conclude about the existence of a fractional order on the inertance term, and would reduce uncertainty on respiratory system parameters by alleviating the need to fit the three $F(f)$ parameters.

3.2.6 Conclusion

A procedure for measuring the respiratory mechanics in TLV was presented. It consists of an adaption of the standard low-frequency FOT method, with nonlinear regression of the data in the frequency domain to obtain relevant parameter estimation. The identification was validated on 1000 randomly generated data sets, and the complete measurement protocol was validated by measuring the parameters of a mechanical RIC setup.

A 5-CPM lung model was used to describe observed *in-vivo* data. While a fractional order on the compliance term is mandatory to explain the low-frequency behavior, no conclusion can be made regarding the presence of a fractional order on the inertance term. Consequently, a usual CPM description of the respiratory mechanics seems appropriate in TLV until more is known on the respiratory mechanics above 2 Hz. However, expressing the CPM in terms of $RIC\alpha$ is currently preferred over a $RIGH$ parameterization, the former being more generic, because there are no experimental facts justifying that the fractional order would indicate tissue dynamics.

Even though the 5-CPM and fluid system parameters present noticeable variability between experiments, these eight values will be useful for future design of pressure controllers for TLV systems. Good knowledge of the ventilator and respiratory system dynamics, together with their expected variation range, will allow more efficient and robust loop shaping, improving the safety and efficacy of TLV pressure regulated modes.

The further step in impedance studies in TLV should involve more detailed mechanistic impedance models that could predict and explain the fractional order based on lung morphology and fluid dynamics in TLV.

Acknowledgment

The authors would like to thank Nathalie Samson for her assistance for *in-vivo* experiments as well as Raymond Robert for the development the prototype used in the experiments.

CHAPITRE 4

Résultats

4.1 Article : «Ventilation liquidienne totale néonatale : est-ce que la technique des oscillations forcées à basse fréquence est appropriée pour la détermination de la mécanique respiratoire ?»

4.1.1 Avant-propos

Auteurs et affiliation : D. Bossé : étudiant au MD-MSc, Université de Sherbrooke, Faculté de médecine et des sciences de la santé, Département de physiologie-biopysique.

A. Beaulieu : étudiant à la maîtrise, Université de Sherbrooke, Faculté de génie, Département de génie mécanique.

O. Avoine : étudiant au doctorat, Université de Sherbrooke, Faculté de médecine et des sciences de la santé, Département de physiologie-biopysique.

P. Micheau : Professeur titulaire, Université de Sherbrooke, Faculté de génie, Département de génie mécanique.

J.P. Praud : Professeur titulaire, Université de Sherbrooke, Faculté de médecine et des sciences de la santé, Département de pédiatrie.

H. Walti : Professeur titulaire, Université de Sherbrooke, Faculté de médecine et des sciences de la santé, Département de pédiatrie.

Date de soumission : 15 septembre 2009

Date d'acception : 8 juin 2010

État de l'acceptation : version finale publiée

Revue : Journal of Applied Physiology

Titre français : Ventilation liquidienne totale néonatale : Est-ce que la technique des oscillations forcées à basse fréquence est appropriée pour la détermination de la mécanique respiratoire ?

Contribution au document : Cet article contribue au mémoire en précisant la méthodologie des expérimentations *in vivo*, les résultats et leur interprétation physiologique. La présentation des résultats d'impédance pour différentes conditions expérimentales ainsi que leur analyse sous l'angle de la physiologie, contiennent donc l'information jusqu'ici manquante et permettant de mieux saisir le projet dans sa globalité.

Résumé français : *Introduction* Cette étude vise à implanter la technique des oscillations forcées à basse fréquence (TOF-BF) en ventilation liquidienne totale (VLT) néonatale, et a fournir un premier aperçu de l'impédance respiratoire sous cette nouvelle méthode de ventilation. *Méthode* Treize agneaux nouveau-nés d'une masse de 2.5 ± 0.4 kg (moyenne±écart-type) ont été intubés, anesthésiés, puis placés en VLT en utilisant un respirateur liquidien spécifiquement conçu et un perfluorocarbone liquide. Le protocole de mesure de la mécanique respiratoire est débuté immédiatement après le début de la VLT. Trois blocs de mesures ont tout d'abord été réalisés : un durant l'adaptation du système respiratoire à la VLT, suivi de deux autres en condition de régime établi. Les agneaux ont été ensuite divisés en deux groupes avant une autre série de trois blocs de mesure : le premier groupe a reçu une injection i.v de salbutamol (1.5μg/kg/min) pendant 10 min, alors que le second a reçu un bandage de poitrine. L'impédance du système respiratoire a été mesurée en utilisant une série d'essais harmoniques entre 0.05 Hz et 2 Hz, et le modèle à phase constante (« *constant-phase model* ») a été ajusté sur la réponse en fréquence. *Résultats* La résistance et l'inertance des voies aériennes sont grandement augmentés en VLT en comparaison de la ventilation gazeuse, avec une fréquence de résonnance ≤ 1.2 Hz. La résistance et la réactance à 0.2 Hz sont sensibles à la bronchoconstriction et

dilatation, autant que lors de la réduction de compliance. *Conclusions* Nous présentons une application réussie de la TOF-BF en ventilation liquidienne néonatale, ainsi qu'un premier aperçu de l'impédance respiratoire sous cette nouvelle méthode de ventilation. Nous montrons que la TOF-BF est un outil efficace pour suivre la mécanique respiratoire en VLT.

Note : Bien que A. Beaulieu ne soit pas le premier auteur de cet article, les résultats présentés sous l'angle de la physiologie sont jugés pertinents dans le cadre du mémoire pour comprendre les implications du projet dans son ensemble. La contribution de M. Beaulieu au travail de recherche décrit dans cet article est axée sur le développement de la méthode expérimentale et le traitement des résultats.

Neonatal Total Liquid Ventilation: Is Low Frequency Forced Oscillation Technique Suitable for Respiratory Mechanics Assessment ?

D. Bossé[a], A. Beaulieu[b], O. Avoine[a], P. Micheau[b], J.-P. Praud[a,c], H. Walti[a,c]

[a] *Faculté de Médecine et des Sciences de la Santé de l'Université de Sherbrooke, Département de Pédiatrie, Sherbrooke, Québec, Canada.*

[b] *Faculté de Génie de l'Université de Sherbrooke, Département de Génie Mécanique, Sherbrooke, Québec, Canada.*

[c] *Faculté de Médecine et des Sciences de la Santé de l'Université de Sherbrooke, Département de Physiologie et de Biophysique, Sherbrooke, Québec, Canada.*

Abstract

Background. This study aimed to implement low-frequency forced oscillation technique (LFFOT) in neonatal total liquid ventilation (TLV) and to provide the first insight into respiratory impedance under this new modality of ventilation. *Method.* Thirteen newborn lambs weighing 2.5±0.4 kg (mean±SD) were premedicated, intubated, anesthetized, and then placed under TLV using a specially-design liquid ventilator and a perfluorocarbon. The respiratory mechanics measurements protocol was started immediately after TLV initiation. Three blocks of measurements were first performed: one during initial respiratory system adaptation to TLV, followed by two others series during steady state conditions. Lambs were then divided into two groups prior to undergoing another three blocks of measurements: the first group received a 10-min i.v. infusion of salbutamol (1.5 μg/kg/min) after continuous infusion of methacholine (9 μg/kg/min) while the second group of lambs was chest-strapped. Respiratory impedance was measured using serial single-frequency tests at frequencies ranging between 0.05-2 Hz and then fitted with a constant-phase model. 0.2 Hz harmonic test signals were also launched every ten minutes throughout the measurement protocol. *Results.* Airway resistance and inertance were starkly increased in TLV compared to gas ventilation with a resonant frequency $\leq$ 1.2 Hz. 0.2 Hz resistance and reactance were sensitive to bronchoconstriction and dilation as well as during compliance reduction. *Conclusions.* We report successful implementation of LFFOT to neonatal total liquid ventilation and present the first insight into respiratory impedance under this new modality of ventilation. We show that LFFOT is an effective tool to track respiratory mechanics under TLV.

Key Words: Lung Function Test ; Perfluorocarbons ; Mechanical ventilation ; Sheep ; Metacholine Chloride

4.1.2 Introduction

The advent of neonatal liquid assisted ventilation (LAV) has concurred with global efforts to perfect strategies of ventilation improving the morbidity and mortality of several clinical conditions such as meconium aspiration and infant respiratory distress syndrome, while minimizing ventilator induced injuries. To date, two type of LAV have been used: partial liquid ventilation (PLV) (Fuhrman *et al.*, 1991) and total liquid ventilation (TLV) (Wolfson et Shaffer, 2004, 2005). The former consists in partly filling the lungs with a liquid, usually a perfluorocarbon (PFC), while a conventional gas ventilator allows gas exchanges. In contrast, during TLV, lungs are completely filled with PFC and a dedicated liquid ventilator (Robert *et al.*, 2006) ensures the oxygenation of the fluid and the renewal of a tidal volume of liquid. TLV appears to be superior to VLP (Tarczy-Hornoch *et al.*, 2000; Wolfson et Shaffer, 2005) and offers many advantages over conventional mechanical ventilation. Among others, TLV has anti-inflammatory (Rossman *et al.*, 1996; Smith *et al.*, 1995; Thomassen *et al.*, 1997; Varani *et al.*, 1996), recruits atelectatic zones of the lung (Wolfson *et al.*, 1992), homogenizes ventilation (Wolfson et Shaffer, 2005) and pulmonary blood flow distribution (Lowe et Shaffer, 1986), and reduces inflation pressure by increasing lung compliance (Wolfson et Shaffer, 2005). Thus, TLV improves blood oxygenation and reduces occurrence of baro-/volutrauma (Greenspan *et al.*, 2000; Wolfson et Shaffer, 2005). Moreover, tidal volumes of liquid allow meconium, exudate, and mucus removal and filtering (Wolfson *et al.*, 2008) while ensuring adequate ventilation.

A total liquid ventilator must resemble other conventional ventilators except that it must be able to conduct ventilation with a perfluorocarbon fluid (Costantino *et al.*, 2009). Various types of liquid ventilators have been developed for conducting animal experiments (Baba *et al.*, 1996; Heckman *et al.*, 1999; Larrabe *et al.*, 2001; Parker *et al.*, 2009), however our fourth prototype developed at the Université de Sherbrooke for experimental research on animal models of newborns (Inolivent-4) includes the latest up-to-date devices, findings and control algorithms. In vivo experimental results with this prototype have demonstrated its efficiency in maintaining adequate gas exchange, normal acid-base equilibrium and greater minute ventilation whilst nearing flow limits (Robert *et al.*, 2009a).

As during conventional mechanical ventilation, knowledge of the respiratory mechanics during TLV is of great interest since it affords valuable insight into the lung state as well as into underlying disease pathophysiology. Similarly, knowledge of the respiratory mechanics helps clinicians to optimize ventilation, follow treatment progression, plan timely weaning, and prevent iatrogenic injuries (Grinnan et Truwit, 2005a; Pelosi et Gattinoni, 2000; Polese *et al.*, 2005). The low-frequency forced oscillation technique (LFFOT) (Sly

et al., 1996) appears particularly well suited for this purpose. Readers are referred to review articles for a complete understanding of the technique (Goldman, 2001; Navajas et Farré, 1999; Oostveen *et al.*, 2003). Briefly, LFFOT is a non-invasive technique to measure respiratory impedance (ZRS), from which mechanical properties of the overall respiratory system (resistance, elastance, and inertance) can be derived. Interestingly, this technique also enables the use of parametric models to discriminate the contribution of both tissues and airways to respiratory mechanics (Goldman *et al.*, 2005; Hall *et al.*, 2000; Pillow *et al.*, 2005). Furthermore, it appears to be more sensitive to subtle mechanical changes than other lung function testing (Skloot *et al.*, 2004) and has already been used successfully in human infants (Beydon *et al.*, 2007; Petak *et al.*, 1997; Pillow *et al.*, 2005; Sly *et al.*, 1996) and a preterm ovine model (Pillow *et al.*, 2004a,b), as well as during bronchoprovocation challenges (Bayat *et al.*, 2009; Hall *et al.*, 2001). Finally, since it does not require active collaboration of the patient, LFFOT can be easily performed during mechanical ventilation, especially under general anesthesia and curarization (Farre *et al.*, 1995; Navajas *et al.*, 1990).

However, unlike conventional mechanical ventilation, there is so far only scarce information relative to dynamic respiratory mechanics during TLV (Alvarez *et al.*, 2009; Larrabe *et al.*, 2001; Wolfson *et al.*, 1992). In the present study, we implement for the first time LFFOT to a total liquid ventilator and test whether this technique enables reliable respiratory mechanics characterization during neonatal total liquid ventilation. For this purpose, we used healthy newborn lambs under steady state ventilation conditions and assessed LFFOT responsiveness to changes in respiratory mechanics using methacholine (MCh) and salbutamol infusion as well as chest bandage.

Glossary

CPM	Constant-phase model
f	Frequency (Hz)
f_{res}	Resonant frequency (Hz)
FRF_1	Frequency-response complex function (cmH_2O / mL)
G	Tissue damping ($cmH_2O \cdot s$ / mL at 1 rad/s)
GV	Gas ventilation
$\hat{G}_{XY}$	Cross-spectral density function estimate between X and Y
H	Tissue elastance ($cmH_2O \cdot s$ / mL at 1 rad/s)
$\mathrm{Im}(Z_{RS})$	Imaginary part of respiratory system impedance ($cmH_2O \cdot s$ / mL)
I_{RS}	Respiratory system inertance ($cmH_2O \cdot s^2$ / mL)
j	Imaginary unit ($\sqrt{-1}$)

LFFOT	Low frequency forced oscillation technique
MCh	Methacholine
P	Indicates pressure signal (subscripts)
P_{aw}	Airway pressure (cmH_2O)
$PEEP$	Positive end-expiratory pressure (cmH_2O)
$PEEP_{ref}$	Reference positive end-expiratory pressure (cmH_2O)
PFC	Perfluorocarbon fluid
R_{aw}	Airway resistance ($cmH_2O \cdot s$ / mL)
$\mathrm{Re}(Z_{RS})$	Real part of respiratory system impedance ($cmH_2O \cdot s$ / mL)
RN	random noise
R_{RS}	Respiratory system resistance ($cmH_2O \cdot s$ / mL)
SD	Standard deviation
TLV	Total liquid ventilation
V	Indicates volume signal (subscripts)
V_{pump}	Volume measured at the piston pump (mL)
X_{RS}	Respiratory system reactance ($cmH_2O \cdot s$ / mL)
Z_{RS}	Respiratory system impedance ($cmH_2O \cdot s$ / mL)
Z_{total}	Total impedance (respiratory system + ventilator components) ($cmH_2O \cdot s$ / mL)
α	Fractional exponent
γ^2	Coherence function
η	Tissue hysteresivity $= G/H$
ω	Angular frequency (rad/s)

4.1.3 Materials and Methods

Experimentation was performed in accordance with the Canadian Council on Animal Care guidelines for the care and use of laboratory animals and was approved by our institutional Ethics Committee for Animal Care and Experimentation.

Animal Preparation

Thirteen term and healthy newborn Romanov lambs (six females and seven males) weighing on average 2.5 (0.4 kg (SD) and < 5 days of age (see table 1 for lamb characteristics), were premedicated with intramuscular injections of ketamine (10 mg/kg), atropine (0.1 mg/kg) and midazolam (0.1 mg/kg) together with antibiotics (0.05 mg/kg duplocillin and 5 mg/kg gentamicin). Lambs were secured in supine position on an open cot equipped with a warming carpet and a radiant heater to maintain their central temperature at

Tableau 4.1 Lamb characteristics

Lamb No.	Group	Sex	Weight (kg)
1	Chest-Strapped	M	2.85
2*	Chest-Strapped	M	2.50
3	Chest-Strapped	F	2.06
4	Chest-Strapped	M	1.90
5	Chest-Strapped	F	2.34
11**	Chest-Strapped	F	3.09
13	Chest-Strapped	F	2.45
6*	MCh/Salbutamol	M	3.04
7	MCh/Salbutamol	F	2.54
8	MCh/Salbutamol	F	2.00
9	MCh/Salbutamol	M	2.10
10	MCh/Salbutamol	M	2.06
12	MCh/Salbutamol	M	3.01

Sex and weight distribution within both groups. *Lambs were not considered in the results since lamb 2 had perfluorothorax and *lamb 6* had idiopathic hemothorax (before total liquid ventilation initiation). **Impedance of chest-strapped *lamb 11* was not counted due to a loosening of the bandage during the experiment. M, male; F, female; MCh, methacholine.

39.5 (0.5 °C throughout the experiment. Pressure-regulated volume-control ventilation was initiated (Servo 300 ventilator, Siemens-Elema AB, Solna, Sweden) following orotracheal intubation performed using a 5.5 G cuffed endotracheal tube (Mallinckrodt, St. Louis (MO) USA). Ventilation settings were adjusted as follows: 55 breaths/min with an inspiratory:expiratory ratio = 1:2; tidal volume = 10 mL/kg; positive end expiratory pressure (PEEP) = 4 cm H_2O and fraction of inspired oxygen = 1.0. Oxygen saturation was monitored using a pulse oximeter probe placed on the base of the tail (Radical, Masimo, Irvine (CA), USA) and heart rate was recorded using a Hewlett-Packard cardio respiratory monitor (model HP78342A, Palo Alto (CA), USA). Anesthesia was induced with one intraperitoneal loading dose of thiopental (20 mg/kg) and followed by continuous infusion of 2 mg/kg/h via the left jugular vein. Complete paralysis was achieved with i.v. administration of vecuronium bromide (0.1 mg/kg) every two hours and continuous jugular infusion of 5% dextrose was given at 4 mL/kg/h. The right jugular vein was cannulated in turn to provide eventual i.v. access for methacholine and salbutamol delivery during the respiratory mechanics measurement protocol. A 3Fr 7-cm catheter (PV2013L07, PiCCO catheter, Pulsion Medical System, Munich, Germany) was positioned into the femoral artery using a cut-down procedure for continuous monitoring of blood temperature and mean arterial, systolic, and diastolic pressures. The catheter also provided access for arterial blood gas sampling.

Study design

Total liquid ventilation. Lambs were allowed 20 min for recovery and then gradually shifted from conventional mechanical ventilation to a volume-controlled pressure-limited total liquid ventilation using our specially-designed ventilator (Robert *et al.*, 2009a). Transition was made as quickly as possible using 10 mL aliquots of warmed (39°C), preoxygenated perfluorodecalin (F2 Chemical, Lancashire, UK) and by increasing gas-ventilator PEEP from 4 to 7 cm H_2O . Total number of PFC aliquots was adjusted to achieve lamb calculated functional residual capacity (25 mL/kg). Gas ventilation was then interrupted and total liquid ventilation was intitiated as followed : volume controlled mode, 5.6 breaths/min with an inspiration:expiration ratio = 1:3 ; end-inspiratory and end-expiratory pause = 0.5 s ; tidal volume = 28 mL/kg ; $PEEP_{ref}$ = 5 cmH_2O and fraction of inspired oxygen at 0.95. Inspiration was volume-controlled (Robert *et al.*, 2009a) while expiration was pressure-regulated and volume targeted ; both were pressure limited and time cycled (Robert *et al.*, 2006).

Additional interventions. Sodium bicarbonate or tromethamine was used to maintain pH > 7.25. Crystalloids (bolus of 10 mL/kg lactated Ringer's solution) or vasopressor (dopamine 5 - 20 μg/kg-min) were used as needed to maintain a mean arterial pressure $\geq$ 50 mmHg. The rate of i.v. dextrose infusion was adjusted to maintain glucose blood level at 40-100 mg/dL. Once the protocol completed, the lambs were euthanized with pentobarbital (60 mg/kg) and the lung and thoracic cavity carefully inspected for evidence of perfluorothorax or gross abnormalities.

LFFOT equipment. Our total liquid ventilator prototype (Robert *et al.*, 2009a) was used to generate volumetric harmonic oscillations and record pressure and volume signals at specified expiratory or inspiratory pauses. Airway pressure was measured using a stainless steel capillary tube inserted in the endotracheal tube (ET), its capped end being located approximately 1 cm before ET distal end, thus reducing Venturi effect by measuring pressure in a constant section duct. Four equidistant radial holes ensured static pressure measurements by minimizing dynamic pressure effects. The capillary was connected to the pressure sensor (Model 1620, Measurement Specialties inc, Hampton (VA), USA) with 30-cm long perfusion flexible tubing. The sensor was calibrated *in vitro* using a 1 m high water column, has a precision of $\pm$ 1% and 1.2 kHz bandwidth. Volumetric excitation signals were generated using the ventilator expiratory piston pump while a linear position

sensor (CS-250-AD, MTS Sensors, Cary (NC), USA) measured piston displacement, and hence the volume of PFC in the pump, with a precision of ± 0.15 mL and a bandwidth over 2 kHz. Flow spectra were obtained from Fourier analysis of the position sensor signals as detailed below in the signal-processing section. However, the flexible ventilator tubing adds a resonant behavior to the system and the pressure sensor tubing adds a time delay, which must be measured and compensated for in order to retrieve the respiratory impedance Z_{RS} from the total impedance of the experimental system Z_{total}.

Respiratory mechanics measurement protocol. Respiratory mechanics measurements were divided in six blocks (B) *(figure 4.1)*. While the first block was performed immediately after onset of TLV in order to monitor initial adaptation of the respiratory system to TLV, the next two blocks were performed to characterize TLV steady state. These first series of measurements were conducted similarly on every lamb whereas the last three blocks where used to assess LFFOT sensibility to induced changes in respiratory mechanics *(detailed below)*.

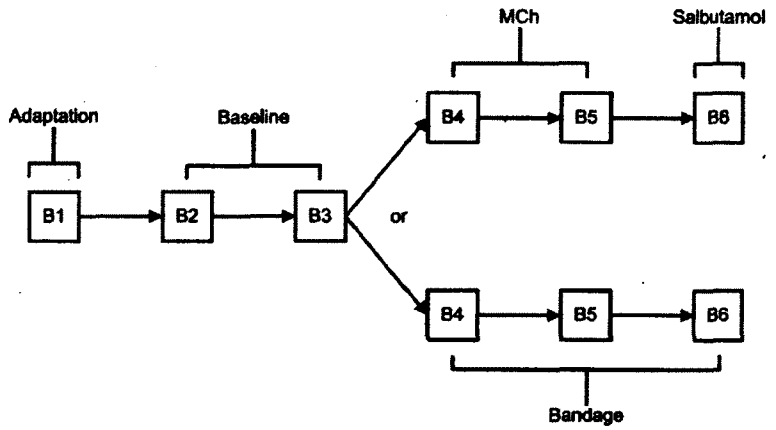

Figure 4.1 Sequential arrangement of the six blocks (B) of measurements over time. Each block was composed of a complete frequency spectrum. Following performance of B1 (adaptation) and B2 and B3 (baseline) in every lamb at the beginning of the experiment, lambs were separated in two groups: one group receiving methacholine (MCh) for two blocks (B4 and B5) followed by salbutamol (B6), and the second group in which lambs were chest-strapped (B4 to B6).

All experimental blocks were started and ended with one random noise signal test for respiratory mechanics assessment between 2 and 4 Hz. Single-frequency signals (DuBois *et al.*, 1956) were launched after the first random noise (Michaelson *et al.*, 1975) and over a narrow spectrum of 0.05 to 2 Hz inclusively, beginning with oscillations at 2 Hz and decreasing up to 0.05 Hz. Tests were interspaced every 0.2 Hz between 2 and 1 Hz

and every 0.1 Hz between 1 and 0.1 Hz with a final test at 0.05 Hz in order to closely characterize low frequency respiratory system impedance. All oscillations were performed at fixed flow amplitude of 7.5 mL/s (i.e., a volume from 11.9 mL at 0.1 Hz down to 0.6 mL at 2Hz), except for the 0.05 Hz sine wave, in which amplitude was set at 5 mL/s (15.9 mL volume) in order to avoid airway collapse and other nonlinearities associated with high volumetric oscillation amplitude.

Forced oscillations were performed during a 30 s apnea except for the 0.05 Hz sinusoid, which necessitated a 45 s apnea to lower the influence of the transients on the spectra. All signals were launched in pairs and at two different lung volumes: the first at end-expiration, the other at end-inspiration. Lambs were allowed a minimum of 30 s between each pair of tests in order to maintain normal blood gases. Consequently, each block lasted between 60 and 90 min. 0.2 Hz tests were repeated every 10-12 min to assess LFFOT and short time variability of respiratory system mechanics, independently of frequency. Arterial blood gas analyses were performed after each 10-min break between the five first blocks of measurements for ventilation recovery.

Lambs were then divided in two groups to assess LFFOT sensitivity to induced respiratory mechanics alterations. Sensitivity to compliance reduction was assessed in 5 lambs by gently wrapping the chest using a 10-cm wide elastic bandage (Elastoplast, BSN medical Ltd, Brierfield, UK). LFFOT performance in tracking resistance changes was assessed in 5 other lambs in two steps. Two blocks of measurement (B4 & B5) were first performed during methacholine (MCh)-induced rise of respiratory resistance. Continuous infusion of MCh was started at 6 μg/kg/min while preventing MCh-induced decline of mean systemic arterial pressure (Welch, 1967a) below 50 mmHg. Dosage was then raised to 9 μg/kg/min after hemodynamic stabilization. Respiratory mechanics measurements began 10 min after ventilator peak pressure reached plateau. Then, a last block of measurements (B6) was carried out after 10-min i.v. infusion of salbutamol (1.5 μg/kg/min) to assess whether bronchodilation can be tracked by LFFOT.

Signal processing. The signal processing methodology followed a typical Welch's overlapped segmented average frequency analysis procedure (Seber et Wild, 2003; Welch, 1967a). Pressure and volume signals were digitized (PCI-DAS1602/16, Measurement Computing, Norton (MA), USA (16 bits resolution, 2 kHz sampling rate)), then digitally low-pass filtered (6^{th} order Butterworth, -3dB cutoff at 10 Hz) and downsampled at 50 Hz for recording. Each recorded test was then divided into overlapping segments (20 s for single-frequency signal, 10 s for noise, 67% overlap) and Hanning windowed. The fre-

quency–response function estimate $FRF_1(f)$, i.e. the transfer function between pump volume and airway pressure, was computed using

$$H_1(f) = \frac{\hat{G}_{VP}(f)}{\hat{G}_{VV}(f)} \tag{4.1}$$

where $\hat{G}_{VP}(f)$ is the averaged cross-spectral density function between airway pressure P_{aw} and pump volume V_{pump} and $\hat{G}_{VV}(f)$ is the averaged autospectral density function of V_{pump}. The total impedance of the respiratory system and the ventilator tubing system, $Z_{total}(f)$, is then given by

$$Z_{total}(f) = \frac{P_{aw}(f)}{\dot{V}_{pump}(f)} = \frac{1}{j2\pi f} H_1(f) \tag{4.2}$$

with $j^2 = -1$..

Finally, coherence function (γ^2) was computed from the spectral analysis of pressure and flow signals.

$$\gamma^2(f) = \frac{\left|\hat{G}_{VP}(f)\right|}{\hat{G}_{PP}(f)\,\hat{G}_{VV}(f)} \tag{4.3}$$

A value of $\gamma^2 \geq 0.95$ was used as the criterion for test acceptance . This overall process is very similar to typical conventional mechanical ventilation forced oscillation technique analysis (Polak *et al.*, 2006).

Parametric identification . Similar blocks of measurements *(see figure 4.1)* were ensemble averaged when possible and a seven-parameter inverse model was fitted to the average spectrum to improve fitting performance. Hence, prechallenge blocks were grouped (B2 & B3) as well as blocks performed during MCh infusion (B4 & B5) and on chest-strapped lambs (B4, B5, & B6). The complete system inverse model (*equation 4.4*) for which parameters needed to be identified consisted of the four-parameter constant-phase model (CPM),$Z_{RS}(j\omega)$ *(equation 4.5)*(Hantos *et al.*, 1992), and a three-parameter linear transfer function representing ventilator flexible tubing dynamics, $Z_{tubing}(j\omega)$ (equation 4.6).

$$Z_{total}(j\omega) = Z_{RS}(j\omega) \cdot Z_{tubing}(j\omega) \tag{4.4}$$

where the respiratory system impedance is

$$Z_{RS}(j\omega) = R_{aw} + j\omega I_{RS} + \frac{G - jH}{\omega^{\alpha}} \tag{4.5}$$

and the flexible tubing impedance is

$$Z_{tubing}(j\omega) = \frac{\omega_n^2}{(j\omega)^2 + 2\zeta\omega_n j\omega + \omega_n^2} e^{-d\,j\omega} \tag{4.6}$$

In the $Z_{RS}(j\omega)$ model, ω is the angular frequency, R_{aw} is the airway resistance, I_{RS} the respiratory system inertance, G the tissue damping, H the tissue elastance and $\alpha = (2/\pi)\cdot\arctan(G/H)$ is a fractional exponent. The flexible tubing impedance was represented by an underdamped oscillation of natural pulsation ω_n and damping factor ζ(Robert, 2007), and a time delay d associated with pressure wave propagation in all flexible tubing (Wang *et al.*, 1997). While these parameters gave no physiological information, their estimation was necessary for ventilator dynamics compensation and respiratory impedance $Z_{RS}(j\omega)$ estimation *(figure 4.2)*.

The seven parameters (i.e. R_{aw}, I_{RS}, G, H, ω_n, ζ and d) were identified by a nonlinear weighted least squares error minimization routine (Seber et Wild, 2003), the Matlab's lsqnonlin function (The MathWorks, Natick (MA), USA), using experimental total impedance from equation 4.2. After a first seven-parameter curve-fit, the ventilator-associated parameters were set constant at the estimated value. The routine was launched a second time over a limited frequency range (0.05-1.75 Hz) to gain more precision on the four CPM parameters. This helped reduce computed parameter confidence intervals, yielding more precise physiological parameter values.

The real part of the respiratory impedance $\mathrm{Re}(Z_{RS})$ is also called the respiratory system resistance (R_{RS}), and comprises airway resistance and tissue damping parameters. Respiratory system inertance and tissue elastance form respiratory system reactance (X_{RS}) which is related to the imaginary part of the impedance $\mathrm{Im}(Z_{RS})$ by $\mathrm{Im}(Z_{RS}) = jX_{RS}$..Graphically, G refers to the frequency-dependent pattern on R_{RS} curve and R_{aw} to its mainly frequency-independent part. H mainly influences X_{RS} at low frequencies, whereas I_{RS} determines its shape for higher f. The discrete frequency that graphically discriminates H and I_{RS} contributions is where $X_{RS} = 0$, and is called the resonant frequency (f_{res}) *(figure 4.2b)*. Hysteresivity was calculated as the ratio between tissue damping and elastance: $\eta = G\ /\ H$(Fredberg et Stamenovic, 1989).

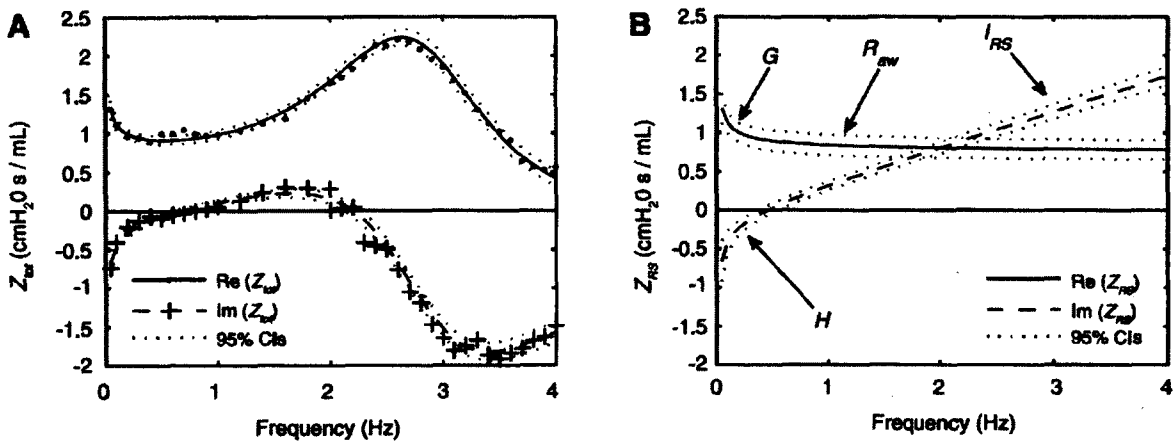

Figure 4.2 **A**: typical experimental total impedance (Z_{tot}) distribution over frequency, with the line representing the seven-parameter inverse model fit on the data. Data are from lamb 11, baseline, end-inspiratory spectrum, fitting error = 0.033. **B**: respiratory system impedance (Z_{rs}) spectrum, given by the constant-phase model fit, after retrieval from the Ztot. Dashed lines and plus signs represent the imaginary part of impedance [Im(Z_{rs})] ; solid lines and dots represent the real part of impedance [Re(Z_{rs})]. Constant-phase model parameters are graphically represented with G (tissue damping). R_{aw} (airway resistance) and H (elastance) were separated from I_{rs} (respiratory system inertance) by f_{res} (resonant frequency). CIs, confidence intervals.

Statistical Methods. Changes in respiratory mechanics parameter following adaptation, MCh and salbutamol infusion, chest-strapping, and between respiratory volumes were computed using Wilcoxon signed-rank tests (SPSS software, v16.0). All data are presented as median and interquartile range (25^{th} - 75^{th} percentile). Statistical significance was assumed at $p \leq 0.05$.

4.1.4 Results

LFFOT implementation in TLV. LFFOT implementation to our total liquid ventilator *Inolivent-4* was straightforward and allowed easy measurement of Z_{RS} in healthy newborn lambs. Ventilator piston pump forced oscillations enabled reliable assessment of total system mechanics using single-frequency signal as well as random noise. Respiratory system impedance was measured at very low frequency ($f \leq$ 2 Hz) using single-frequency testing while impedance of ventilator flexible tubing was dominant over 2 Hz and measured by random noise. For the sake of simplicity, the reader is reffered to table 2 for results concerning 0.2 Hz single-frequency resistance and reactance ($\text{R}_{\text{RS}_0}.2$ and $\text{X}_{\text{RS}_0}.2$) and to table 3 for CPM-derived parameter estimations (R_{aw}, I_{RS}, G, H) throughout the text.

Measurements, performed during several consecutive apneas yielded moderate hypercarbia but no significant hypoxia (see figure 4.3). Arterial oxygen saturation stayed close to 100% but during the methacholine, where saturation decreased down to about 90%. Data are not available after salbutamol infusion since blood gas analyses have been performed following each block of measurements, except after that last one since lambs were euthanized.

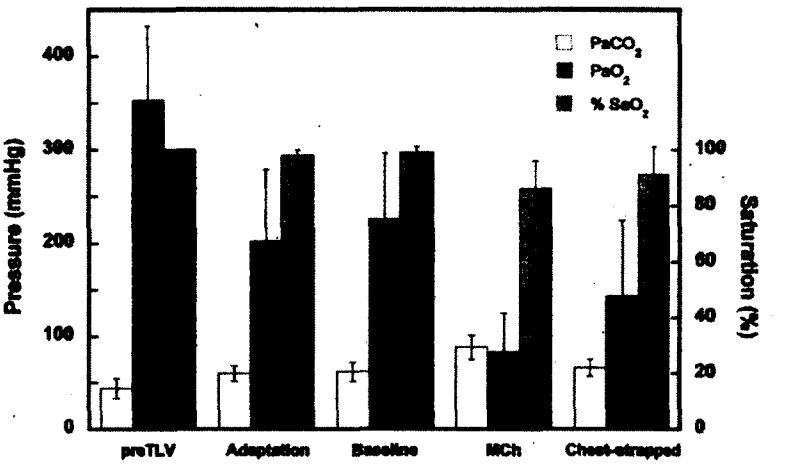

Figure 4.3 Averaged partial pressure of carbon dioxide (PaCO2) and oxygen (PaO2) and arterial saturation in oxygen (%SaO2) for all of the lambs. TLV, total liquid ventilation.

Variability. Mean short-term intra-individual variability that mirrored both the variation in the respiratory resistance over time and the variability of LFFOT was computed using $RRS_0.2$. Interestingly, the coefficient of variation was always lower at end-inspiration than at end- expiration, such that steady state values obtained during baseline for the eleven lambs were 12.4 and 18.5% respectively *(table 2)*. The variability was also higher immediately after TLV initiation (21%) and lower after salbutamol-induced bronchodilation (7%), when the resistive part of impedance was lower. Intra-individual variability was otherwise maintained within 10 – 15 % at end-inspiration and within 16 – 23 % at end-expiration.

Constant-phase model. During baseline conditions *(figure 4.3)*, the frequency-independent part of the R_{RS} curve, associated with airways resistance, was within 0.3 and 1.2 $cmH_2O{\cdot}s/mL$ and preceded by a short frequency-dependent segment related to tissue damping. Note that the pattern of the R_{RS} curves was very similar amongst lambs. Conversely, the dispersion of the X_{RS} curve raised towards higher frequencies, suggesting greater variability of the inertance term. Furthermore, there was a significant inverse Pearson correlation between

Tableau 4.2 Resistance and reactance (in $cmH_2O \cdot s \cdot ml^{-1}$) of the respiratory system as measured using a 0.2-Hz single-frequency signal

	End Inspiration					End Expiration				
	$R_{rs_{0.2}}$		$X_{rs_{0.2}}$			$R_{rs_{0.2}}$		$X_{rs_{0.2}}$		
	Median	IQR	Median	IQR	CV, %	Median	IQR	Median	IQR	CV, %
Adapt	0.75 *†	0.43-0.82	-0.21	-0.44-0.16	20.7	0.87†	0.58-1.19	-0.23	-0.31-0.19	20.7
BL	0.60	0.41-0.81	-0.17	-0.26-0.13	12.4	0.62	0.44-0.86	-0.21	-0.28-0.13	18.5
BL	0.73	0.60-0.75	-0.22	-0.33-0.11	13.4	0.62	0.61-0.86	-0.21	-0.31-0.12	19.0
MCh	0.93*†	0.78-0.99	-0.28	-0.38-0.15	11.4	1.26†	0.95-1.37	-0.26†	-0.53-0.20	16.4
Salbut	0.43†‡	0.35-0.52	-0.15†‡	-0.20-0.09	6.5	0.66	0.64-0.82	-0.17	-0.35-0.12	6.9
BL	0.41	0.36-0.50	-0.16	-0.22-0.12	11.2	0.53	0.42-0.74	-0.24	-0.26-0.13	17.9
Bandage	0.42*	0.40-0.79	-0.22*	-0.54-0.17	15.5	0.74†	0.58-1.11	-0.43†	-0.53-0.24	22.6

Group median respiratory system resistance ($R_{rs_{0.2}}$) and reactance at 0.2 Hz ($X_{rs_{0.2}}$) for each experimental block. Values are presented as median with their respective interquartile range (IQR)=25th to 75th. Coefficient of variation (CV, in percent) provides an insight into mean intraindividual variability within blocks and was computed using $R_{rs_{0.2}}$. Measurements have been performed during initial respiratory system adaptation to total liquid ventilation (Adapt), during continuous MCh infusion (MCh), then after a 10-minutes salbutamol infusion (Salbut), and while lambs were chest-strapped (Bandage). Baseline steady-state condition (BL) values are provided for each of the three conditions. †Statistical difference from the respective baseline; ‡comparison between MCh and salbutamol; *end-inspiration values statistically different from end-expiration values: $p \leq 0.05$.

the lamb weight and f_{res}, with end-inspiratory r = -0.634 ($p = 0.018$) and end-expiratory r = -0.541 ($p = 0.043$). I_{RS} also correlated with weight at both respiratory volumes: (r = 0.627, $p = 0.019$) and ($r = 0.619$, $p = 0.021$) at end-inspiration and end-expiration respectively. Correlation between R_{RS} and weight did not otherwise reach statistical significance.

Continuous intravenous infusion of methacholine. An example of impedance spectra measured pre- and post-methacholine challenge is presented in figure 5a and 5b. Plots show vertical shift of R_{RS} at both respiratory volumes, consistent with an increase in airway resistance. Likewise, $R_{RS_0}.2$ was statistically higher during MCh infusion (*table 2*), although absolute values of CPM-derived resistive parameters (R_{aw} and G) failed to show a significant increase (*table 3*). Finally, $X_{RS_0}.2$was significantly decreased at end-expiration. Note that conversely to the R_{RS} curve, graphical modulations of X_{RS} were quite variable among lambs and therefore no conclusion could therefore be drawn: if elastance appeared right shifted (at frequencies close to zero) owing to MCh infusion, steepness of the curve of reactance however was not consistent among lambs.

Intravenous infusion of salbutamol. Again, figure 5a shows a clear downward shift of the X_{RS} curve after salbutamol infusion as compared to the resistance plateau during methacholine infusion and before challenge. This difference was however substantially reduced at end-expiration (*figure 4b*) compared to end-inspiration. Similarly, both $R_{RS_0}.2$ and $X_{RS_0}.2$ decreased significantly at end-inspiration but not at end-expiration volume, a

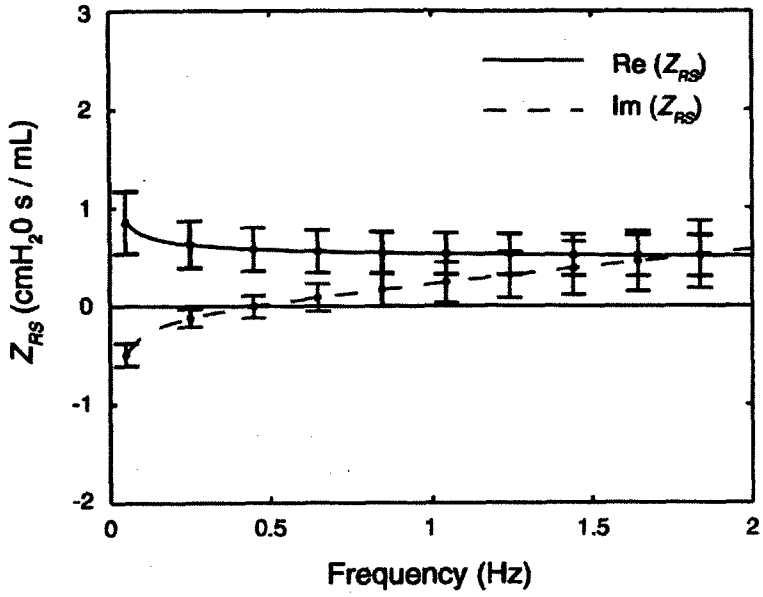

Figure 4.4 End-inspiration Z_{rs} curves of lambs at baseline conditions ($n = 11$). The zero crossing point on the reactance curves represents the f_{res}.

finding that concurs with the plots. CPM parameters failed to report a significant decrease in R_{aw} and G compared to baseline.

Chest-strapping. Respiratory impedance of lambs with a bandage strapped around theirs chest shows graphically revealed an increase in frequency-dependence of R_{RS} at low frequencies (*figure 6a and b*) and a right shift of the X_{RS} curve, consistent with a higher elastance (lower compliance). The later was more convincing at end-expiration (*figure 6b*) than at end-inspiration. $X_{RS_0}.2$ was significantly lower at end-expiration as compared to baseline, but no change in $R_{RS_0}.2$ was found at either volumes. CPM tissue parameters G and H were significantly higher than that observed during baseline at end-expiration volume, while only H was significantly increased at end-inspiration. $R_{RS_0}.2$ and $X_{RS_0}.2$, as G and H, were however all statistically different at end-inspiration as compared to end-expiration.

4.1.5 Discussion

Clinical and physiological implications. We report herein the first implementation of LFFOT to total liquid ventilation as well as provide the first insight into respiratory impedance of newborn lambs under this new modality of ventilation. We present spectral impedance within a very low range of frequencies (0.05 - 2 Hz inclusively) and show that

Tableau 4.3 Low-frequency forced oscillation technique respiratory mechanics during neonatal total liquid ventilation

	Baseline				Challenges			
	End inspiration		End expiration		End inspiration		End expiration	
	Mean	IQR	Mean	IQR	Mean	IQR	Mean	IQR
	Baseline (n=11)				*Adaptation (n=11)*			
R_{aw}, $cmH_2O \cdot s \cdot ml^{-1}$	0.37	0.26-0.53	0.40	0.32-0.55	0.40	0.29-0.64	0.47	0.23-0.86
I_{rs}, $cmH_2O \cdot s^2 \cdot ml^{-1}$	0.06	0.02-0.07	0.06	0.02-0.09	0.05*	0.01-0.08	0.04	0.01-0.07
G, $cmH_2O \cdot ml^{-1}$	0.25	0.05-0.34	0.17	0.11-0.44	0.15	0.04-0.26	0.18	0.02-0.33
H, $cmH_2O \cdot ml^{-1}$	0.25	0.18-0.33	0.28	0.18-0.29	0.26	0.19-0.43	0.31	0.20-0.35
η	0.80	0.25-1.15	0.85	0.32-1.46	0.61	0.26-0.86	0.62	0.15-1.67
	Baseline (n=5)				*Metacholine (n=5)*			
R_{aw}, $cmH_2O \cdot s \cdot ml^{-1}$	0.49	0.29-0.52	0.40	0.32-0.51	0.64	0.27-0.68	0.53	0.25-0.66
I_{rs}, $cmH_2O \cdot s^2 \cdot ml^{-1}$	0.07	0.02-0.09	0.06	0.02-0.09	0.04	0.01-0.09	0.05	0.01-0.08
G, $cmH_2O \cdot ml^{-1}$	0.34	0.16-0.51	0.44	0.24-0.57	0.36	0.19-0.73	0.74	0.30-1.18
H, $cmH_2O \cdot ml^{-1}$	0.30	0.21-0.36	0.29	0.24-0.33	0.34	0.23-0.39	0.34	0.26-0.63
η	1.15	0.58-1.51	1.46	0.74-1.96	0.98	0.68-2.62	1.85	1.17-2.06
	Baseline (n=5)				*Salbutamol (n=5)*			
R_{aw}, $cmH_2O \cdot s \cdot ml^{-1}$	0.49	0.29-0.52	0.40	0.32-0.51	0.30	0.13-0.38	0.34	0.15-0.49
I_{rs}, $cmH_2O \cdot s^2 \cdot ml^{-1}$	0.07	0.02-0.09	0.06	0.02-0.09	0.06	0.02-0.07	0.03	0.02-0.06
G, $cmH_2O \cdot ml^{-1}$	0.34	0.16-0.51	0.44	0.24-0.57	0.09*‡	0.09-0.38	0.30‡	0.20-0.55
H, $cmH_2O \cdot ml^{-1}$	0.30	0.21-0.36	0.29	0.24-0.33	0.21‡	0.19-0.27	0.37	0.28-0.51
η	1.15	0.58-1.51	1.46	0.74-1.96	0.48‡	0.38-1.75	0.92	0.60-1.19
	Baseline (n=5)				*Chest-strapped (n=5)*			
R_{aw}, $cmH_2O \cdot s \cdot ml^{-1}$	0.30	0.25-0.65	0.33	0.28-0.74	0.29	0.09-0.60	0.28	0.00-0.58
I_{rs}, $cmH_2O \cdot s^2 \cdot ml^{-1}$	0.05	0.01-0.06	0.05	0.01-0.07	0.05	0.02-0.07	0.05	0.02-0.07
G, $cmH_2O \cdot ml^{-1}$	0.06	0.05-0.19	0.13	0.07-0.21	0.14*	0.07-0.52	0.53†	0.14-0.96
H, $cmH_2O \cdot ml^{-1}$	0.21	0.17-0.25	0.25	0.20-0.32	0.25*†	0.20-0.30	0.40†	0.26-0.67
η	0.26	0.23-0.87	0.56	0.24-0.83	0.81†	0.27-1.65	0.83	0.55-1.72

Values are presented as median with IQR = 25th to 75th for parameters airway resistance (R_{aw}), respiratory system inertance (I_{rs}), tissue damping (G), tissue elastance (H), and hysteresivity (η), as provided by constant-phase model fitting on respiratory impedance, between 0.05 and 2 Hz. n, No. of animals. Parameter values are given for end-inspiration and end-expiration volumes. *Statistically significant differences; †significant difference between parameters for each condition and its respective baseline; ‡significant difference between MCh and salbutamol: $p \leq 0.05$.

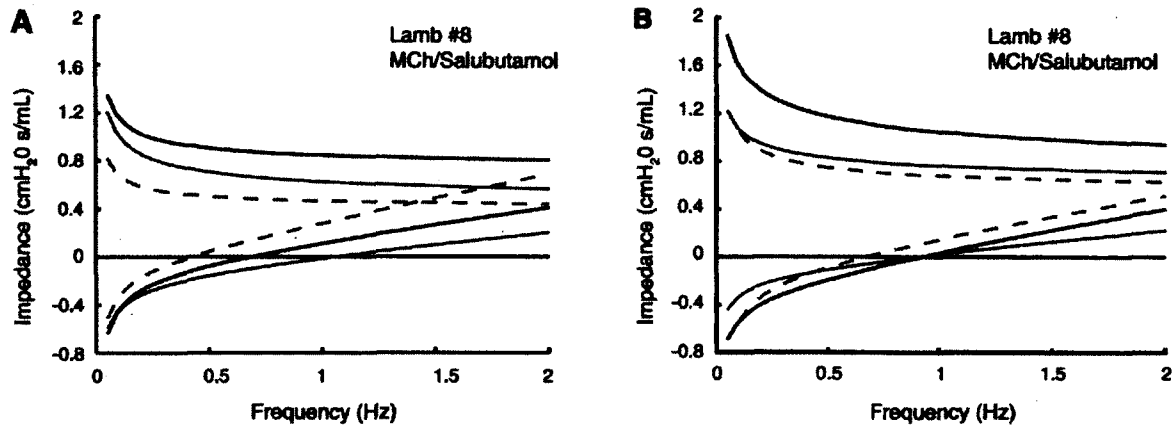

Figure 4.5 Plots exemplifying typical changes (in one lamb) in Z_{rs} during continuous infusion of MCh (dark solid lines) and after a 10-min infusion of salbutamol (dashed shaded lines) compared with baseline Z_{rs} conditions (thin solid lines) at both end-inspiration (**A**) and end-expiration (**B**) volumes.

a single-frequency signal of 0.2 Hz can be a simple and reliable tool to track pulmonary mechanics changes in TLV.

Likewise, since TLV prevents the lung from collapsing below functional residual capacity, several consecutive apneas can be induced without marked hypoxemia. Figure 4.3 shows no significant hypoxemia and moderate hypercarbia throughout the experiment. Blood gas data deteriorated following MCh infusion mainly because of bronchoconstriction. However, theoretical effects of these variations in $PaCO_2$ and PaO_2 on respiratory mechanics were not investigated in the present study.

Methodological considerations. In spite of providing a good fit on our experimental data, the resistive parameters G and R_{aw} were found dependent from each other during the parametric identification process (data not shown). This issue has also been reported by previous investigators (Hantos *et al.*, 2003; Thamrin *et al.*, 2004; Yuan *et al.*, 1998) on conventional gas ventilation and is therefore unlikely to be attributable to PFC fluid in lungs but to the mathematical structure of Z_{RS}. Nevertheless, the dependence between both parameters decreases the sensitivity of the CPM, and excludes reliable partitioning of tissue and airway resistance. This phenomenon may also explain why no significant changes in R_{aw} were found during MCh and salbutamol challenge, albeit R_{RS} modulations were graphically appreciable and noticeable by 0.2 Hz single-frequency signal tests.

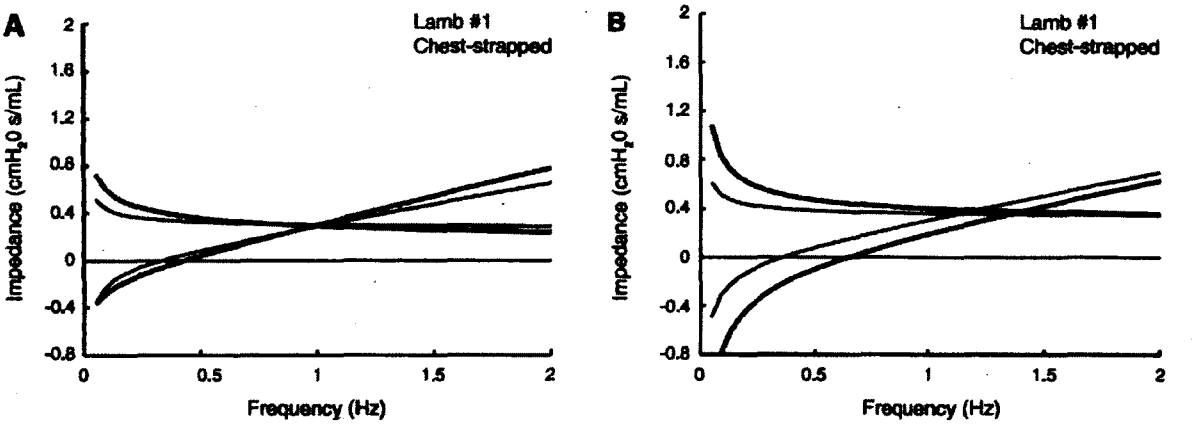

Figure 4.6 Plots exemplifying typical changes in Z_{rs} following chest-strapping of one lamb at both end-inspiration (**A**) and end-expiration (**B**) volumes. Thin line, Z_{rs} at baseline conditions; thick line: Z_{rs} on chest-strapped lamb.

Respiratory mechanics in TLV. Respiratory mechanics of newborn lambs under TLV contrast with that found by other authors working with lambs under gas ventilation (Pillow *et al.*, 2001), mainly by I_{RS} predominance of the reactance spectrum under 2 Hz and a roughly 30 to 40-fold increase in R_{aw}(Robert *et al.*, 2009b). Likewise, we found that f_{res} was predominantly below 1.2 Hz with PFC fluid into the lung *(see figure 4.3)*, comparatively to about 10 Hz with air (Pillow *et al.*, 2001). This left shift of the reactance as well as the increase in I_{RS} and $R_{aw}$where to be expected since 39 (C perfluorodecalin density (1880 kg/m^3) and dynamic viscosity (3.4 mPa·s) are starkly greater than air at the same temperature. These observations also concur with results obtained at low pulmonary volume in partial liquid ventilation (when PFC/air ratio is maximal in the lungs) (Schmalisch *et al.*, 2003). However, compared this latter type of liquid assisted ventilation, respiratory mechanics is much less dependent of lung volumes in TLV and the clinically relevant range of frequency is more confined to very low frequencies ($f \leq$ 2 Hz instead of $f \geq$ 4 Hz in partial liquid ventilation).

CPM spectra, as displayed on figure 4, showed some variability amongst lambs. Of note, part of this variability is inherent to the neonatal animal model itself given that respiratory mechanics varies with height, lung maturity, and alveolarisation of each newborn lamb (Oostveen *et al.*, 2003; Pillow *et al.*, 2005). On the other hand, the contribution of the method, especially the deconvolution process used for separating ventilator tubing dynamics from the respiratory system parameters could not be overlooked as being a contributor to the observed variability.

Adequacy of the constant-phase model to TLV and interpretation. Adequacy of the CPM to explain TLV lung impedance spectra was one of the research hypotheses. While the model could be effectively fitted to TLV experimental data, questions arise regarding its interpretation. While in gas ventilation R_{aw} and I_{aw} refer to the airways mechanics and G and H to the tissue, these assumptions could be misleading in TLV. For instance, a high density PFC flow in the airways could yield non negligible fluid-structure interactions such as elastic deformations and associated structural damping. Therefore, if the general behavior of the respiratory impedance is similar, further evidence is needed to give the gas-CPM parameters the same meaning in TLV.

According to the gas constant-phase theory, tissue damping and elastance should be elementary coupled and therefore, changes in G value should always be followed by H, such as hysteresivity $\eta = G / H$ remains constant (Fredberg et Stamenovic, 1989). However, we observed relatively high variability in parameter η among lambs within the same experimental block as well as from one block to another (*see table 3*). This indicates that Gcould possibly account for other phenomena than pure tissue viscance and therefore its value should be interpreted with precaution. In gas ventilation, the artefactual rise in G has been extensively ascribed to airway inhomogeneities, a phenomenon well described by Lutchen and coworkers (Rossman *et al.*, 1996) and particularly apparent during inhalated MCh challenge, when inhomogeneities are probably greater (Sakai *et al.*, 2001; Tgavalekos *et al.*, 2005; Varani *et al.*, 1996). On the other hand, explanation is unlikely to be true in TLV since airway recruitment and uniform distribution of PFC into the respiratory system enhance ventilation homogeneity and uphold alveolar patency even at end-expiration volume (Greenspan *et al.*, 2000; Wolfson et Shaffer, 2004).

Herein, figure 4.3 shows that the real part of the impedance response, which refers to respiratory system resistance, is only frequency dependent at very low frequencies (typically 0.05 and 0.1 Hz) and constant at upper frequencies. Such distribution of the measured impedance real part implies two possible biases on the value of G: i) parameter G in the CPM equation (*equation 4.4*) is the gain of the frequency-dependence on the real part (inverse of the frequency). However, a good fit is not a guarantee for identification of parameter G of the CPM: if an increase in airway resistances for these low frequency experiments is indeed generated, it will be identified by parameter G. Indeed, it was observed that a too large volume amplitude at low frequencies could generate a nonlinear response of the airways (and eventually collapses, which is equivalent to an increase in airway resistance). Actually, few collapses were observed for the high volume 0.05 Hz tests, but the results were always rejected based on the resulting low coherence values. As suggested in , air-

way collapses in TLV induce neither structural changes in the respiratory system nor any noticeable airway injury, so we can expect that subsequent measurements were unaffected by these events. In spite of the fact that heavily nonlinear responses were discarded from our analysis, an undetected nonlinear behavior of the airways could explain the increase in resistance, and consequently create a bias for the value of G. A recommendation could be to perform measurements at the lowest amplitudes in order to ensure a linear response of the airways. ii) The identification of the parameter G, which characterizes the frequency-dependence, is strongly sensitive of the few very low frequency measurements: a potential noisy measurement on one recording would strongly affect the identified parameter G (and indirectly the estimated parameter R_{aw}). This could explain the large dispersion on the value of G from one experimental block to the other. A recommendation could be to perform more measurements at very low frequencies in order to obtain additional data showing the frequency-dependence of the real part in TLV.

Single-frequency vs. spectral analysis. Authors are aware that spectral analysis would have required multiple-frequency signal tests which afford a more straightforward approach to track respiratory mechanics and reduce temporal bias. However, as a first step in TLV, we reasoned that is was better to use single-frequency signals at $f \leq 2$ Hz, in order to closely characterize respiratory mechanics at very low frequencies with high signal-to-noise ratio (SNR $\geq$ 20 dB) by avoiding flexible tubing resonance excitation. On the other hand, fixed-frequency tests are easy to implement and fairly understandable by clinicians. $\mathrm{RRS}_0.2$ and $\mathrm{XRS}_0.2$ seem particularly suitable in newborn lambs under TLV since they provide a quick overview of respiratory mechanics and show good responsiveness to bronchoconstriction and bronchodilation challenges, as well as to compliance reduction. In fact, the reduction in compliance using bandage wrapping around the lamb's chest induced a significant lowering of $\mathrm{XRS}_0.2$whereas MCh bronchoconstriction induced a significant increase in $\mathrm{RRS}_0.2$, that is at both pulmonary volumes. A higher frequency (*e.g.* 1.0 or 1.5 Hz) reflecting only the frequency-independent resistance (airway resistance) could also be used, for instance, to track airway or endotracheal tube obstruction.

4.1.6 Conclusion

In summary, we have successfully implemented the low frequency forced oscillation technique to neonatal total liquid ventilation and present the first report of respiratory impedance under this modality of ventilation. The process revealed considerable differences between conventional mechanical ventilation and TLV lung mechanics. Namely, the high

viscosity and density of PFC shift frequencies of interest towards lower values and yield considerably higher inertance and resistance values. In addition, we show that a 0.2 Hz single-frequency signal represents an optimal tool to track pulmonary mechanics modulations under diverse physiological circumstances such as bronchoconstriction and dilation as well as compliance reduction. This experiment, the first of a series, is a key element toward enhancing our knowledge of lung dynamics in total liquid ventilation. Further studies will be needed to adapt multiple-frequency signal to TLV in order to improve and enable a more effective assessment of spectral respiratory mechanics at $f \leq 2$ Hz. Moreover, the physiological explanation of the model parameter meaning, mostly unusual G and η values, is yet to be determined. The main long-term objective is to achieve the implementation of LFFOT in future total liquid ventilators ready to be introduced in neonatal intensive care units. Hence, as in gas ventilation, LFFOT is expected to provide insight into treatment progression and help plan optimal weaning procedures in total liquid ventilation.

Acknowledgements

The authors gratefully acknowledge Mrs. Nathalie Carrier for statistical consultations, together with Mr. Raymond Robert and Mrs. Nathalie Samson for their technical assistance. We also acknowledge Pulsion Medical Systems for providing the PiCCO device used for hemodynamic monitoring.

Grants

This work was supported in part by the Fondation des Étoiles and the Faculté de Médecine et des Sciences de la Santé of the Université de Sherbrooke (Perinatal Research Team on Ovines), the Natural Sciences and Engineering Research Council of Canada (NSERC) and the Fonds québécois de la recherche sur la nature et les technologies (FQRNT). P Micheau, J-P Praud and H Walti are members of the FRSQ-funded Centre de Recherche Clinique Étienne-Le Bel of the Centre Hospitalier Universitaire de Sherbrooke.

CHAPITRE 5

Conclusion

5.1 Sommaire

Le but du projet de recherche était de développer du matériel et des méthodes de caractérisation de la dynamique pulmonaire en ventilation liquidienne totale. À cette fin, un débitmètre instationnaire a été conçu et validé. Sa plage de mesure, pour des débits stationnaires, est de 5 ml/s à 60 ml/s, et le dispositif permet de mesurer des débits pulsés d'une fréquence allant jusqu'à 3 Hz.

De plus, la technique des oscillations forcées a été appliquée pour une première fois en VLT. Des mesures ont été réalisées à l'aide de nouvelles fonctionnalités logicielles implantées sur le prototype Inolivent-4. Pour des raisons de synchronisme avec l'étudiant en physiologie qui travaillait sur le même projet, toutefois, toutes ces mesures ont été réalisées avant que le débitmètre instationnaire ne soit implanté. Les spectres d'impédance pulmonaire montrent le comportement d'un système à ordre fractionnaire, lequel peut être décrit par le «*constant-phase model*» tiré de la ventilation gazeuse ou encore par un modèle incluant un ordre fractionnel à la fois sur le terme de compliance et sur celui d'inertance. Toutefois, l'existence de l'ordre fractionnaire sur le terme d'inertance ne peut être affirmée hors de tout doute, car il s'exprime aux mêmes fréquences que les résonances des tubes flexibles du respirateur qui masquent toute autre dynamique. Par ailleurs, l'étude a confirmé que les dynamiques observées se produisent à beaucoup plus basses fréquences en VLT que ce que l'on retrouve en VMC.

Finalement, l'influence de différents challenges pulmonaires sur les données fournies par la TOF en VLT a été étudiée afin de montrer que l'on peut bien suivre l'état du patient avec cette méthode. Les résultats montrent que des essais à une fréquence pure de 0.2 Hz permettent de suivre les changements de mécanique pulmonaire tels que la bronchoconstriction, la bronchodilatation ou la réduction de compliance.

Chacun de ces éléments répond donc à un ou plusieurs objectifs du projet de recherche, et ils proposent ensemble une façon facilement applicable pour mesurer la dynamique pulmonaire en ventilation liquidienne totale.

5.2 Contributions

Les contributions scientifiques amenées par le projet de recherche concernent à la fois le développement des respirateurs liquidiens ainsi que la mesure des propriétés physiologiques des poumons en VLT.

Premièrement, la mesure du débit en continu à la trachée constitue une amélioration aux prototypes Inolivent. En effet, ce débit a toujours été estimé à partir de mesures du volume des pompes. Alors que l'estimation actuelle est validée pour les écoulements stationnaires, l'approche proposée permettra de mieux caractériser les oscillations de débit aux ouvertures et fermeture de valves, et permettra une mesure plus directe pendant les essais d'oscillations forcées. De plus, bien que le concept proposé pour le débitmètre est déjà connu (Foucault *et al.*, 2005), son emploi avec des liquides denses n'avait jamais été expérimenté et a fait l'objet d'un article publié dans *Flow measurement and Instrumentation* (Beaulieu *et al.*, 2011). Dans un autre ordre d'idées, le débitmètre apporte un élément de sécurité à la machine de par la vérification continuelle des volumes lus par les capteurs de position des pompes.

Deuxièmement, le développement de la technique pour appliquer la TOF ainsi que sa validation *in vitro* fera l'objet d'une publication soumise à l'*IEEE Transactions on Biomedical Engineering*. Comme une telle procédure n'a jamais été, à notre connaissance, développée en VLT, il s'agit bien là d'une percée originale réalisée au cours du projet de maîtrise.

La dernière contribution principale concerne la connaissance de la physiologie pulmonaire en VLT. Des spectres d'impédance du système respiratoire en VLT sont en effet pour la première fois publiés (Bossé *et al.*, 2010). Ces données existaient pour la ventilation mécanique conventionnelle et la ventilation liquidienne partielle, mais pas pour le cas de la VLT. L'allure du spectre, son ordre et ses fréquences caractéristiques apporteront à la

communauté une base plus solide pour le développement de modèles d'impédance plus évolués.

5.3 Perspectives

Tout d'abord en ce qui concerne le débitmètre instationnaire, l'étude de validation n'a pas permis de déterminer la cause de la limitation à des fréquences inférieures à 3 Hz du dispositif réalisé. Il sera donc pertinent d'approfondir la caractérisation, que ce soit en utilisant une autre référence liée de façon rigide au venturi ou encore par le développement d'un modèle numérique plus détaillé du comportement lorsque les non-stationnarités deviennent importantes.

Ensuite, comme le projet dans son ensemble consistait en une première exploration de la TOF en VLT, il a pointé plusieurs avenues qu'il serait intéressant d'emprunter. La prochaine étape devrait être de réaliser des mesures d'impédance avec la mesure du débit instantané à la trachée. En ne se préoccupant plus des dynamiques des tubulures entre la pompe et le patient, les mesures du comportement à de plus hautes fréquences gagneront beaucoup en fiabilité. Par la suite, les spectres d'impédance recueillis permettront le développement d'un modèle physiologique du système respiratoire plus évolué. Celui-ci liera le ou les ordres fractionnaires à la géométrie récursive des poumons, un peu comme ce qui a été développé en ventilation gazeuse ces dernières années par l'équipe de Ionescu.

Enfin, d'un point de vue plus clinique, l'amélioration la plus importante de la technique serait d'utiliser des signaux-tests multifréquentiels au lieu d'ondes sinusoïdales. La confirmation de la linéarité du système mesuré ainsi que la détermination du type de signal-test le plus approprié considérant les données ici présentées seront des étapes préalables qui mèneront à cette implantation. Cette dernière, en permettant de recueillir l'ensemble du spectre d'impédance pulmonaire en un seul essai, est nécessaire avant de considérer l'utilisation de la TOF en VLT dans un contexte clinique ou même préclinique.

Liste des références

Alvarez, F. J., Gastiasoro, E., Rey-Santano, M. C., Gomez-Solaetxe, M. A., Publicover, N. G. et Larrabe, J. L. (2009). Dynamic and quasi-static lung mechanics system for gas-assisted and liquid-assisted ventilation. *IEEE Transactions on Biomedical Engineering*, volume 56, numéro 7, p. 1938–1948.

Avoine, O., Bossé, D., Beaudry, B., Beaulieu, A., Albadine, R., Praud, J.-P., Robert, R., Micheau, P. et Walti, H. (2011). Total liquid ventilation efficacy in an ovine model of severe meconium aspiration syndrome. *Crit Care Med.*

Baba, Y., Taenaka, Y., Akagi, H., Nakatani, T., Masuzawa, T., Tatsumi, E., Wakisaka, Y., Toda, K., Eya, K., Tsukahara, K. et Takano, H. (1996). A volume-controlled liquid ventilator with pressure-limit mode: imperative expiratory control. *Artif Organs*, volume 20, p. 1052–1056.

Bagnoli, P., Vismara, R., Fiore, G. B. et Costantino, M. L. (2005). A mechanical model lung for hydraulic testing of total liquid ventilation circuits. *Int J Artif Organs*, volume 28, numéro 12, p. 1232–1241.

Bayat, S., Strengell, S., Porra, L., Janosi, T., Petak, F., Suhonen, H., Suortti, P., Hantos, Z., Sovijarvi, A. et Habre, W. (2009). Methacholine and ovalbumin challenges assessed by forced oscillations and synchrotron lung imaging. *Am J Respir Crit*, volume Car, p. Me.

Beaudry, B. (2009). *L'évaluation et l'optimisation des échanges gazaux dans un oxygénateur de respirateur liquidien.* Mémoire de maîtrise, Université de Sherbrooke.

Beaulieu, A., Foucault, E., Braud, P., Micheau, P. et Szeger, P. (2011). A flowmeter for unsteady liquid flow measurements. *Flow Measurement and Instrumentation*, volume 22, numéro 2, p. 131 – 137.

Beaulieu, A., Micheau, P., Bossé, D., Robert, R., Avoine, O., Praud, J. et Walti, H. (2010). Mechanical impedance of the respiratory system during total liquid ventilation. Dans *1st International Conference on Applied Bionics and Biomechanics.*

Bendat, J. S. et Piersol, A. G. (1980). *Engineering Applications of Correlation and Spectral Analysis.* John Wiley & Sons, New-York.

Beydon, N., Davis, S., Lombardi, E., Allen, J., Arets, H., Aurora, P., Bisgaard, H., Davis, G., Ducharme, F., Eigen, H., Gappa, M., Gaultier, C., Gustafsson, P., Hall, G., Hantos, Z., Healy, M., Jones, M., Klug, B., Lodrup, Carlsen, K., McKenzie, S., Marchal, F., Mayer, O., Merkus, P., Morris, M., Oostveen, E., Pillow, J., Seddon, P., Silverman, M., Sly, P., Stocks, J., Tepper, R., Vilozni, D. et Wilson, N. (2007). An official american thoracic society/european respiratory society statement: pulmonary function testing in preschool children. *Am J Respir Crit Care Med*, volume 175, p. 1304–1345.

Bhutani, V. et Sivieri, E. (2001). Clinical use of pulmonary mechanics and waveform graphics. *Clin Perinatol.*, volume 28, numéro 3, p. 487–503.

Birch, M., MacLeod, D. et Levine, M. (2001). An analogue instrument for the measurement of respiratory impedance using the forced oscillation technique. *Physiol Meas*, volume 22, numéro 2, p. 323–339.

Blom, J. A. (2004). *Monitoring of Respiration and Circulation.* Biomedical Engineering, CRC Press, Boca Raton.

Bossé, D., Beaulieu, A., Avoine, O., Micheau, P., Praud, J.-P. et Walti, H. (2010). Neonatal total liquid ventilation: Is low frequency forced oscillation technique suitable for respiratory mechanics assessment ? *J Appl Physiol*, volume 109, numéro 2, p. 501 – 510.

Brereton, G., Schock, H. et Bedford, J. (2008). An indirect technique for determining instantaneous flow rate from centerline velocity in unsteady duct flows. *Flow Measurement and Instrumentation*, volume 19, numéro 1, p. 9 – 15.

Brereton, G. J., Schock, H. J. et Rahi, M. A. A. (2006). An indirect pressure-gradient technique for measuring instantaneous flow rates in unsteady duct flows. *Experiments in Fluids*, volume 40, numéro 2, p. 238 – 244.

Catania, A. et Ferrari, A. (2009). Development and assessment of a new operating principle for the measurement of unsteady flow rates in high-pressure pipelines. *Flow Measurement and Instrumentation*, volume 20, numéro 6, p. 230 – 240.

Çarpinlioglu, M. O. et Yasar Gündogdu, M. (2001). A critical review on pulsatile pipe flow studies directing towards future research topics. *Flow Measurement and Instrumentation*, volume 12, numéro 3, p. 163 – 174.

Chatburn, R. et Primiano, F. (2001). A new system for understanding modes of mechanical ventilation. *Respiratory Care*, volume 46, numéro 6, p. 604–621.

Coleman, T. et Li, Y. (1996). An interior, trust region approach for nonlinear minimization subject to bounds. *SIAM Journal on Optimization*, volume 6, p. 418–445.

Corno, C., Fiore, G. B., Martelli, E., Dani, C. et Costantino, M. L. (2003). Volume controlled apparatus for neonatal tidal liquid ventilation. *ASAIO J*, volume 49, numéro 3, p. 250–258.

Costantino, M. L. et Fiore, G. B. (2001). A model of neonatal tidal liquid ventilation mechanics. *Med. Eng. Phy.*, volume 23, numéro 7, p. 459 – 473.

Costantino, M. L., Micheau, P., Shaffer, T. H., Tredici, S., Wolfson, M. R., 6th Internationl Symposium on Perfluorocarbon Application et Ventilation, L. (2009). Clinical design functions: round table discussions on the bioengineering of liquid ventilators. *ASAIO J*, volume 55, numéro 3, p. 206–208.

Donaldson, J. R. et Schnabel, R. B. (1987). Computational experience with confidence regions and confidence intervals for nonlinear least squares. *Technometrics*, volume 29, numéro 1, p. 67–82.

Draper, N. et Smith, H. (1998). *Applied Regression Analysis*, 3e édition. John Wiley & Sons, 706 pp. p.

DuBois, A. B., Brody, A. W., Lewis, D. H. et Burgess, B. Franklin, J. (1956). Oscillation mechanics of lungs and chest in man. *J Appl Physiol*, volume 8, numéro 6, p. 587–594.

Durst, F., Melling, A., Trimis, D. et Volkholz, P. (1996). Development of a flow meter for instantaneous flow rate measurements of anaesthetic liquids. *Flow Measurement and Instrumentation*, volume 7, numéro 3-4, p. 215–22.

Durst, F., Ünsal, B., Ray, S. et Trimis, D. (2007). Method for defined mass flow variations in time and its application to test a mass flow rate meter for pulsating flows. *Measurement Science and Technology*, volume 18, numéro 3, p. 790.

Farre, R., Ferrer, M., Rotger, M. et Navajas, D. (1995). Servocontrolled generator to measure respiratory impedance from 0.25 to 26 hz in ventilated patients at different peep levels. *Eur Respir J*, volume 8, p. 1222–1227.

Farre, R., Peslin, R., Rotger, M. et Navajas, D. (1994). Human lung impedance from spontaneous breathing frequencies to 32 hz. *J Appl Physiol*, volume 76, numéro 3, p. 1176–1183.

Farre, R., Rotger, M. et Navàjas, D. (1997). Estimation of random errors in respiratory resistance and reactance measured by the forced oscillation technique. *Eur Respir J*, volume 10, numéro 3, p. 685–689.

Foucault, E., Szeger, P., Laumonier, J. et Micheau, P. (2005). DébitmÃ¨tre instationnaire. Brevet international WO 2005/080924.

Foust, R., Tran, N. N., Cox, C., Miller, T. F., Greenspan, J. S., Wolfson, M. R. et Shaffer, T. H. (1996). Liquid assisted ventilation: An alternative ventilatory strategy for acute meconium aspiration injury. *Pediatr Pulmonol*, volume 21, p. 316–322.

Fredberg, J. J. et Stamenovic, D. (1989). On the imperfect elasticity of lung tissue. *J Appl Physiol*, volume 67, numéro 6, p. 2408–2419.

Fuhrman, B., Paczan, P. et DeFrancisis, M. (1991). Perfluorocarbon-associated gas exchange. *Crit Care Med*, volume 19, p. 712–722.

Goldman, M. (2001). Clinical application of forced oscillation. *Pulm Pharmacol Ther*, volume 14, p. 341–350.

Goldman, M., Saadeh, C. et Ross, D. (2005). Clinical applications of forced oscillation to assess peripheral airway function. *Respir Physiol Neurobiol*, volume 148, p. 179–194.

Gollan, F. et Clark, L. (1966). Survival of mammals breathing organic liquids equilibrated with oxygen at atmospheric pressure. *Science*, volume 152, p. 1755–1766.

Gómez, M. A., Hilario, E., Alvarez, F. J., Gastiasoro, E., Alvarez, A., et Larrabe, J. L. (2005). Respirator system for total liquid ventilation. *World Academy of Science, Engineering and Technology*, volume 11, p. 445 – 450.

Greenspan, J., Wolfson, M. et Shaffer, T. (2000). Liquid ventilation. *Semin Perinatol*, volume 24, p. 396–405.

Grinnan, D. et Truwit, J. (2005a). Clinical review: respiratory mechanics in spontaneous and assisted ventilation. *Crit Care*, volume 9, p. 472–484.

Grinnan, D. C. et Truwit, J. D. (2005b). Clinical review: respiratory mechanics in spontaneous and assisted ventilation. *Crit Care*, volume 9, numéro 5, p. 472–484.

Hall, G., Hantos, Z., Petak, F., Wildhaber, J., Tiller, K., Burton, P. et Sly, P. (2000). Airway and respiratory tissue mechanics in normal infants. *Am J Respir Crit Care Med*, volume 162, p. 1397–1402.

Hall, G., Hantos, Z., Wildhaber, J., Petak, F. et Sly, P. (2001). Methacholine responsiveness in infants assessed with low frequency forced oscillation and forced expiration techniques. *Thorax*, volume 56, p. 42–47.

Hantos, Z., Collins, R., Turner, D., Janosi, T. et Sly, P. (2003). Tracking of airway and tissue mechanics during tlc maneuvers in mice. *J Appl Physiol*, volume 95, p. 1695–1705.

Hantos, Z., Daroczy, B., Suki, B., Nagy, S. et Fredberg, J. J. (1992). Input impedance and peripheral inhomogeneity of dog lungs. *J Appl Physiol*, volume 72, numéro 1, p. 168–178.

He, X. et Ku, D. N. (1994). Unsteady entrance flow development in a straight tube. *Journal of biomechanical engineering*, volume 116, numéro 3, p. 355–360.

Heckman, J., Hoffman, J., Shaffer, T. et Wolfson, M. (1999). Software for real-time control of a tidal liquid ventilator. *Biomed Instrum Technol*, volume 33, p. 268–276.

Hirschl, R., Croce, M., Gore, D., Wiedemann, H., Davis, K., Zwischenberger, J. et Bartlett, R. (2002). Prospective, randomized, controlled pilot study of partial liquid ventilation in adult acute respiratory distress syndrome. *Am J Respir Crit Care Med*, volume 165, p. 781–787.

Hirschl, R. B. (2004). Current experience with liquid ventilation. *Paediatric Respiratory Reviews*, volume 5(Suppl A), p. S339 ?S345.

Ionescu, C. et De Keyser, R. (2006). On the potential of using fractional-order systems to model the respiratory impedance. *Annals of Dunarea de Jos University of Galati*, volume Fascicle 3, p. 57–62.

Ionescu, C. et De Keyser, R. (2008). Parametric models for characterizing respiratory input impedance. *J Med. Eng. Tech.*, volume 32, p. 315–324(10).

Ionescu, C. et De Keyser, R. (2009). Relations between fractional-order model parameters and lung pathology in chronic obstructive pulmonary disease. *IEEE Transactions on Biomedical Engineering*, volume 56, numéro 4, p. 978–987.

Ionescu, C., Derom, E. et Keyser, R. D. (2010a). Assessment of respiratory mechanical properties with constant-phase models in healthy and copd lungs. *Computer Methods and Programs in Biomedicine*, volume 97, numéro 1, p. 78 – 85.

Ionescu, C., Muntean, I., Tenreiro-Machado, J., De Keyser, R. et Abrudean, M. (2010b). A theoretical study on modeling the respiratory tract with ladder networks by means of intrinsic fractal geometry. *Biomedical Engineering, IEEE Transactions on*, volume 57, numéro 2, p. 246 –253.

Ionescu, C., Oustaloup, A., Levron, F., Melchior, P., Sabatier, J. et De Keyser, R. M. (2009a). A model of the lungs based on fractal geometrical and structural properties. Dans *System Identification, Volume 15, Part 1*, IFAC.

Ionescu, C., Segers, P. et De Keyser, R. (2009b). Mechanical properties of the respiratory system derived from morphologic insight. *Biomedical Engineering, IEEE Transactions on*, volume 56, numéro 4, p. 949 –959.

Ionescu, C.-M., Kosinski, W. et Keyser, R. D. (2010c). Viscoelasticity and fractal structure in a model of human lungs. *Archives of Mechanics*, volume 1, p. 21–48.

ISO (1980). 5167:1980, measurement of fluid flow by means of orifice plates, nozzles and venturi tubes inserted in circular cross-section conduits running full.

ISO/IEC (1995). 98:1995, guide to the expression of uncertainty in measurement.

Johnson, A. T. et Bronzino, J. D. (1995). *The Biomedical Engineering Handbook*, chapitre 7 - Respiratory System. CRC, Boca Raton, p. 70 – 86.

Lambossy, P. (1952). Oscillations forcées d'un liquide incompressible et visqueux dans un tube rigide et horizontal. calcul de la force frottement. *Helvetica Physica Acta*, volume 25, p. 371 – 386.

Larrabe, J., Alvarez, F., Cuesta, E., Valls-i Soler, A., Alfonso, L., Arnaiz, A., Fernandez, M., Loureiro, B., Publicover, N., Roman, L., Casla, J. et Gomez, M. (2001). Development of a time-cycled volume-controlled pressure-limited respirator and lung mechanics system for total liquid ventilation. *IEEE Transactions on Biomedical Engineering*, volume 48, numéro 10, p. 1134–1144.

Lauzon, A. M. et Bates, J. H. (1991). Estimation of time-varying respiratory mechanical parameters by recursive least squares. *J Appl Physiol*, volume 71, numéro 3, p. 1159–1165.

Lee, S., Alexander, J., Blowes, R., Ingram, D. et Milner, A. D. (1999). Determination of resonance frequency of the respiratory system in respiratory distress syndrome. *Archives of Disease in Childhood - Fetal and Neonatal Edition*, volume 80, numéro 3, p. F198–F202.

Lorino, H., Mariette, C., Karouia, M. et Lorino, A. M. (1993). Influence of signal processing on estimation of respiratory impedance. *J Appl Physiol*, volume 74, numéro 1, p. 215–223.

Lowe, C. et Shaffer, T. (1986). Pulmonary vascular resistance in the fluorocarbon-filled lung. *J Appl Physiol*, volume 60, p. 154–159.

Lowe, K. (1991). Perfluorochemicals: Blood substitutes and beyond. *Advanced Materials*, volume 3, numéro 2, p. 87–93.

Maki, B. E. (1986). Interpretation of the coherence function when using pseudorandom inputs to identify nonlinear systems. *IEEE Transactions on Biomedical Engineering*, volume BME-33, numéro 8, p. 775–779.

Marraro, G., Bonati, M., Ferrari, A., Barzaghi, M. M., Pagani, C., Bortolotti, A., Galbiati, A., Luchetti, M. et Croce, A. (1998). Perfluorocarbon broncho-alveolar lavage and liquid ventilation versus saline broncho-alveolar lavage in adult guinea pig experimental model of meconium inhalation. *Intensive Care Med*, volume 24, numéro 5, p. 501–508.

Mathieu, B. et Oustaloup, A. (1999). *LA COMMANDE CRONE. Du scalaire au multivariable*, 2e édition. Collection automatique, Hermes Science Publications, 315 p.

Mead, J. et Whittenberger, J. L. (1953). Physical properties of human lungs measured during spontaneous respiration. *J. Appl. Physiol.*, volume 5, p. 779 – 796.

Michaelson, E. D., Grassman, E. D. et Peters, W. R. (1975). Pulmonary mechanics by spectral analysis of forced random noise. *J Clin Invest*, volume 56, numéro 5, p. 1210–1230.

Morris, C. et Forster, F. (2004). Oscillatory flow in microchannels: Comparison of exact and approximate impedance models with experiments. *Experiments in Fluids*, volume 36, p. 928–937.

Navajas, D. et Farré, R. (1999). *Respiratory Mechanics*, chapitre 7 - Oscillation mechanics, European Respiratory monographs, *volume 4*. European Respiratory Society,, p. 112 – 140.

Navajas, D. et Farre, R. (2001). Forced oscillation assessment of respiratory mechanics in ventilated patients. *Crit Care*, volume 5, numéro 1, p. 3–9.

Navajas, D., Farre, R., Canet, J., Rotger, M. et Sanchis, J. (1990). Respiratory input impedance in anesthetized paralyzed patients. *J Appl Physiol*, volume 69, p. 1372–1379.

Oostveen, E., MacLeod, D., Lorino, H., Farre, R., Hantos, Z., Desager, K., Marchal, F. et Measurements, E. (2003). The forced oscillation technique in clinical practice: methodology, recommendations and future developments. *Eur Respir J*, volume 22, p. 1026–1041.

Oswald-Mammosser, M., Charloux, A., Enache, I. et Lonsdorfer-Wolf, E. (2010). The opening interrupter technique for respiratory resistance measurements in children. *Respirology*, volume 15, numéro 7, p. 1104 – 1110.

Parker, J., Sakla, A., Donovan, F., Beam, D., Chekuri, A., Al-Khatib, M., Hamm, C. et Eyal, F. (2009). A microprocessor-controlled tracheal insufflation-assisted total liquid ventilation system. *Med Biol*, volume En, p. Compu.

Pelosi, P. et Gattinoni, L. (2000). *Respiratory mechanics in ARDS: a siren for physicians ? Intensive Care Med*, volume 26, p. 653–656.

Petak, F., Hayden, M., Hantos, Z. et Sly, P. (1997). Volume dependence of respiratory impedance in infants. *Am J Respir Crit Care Med*, volume 156, p. 1172–1177.

Pierce, R. J., Hillman, D., Young, I. H., O'Donoghue, F., Zimmerman, P. V., West, S. et Burdon, J. G. (2005). Respiratory function tests and their application. *Respirology*, volume 10, numéro S2, p. S1 – S19.

Pilbeam, S. P. et Cairo, J. M. (2006). *Mechanical Ventilation: Physiological and Clinical Applications*, 4e édition. Elsevier Science.

Pillow, J., Hall, G., Willet, K., Jobe, A., Hantos, Z. et Sly, P. (2001). Effects of gestation and antenatal steroid on airway and tissue mechanics in newborn lambs. *Am J Respir Crit Care Med*, volume 163, p. 1158–1163.

Pillow, J., Jobe, A., Collins, R., Hantos, Z., Ikegami, M., Moss, T., Newnham, J., Willet, K. et Sly, P. (2004a). Variability in preterm lamb lung mechanics after intra-amniotic endotoxin is associated with changes in surfactant pool size and morphometry. *Am J Physiol Lung Cell Mol Physiol*, volume 287, p. L992–998.

Pillow, J., Sly, P. et Hantos, Z. (2004b). Monitoring of lung volume recruitment and derecruitment using oscillatory mechanics during high-frequency oscillatory ventilation in the preterm lamb. *Pediatr crit care med*, volume 5, p. 172–180.

Pillow, J., Stocks, J., Sly, P. et Hantos, Z. (2005). Partitioning of airway and parenchymal mechanics in unsedated newborn infants. *Pediatr Res*, volume 58, p. 1210–1215.

Pillow, J. J. (2005). High-frequency oscillatory ventilation: Mechanisms of gas exchange and lung mechanics. *Crit Care Med*, volume 33, numéro 3 (suppl), p. S135–S141.

Polak, A. G., Wysoczanski, D. et Mroczka, J. (2006). A multi-method approach to measurement of respiratory system mechanics. *Metrol. Meas. Syst.*, volume 13, numéro 1, p. 3–18.

Polese, G., Serra, A. et Rossi, A. (2005). Respiratory mechanics in the intensive care unit. *Eur Respir Monogr*, volume 31, p. 195–206.

Robert, R. (2007). *Modélisation numérique et stratégies de commande du débit expiratoire pour éviter le collapsus des voies respiratoires en ventilation liquidienne totale.* Thèse de doctorat, Université de Sherbrooke.

Robert, R., Micheau, P., Avione, O., Beaudry, B., Beaulieu, A. et Walti, H. (2009a). A regulator for pressure controlled total liquid ventilation. *IEEE Transactions on Biomedical Engineering*, volume 57, numéro 9, p. 2267 – 2276.

Robert, R., Micheau, P., Beaulieu, A., Avoine, O., Rochon, M. E., Praud, J. P. et Walti, H. (2010). Control of pressure ventilation modes in total liquid ventilation. Dans *1st International Conference on Applied Bionics and Biomechanics.* Venise, Italie, 14 - 16 Octobre.

Robert, R., Micheau, P., Cyr, S., Lesur, O., Praud, J.-P. et Walti, H. (2006). A prototype of volume-controlled tidal liquid ventilator using independent piston pumps. *ASAIO J*, volume 52, numéro 6, p. 638 – 645.

Robert, R., Micheau, P. et Walti, H. (2009b). Optimal expiratory volume profile in tidal liquid ventilation under steady state conditions, based on a symmetrical lung model. *ASAIO Journal*, volume 55, numéro 1, p. 63–72 10.1097/MAT.0b013e3181911821.

Rossman, J., Caty, M., Rich, G., Karamanoukian, H. et Azizkhan, R. (1996). Neutrophil activation and chemotaxis after in vitro treatment with perfluorocarbon. *J Pediatr Surg*, volume 31, p. 1147–1151.

Sakai, H., Ingenito, E., Mora, R., Abbay, S., Cavalcante, F., Lutchen, K. et Suki, B. (2001). Hysteresivity of the lung and tissue strip in the normal rat: effects of heterogeneities. *J Appl Physiol*, volume 91, p. 737–747.

Schlichting, H. (1979). *Boundary-Layer Theory*, 7^{e} édition. McGraw-Hill series in mechanical engineering, McGraw-Hill, 817 p p.

Schlichting, H. et Gersten, K. (2000). *Boundary-Layer Theory*, 8^{e} édition. Springer, New York, NY, 799 p.

Schmalisch, G., Proquitte, H., Schmidt, M., Rudiger, M. et Wauer, R. R. (2005). Inertance measurements by jet pulses in ventilated small lungs after perfluorochemical liquid (pfc) applications. *Physiol Meas*, volume 26, numéro 3, p. 239–249.

Schmalisch, G., Schmidt, M., Proquitté, H., Foitzik, B., RÃ$\frac{1}{4}$diger, M. et Wauer, R. R. (2003). Measurement of changes in respiratory mechanics during partial liquid ventilation using jet pulses. *Crit Care Med*, volume 31, numéro 5, p. 1435–1441.

Seber, G. A. F. et Wild, C. J. (2003). *Nonlinear Regression*, 2^{e} édition. Wiley Series in Probability and Statistics, John Wiley & Sons, 768 p.

Sekins, K. M., Nugent, L., Mazzoni, M., Flanagan, C., Neer, L., Rozenberg, A. et Hoffman, J. (1999). Recent innovations in total liquid ventilation system and component design. *Biomed Instrum Technol*, volume 33, numéro 3, p. 277–284.

Shaffer, T. et Wolfson, M. (1992). Liquid ventilation. *Pediatr Pulmonol*, volume 14, p. 102–109.

Shashikant, M. P., Badellino, M. M., Cooper, B., Shaffer, T. H., Myers, S. I. et Wolfson, M. R. (2002). Physicochemical properties of perfluorochemical liquids influence ventilatory requirements, pulmonary mechanics, and microvascular permeability during partial liquid ventilation following intestinal ischemia/reperfusion injury. *Critical Care Medicine*, volume 30, numéro 10, p. 2300–2305.

Skloot, G., Goldman, M., Fischler, D., Goldman, C., Schechter, C., Levin, S. et Teirstein, A. (2004). Respiratory symptoms and physiologic assessment of ironworkers at the world trade center disaster site. *Chest*, volume 125, p. 1248–1255.

Slotine, J.-J. et Li, W. (1990). *Applied Nonlinear Control*. Prentice Hall.

Sly, P., Hayden, M., Petak, F. et Hantos, Z. (1996). Measurement of low-frequency respiratory impedance in infants. *Am J Respir Crit Care Med*, volume 154, p. 161–166.

Smith, T., Steinhorn, D., Thusu, K., Fuhrman, B. et Dandona, P. (1995). A liquid perfluorochemical decreases the in vitro production of reactive oxygen species by alveolar macrophages. *Crit Care Med*, volume 23, p. 1533–1539.

Suki, B., Barabasi, A. L. et Lutchen, K. R. (1994). Lung tissue viscoelasticity: a mathematical framework and its molecular basis. *J Appl Physiol*, volume 76, numéro 6, p. 2749–2759.

Suki, B., Yuan, H., Zhang, Q. et Lutchen, K. R. (1997). Partitioning of lung tissue response and inhomogeneous airway constriction at the airway opening. *Journal of Applied Physiology*, volume 82, numéro 4, p. 1349–1359.

Tarczy-Hornoch, P., Hildebrandt, J. et Jackson, J. (2000). Gravitational effects on volume distribution in a model of partial and total liquid ventilation. *Respir Physiol*, volume 120, p. 125–138.

Tgavalekos, N., Tawhai, M., Harris, R., Musch, G., Vidal-Melo, M., Venegas, J. et Lutchen, K. (2005). Identifying airways responsible for heterogeneous ventilation and mechanical dysfunction in asthma: an image functional modeling approach. *J Appl Physiol*, volume 99, p. 2388–2397.

Thamrin, C., Janosi, T., Collins, R., Sly, P. et Hantos, Z. (2004). Sensitivity analysis of respiratory parameter estimates in the constant-phase model. *Ann Biomed Eng*, volume 32, numéro 6, p. 815–22.

Thomassen, M., Buhrow, L. et Wiedemann, H. (1997). Perflubron decreases inflammatory cytokine production by human alveolar macrophages. *Crit Care Med*, volume 25, p. 2045–2047.

Tissier, R., Hamanaka, K., Kuno, A., Parker, J. C., Cohen, M. V. et Downey, J. M. (2007). Total liquid ventilation provides ultra-fast cardioprotective cooling. *J Am Coll Cardiol*, volume 49, numéro 5, p. 601–605.

Uchiyama, M. et Hakomori, K. (1983). Measurement of instantaneous flow rate through estimation of velocity profiles. *Automatic Control, IEEE Transactions on*, volume 28, numéro 3, p. 380–388.

Varani, J., Hirschl, R., Dame, M. et Johnson, K. (1996). Perfluorocarbon protects lung epithelial cells from neutrophil-mediated injury in an in vitro model of liquid ventilation therapy. *Shock*, volume 6, p. 339–344.

Venegas, J. G. et Fredberg, J. J. (1994). Understanding the pressure cost of ventilation: Why does high-frequency ventilation work? *Crit Care Med*, volume 22, numéro 9, p. S49–S57.

von der Hardt, K., Kandler, M. A., Fink, L., Schoof, E., Dotsch, J., Bohle, R. M. et Rascher, W. (2003). Laser-assisted microdissection and real-time PCR detect anti-inflammatory

effect of perfluorocarbon. *Am J Physiol Lung Cell Mol Physiol*, volume 285, numéro 1, p. L55–62.

Wang, Y.-Y. L., Chang, C., Chen, J., Hsiu, H. et Wang, W. (1997). Pressure wave propagation in arteries. a model with radial dilatation for simulating the behavior of a real artery. *IEEE Engineering in Medicine and Biology Magazine*, volume 16, numéro 1, p. 51–54.

Weibel, E. R. (1963). *Morphometry of the human lung*. Springer-Verlag, Berlin, Germany, 151 p.

Welch, P. (1967a). A method based on time averaging over short, modified periodograms. *IEEE Transactions on Audio Electroacoustics*, volume AU-15, p. 70–77.

Welch, P. (1967b). The use of fast fourier transform for the estimation of power spectra: A method based on time averaging over short, modified periodograms. *IEEE Transactions on Audio and Electroacoustics*, volume 15, numéro 2, p. 70–73.

White, F. M. (2008). *Fluid mechanics*, 6^{e} édition. McGraw-Hill series in mechanical engineering, McGraw-Hill.

Wolfson, M. et Shaffer, T. (2004). Liquid ventilation: an adjunct for respiratory management. *Paediatr Anaesth*, volume 14, p. 15–23.

Wolfson, M. R., Greenspan, J. S., Deoras, K. S., Rubenstein, S. D. et Shaffer, T. H. (1992). Comparison of gas and liquid ventilation: clinical, physiological, and histological correlates. *J Appl Physiol*, volume 72, numéro 3, p. 1024–1031.

Wolfson, M. R., Greenspan, J. S. et Shaffer, T. H. (1998). Liquid-assisted ventilation: An alternative respiratory modality. *Paediatric Pulmonology*, volume 26, numéro 1, p. 42–63.

Wolfson, M. R., Hirschl, R. B., Jackson, J. C., Gauvin, F., Foley, D. S., Lamm, W. J. E., Gaughan, J. et Shaffer, T. H. (2008). Multicenter comparative study of conventional mechanical gas ventilation to tidal liquid ventilation in oleic acid injured sheep. *ASAIO J*, volume 54, numéro 3, p. 256–269.

Wolfson, M. R. et Shaffer, T. H. (2005). Pulmonary applications of perfluorochemical liquids: Ventilation and beyond. *Paediatric respiratory reviews*, volume 6, numéro 2, p. 117–127.

Womersley, J. R. (1955). Method for the calculation of velocity, rate of flow and viscous drag in arteries when the pressure gradient is known. *Journal of Applied Physiology*, volume 127, numéro 3, p. 553–563.

Yamanaka, G., Kikura, H., Takeda, Y. et Aritomi, M. (2002). Flow measurement on an oscillating pipe flow near the entrance using the uvp method. *Experiments in Fluids*, volume 32, numéro 2, p. 212–220.

Yoxall, C. W., Subhedar, N. V. et Shaw, N. J. (1997). Liquid ventilation in the preterm neonate. *Thorax*, volume 52, numéro Suppl 3, p. S3–S8.

Yuan, H., Suki, B. et Lutchen, K. R. (1998). Sensitivity analysis for evaluating nonlinear models of lung mechanics. *Ann. Biomed. Eng.*, volume 26, numéro 2, p. 230–241.